Collaborative Report on Disposal Concepts

Fuel Cycle Research & Development

Prepared for :
U.S. Department of Energy
Used Fuel Disposition

E.L. Hardin, D.J. Clayton and M.J. Martinez
Sandia National Laboratories
Gerald Neider-Westermann, DBE TEC GmbH
R.L. Howard, Oak Ridge National Laboratory
H.R. Greenberg, J.A. Blink and T.A. Buscheck
Lawrence Livermore National Laboratory
September, 2013

FCRD-UFD-2013-000170 Rev. 0

Revision History for FCRD-UFD-2013-000170 Rev. 0

Revision	Description
Review Draft A (20Aug13)	Sent to authors and informal reviewers
Review (05Sep13)	Updated DBE TEC contribution, sent to Sandia reviewers

Sandia National Laboratories is a multi-program laboratory managed and operated by Sandia Corporation, a wholly owned subsidiary of Lockheed Martin Corporation, for the U.S. Department of Energy's National Nuclear Security Administration under contract DE-AC04-94AL85000.

Sandia Review and Approval Number: SAND2013-7665P

Table of Contents

1. Introduction 2

2. Disposal Concept Update 3

2.1 Salt Repository Concept Update 4
2.2 Hard Rock (Crystalline) Open Repository Concepts 7
2.3 Backfill Thermal Behavior 8
2.4 Cavern-Retrievable Concepts 8

3. Thermal Analysis Update 11

3.1 Parametric Thermal Analysis for Sedimentary Open-Mode Concepts 11

3.1.1 Initial Parameter Study for Open Modes in Sedimentary Media 12
3.1.2 Additional Parameter Study Cases – Required Ventilation Time 16
3.1.3 Additional Parameter Study Cases – Host Rock Thermal Gradients 19
3.1.4 Summary of Parameter Studies for Sedimentary Open-Mode Concepts 22

3.2 Package Power Limit Calculations for Open-Mode Concepts 23

3.2.1 Analysis Method and Results 23

3.3 Summary 39

4. Vertical Waste Package Movement in a Salt Repository 44

4.1 Analysis Method 44

4.1.1 Thermal-Mechanical 45
4.1.2 Thermal-Viscous Flow 47

4.2 Results 51

4.2.1 Baseline Case 51
4.2.2 Reduced Waste Package Density 53
4.2.3 No Heat Generation 55

4.3 Summary 56

5. Conceptual Design Description for Heavy Shaft Hoists 57

5.1 Shaft Hoisting 58

5.1.1 Shaft Safety Requirements 58
5.1.2 Design Basis Regulatory Requirements 59

5.2 Conceptual Design of the Hoisting System for Shaft Gorleben 2 59

5.2.1 Cable Requirements and Safety Factor 60
5.2.2 Hoist Cage and Cable Attachments 62
5.2.3 Hoist Mechanism 65
5.2.4 Headframe and Shaft House 71
5.2.5 Safety Winder/Hoist System 77
5.2.6 Shaft Cross-Section 78

5.3 Operational Safety Analyses and Demonstration Analysis (Gorleben) 79

5.3.1 Probabilistic Safety Assessment 80
5.3.2 DEAB Demonstration Test 82

5.4 Upscaling to a 175 MT Hoist 83

5.5 Preliminary Cost Estimate for 85 MT and 175 MT Hoist Systems 85
5.6 Summary 86
6. Summary 89
Appendix A – Operational Safety Evaluation 90

Tables

Table 2-1. Reference concepts for small and large waste packages 6
Table 3-1. Ventilation time solutions for cases analyzed (initial parameter study) 13
Table 3-2. Ventilation time results for additional cases 16
Table 3-3. Percentage contributions to peak wall temperature from the central package, adjacent packages, and adjacent drifts 17
Table 3-4. Depth into the drift wall for which peak temperature equals the target value (40 GW-d/MT) 21
Table 3-5. Depth into the drift wall for which peak temperature equals the target value (60 GW-d/MT) 21
Table 3-6. Thermal properties for geologic settings 23
Table 3-7. Geometrical and emissivity parameters 25
Table 3-8. Peak wall and package temperature results for the sedimentary open unbackfilled (10 m package spacing) concept. 33
Table 3-9. Peak wall and package temperature results for the sedimentary open unbackfilled (20 m package spacing) concept. 33
Table 3-10. Peak wall and package temperature results for the sedimentary open backfilled (20 m package spacing) concept. 34
Table 3-11. Peak wall and package temperature results for the hard rock open unbackfilled (10 m package spacing) concept. 35
Table 3-12. Peak wall and package temperature results for the hard rock open unbackfilled (20 m package spacing) concept. 36
Table 3-13. Peak wall and package temperature results for the hard rock open backfilled (20 m package spacing) concept. 37
Table 3-14. Summary of confidence interval statistics (maximum package power to meet temperature limits) for open mode disposal concepts and timing cases. 40
Table 3-15. Summary of confidence interval statistics for backfilled open mode concepts with different backfill temperature limits (120°C, 150°C and 200°C) 41
Table 4-1. Thermal properties for the waste and salt 46
Table 4-2. Mechanical properties used for the waste 47
Table 4-3. Waste package drag coefficient 49
Table 5-1. Hoisting System Design Parameters 65
Table 5-2. Hoist safety system sensors 68
Table 5-3. Preliminary cost estimation for major system components 86

THIS PAGE INTENTIONALLY LEFT BLANK

Figures

Figure 2-1. Heat output per PWR fuel assembly, for three values of burnup showing approximate power limits (at closure) for disposal in 32-PWR size packages..... 5

Figure 2-2. Concept drawing for in-drift emplacement of large waste packages in a salt repository 7

Figure 3-1. Graphical results for 21-PWR and 32-PWR waste packages (initial parameter study)..... 15

Figure 3-2. Peak temperature vs. package spacing for values of depth into the rock (32-PWR size packages, 40 GW-d/MT burnup) 20

Figure 3-3. Peak temperature vs. package spacing for values of depth into the rock (32-PWR size packages, 60 GW-d/MT burnup, 90 m drift spacing) 20

Figure 3-4. Correlation plots for the sedimentary unbackfilled open mode with 10 m drift spacing (timing cases as indicated). 27

Figure 3-5. Correlation plots for the sedimentary unbackfilled open mode with 20 m drift spacing (timing cases as indicated). 28

Figure 3-6. Correlation plots for the sedimentary backfilled open mode with 20 m drift spacing (timing cases as indicated). 29

Figure 3-7. Correlation plots for the hard rock unbackfilled open mode with 10 m drift spacing (timing cases as indicated). 30

Figure 3-8. Correlation plots for the hard rock unbackfilled open mode with 20 m drift spacing (timing cases as indicated). 31

Figure 3-9. Correlation plots for the hard rock backfilled open mode with 20 m drift spacing (timing cases as indicated). 32

Figure 4-1. Schematic of waste package embedded in intact salt 44

Figure 4-2. Near-field grid..... 45

Figure 4-3. Decay curve used in the thermal analysis 46

Figure 4-4. Effective viscosity versus temperature for intact salt calculated using the M-D creep model (Munson 1997). 48

Figure 4-5. Horizontal waste package vertical settling velocity versus salt effective viscosity. 50

Figure 4-6. Horizontal waste package vertical settling velocity versus salt temperature..... 50

Figure 4-7. Maximum temperature in waste package versus time 52

Figure 4-8. Thermal-mechanical modeling, baseline case, waste package vertical displacement versus time 52

Figure 4-9. Thermal-viscous flow modeling, baseline case, waste package vertical displacement versus time 53

Figure 4-10. Thermal-mechanical modeling, reduced density, waste package vertical displacement versus time 54
Figure 4-11. Comparison of thermal-mechanical modeling, baseline and reduced density, waste package vertical displacement versus time 54
Figure 4-12. Thermal-mechanical modeling, no heat generation, waste package vertical displacement versus time 55
Figure 4-13. Thermal-viscous flow modeling, no heat generation, waste package vertical displacement versus time 56
Figure 5-1. Principles of operation for friction and drum winders 60
Figure 5-2. Three-layer oval cable strand (left); and an example of flat balance cables (right) 62
Figure 5-3. Hoisting cage with mounting attachments as planned for a 175 MT system 64
Figure 5-4. Counterweight assembly 66
Figure 5-5. Friction pulley and dual motors 67
Figure 5-6. Brake caliper (Type SIEMAG BE 100) 70
Figure 5-7. Conceptual design of the braking system (left) and structure of the brake caliper (right) 70
Figure 5-8. Design of the shaft hoisting system for the Gorleben 2 design, surface shaft station 73
Figure 5-9. Configuration of surface station systems for loading waste shipments 74
Figure 5-10. Potential Configuration of a Shaft House Surface Station with Safety Systems 75
Figure 5-11. Concept of the SELDA braking system as designed for the shaft sump 76
Figure 5-12. Example catch gears 77
Figure 5-13. Safety Winder Roller Guides 78
Figure 5-14. Schematic of the shaft cross-section 79
Figure 5-15. Configuration of the DEAB demonstration testbed 83
Figure 5-16. Hoisting tower without lining (DIREGT) 85

Acronyms

BVOS	Mining Regulations for Shaft and Inclined Haulage Installations (German)
BWR	Boiling Water Reactor
DBE	German Service Company for the Construction and Operation of Waste Repositories
DC	Direct Current
DEAB	Direct Disposal of Spent Fuel Elements (German)
DIN	German Standards Institute
DIN EN	German Standards Institute – European Standard
DIREGT	Direct Disposal of Transport and Storage Canisters (German)
DOE	U.S. Department of Energy
DPC	Dual-Purpose Canister
EBS	Engineered Barrier System
FEM	Finite Element Method
FY	Fiscal Year
GNS	Nuclear Service Company (German)
GW	Gigawatt
HLW	High-Level Waste
K_{th}	Thermal Conductivity
M-D	Multimechanism-Deformation salt creep model
MT	Metric Tons
MTHM	Metric Tons of Heavy Metal
MTU	Metric Tons Uranium
NWPA	Nuclear Waste Policy Act
OFF	Oldest Fuel First
ONDRAF/ NIRAS	Belgian Agency for Radioactive Waste and Enriched Fissile Materials
PSA	Probabilistic Safety Analysis
PWR	Pressurized Water Reactor
R&D	Research and Development
SELDA	Strain Energy Linear Ductile Arrestor

SFC1	Safety and Feasibility Case – 1 (ONDRAF/NIRAS)
SNF	Spent Nuclear Fuel
SNL	Sandia National Laboratories
TAS	Technical Requirements for Shaft Hoisting Installations and Inclined Hoisting Installations (German)
TEV	Transport-Emplacement-Vehicle
UFD	Used Fuel Disposition
UNF	Used Nuclear Fuel
VSG	Preliminary Safety Analysis–Gorleben (German)
YFF	Youngest Fuel First
yr	years

Collaborative Report on Disposal Concepts

Deliverable: M4FT-13SN0804036
Work Package: FT-13SN080403

E.L. Hardin, D.J. Clayton and M.J. Martinez, Sandia National Laboratories
G. Nieder-Westermann, DBE TECHNOLOGY GmbH
R.L. Howard, Oak Ridge National Laboratory
H.R. Greenberg, J.A. Blink and T.A. Buscheck, Lawrence Livermore National Laboratory

Abstract

Reference geologic disposal concepts for the Used Fuel Disposition R&D campaign, are expanded to include backfill and unbackfilled open-mode alternatives for sedimentary rock (e.g., clay/shale) and hard rock (e.g., crystalline). Also, the cavern-retrievable concept is recognized as a possible alternative that combines elements of storage and disposal packaging.

Thermal analysis of alternative disposal concepts is extended to open emplacement modes (those allowing long-term repository ventilation to remove heat), with calculations of minimum ventilation time for various waste types and geologic settings. Also, waste package thermal power limits at the time of emplacement in the repository, are calculated for a range of package spacings and storage/ventilation timing cases, to be used as input to logistical simulations that model disposition and ultimate disposal of used nuclear fuel. These calculations are sensitive to the maximum temperature target adopted for host rock and engineered materials such as clay-based backfill. Disposal in salt and hard rock, which have relatively high thermal conductivity and tolerance for elevated temperatures on the order of 200°C, allows the highest thermal power limits (10 to 15 kW at emplacement). Use of temperature-sensitive backfill is associated with the lowest emplacement power limits (on the order of 1 kW to meet a 100°C temperature target) which would require protracted surface decay storage.

Questions about the potential for large, hot waste packages to sink due to creep in a salt repository are addressed using coupled thermal-mechanical finite-element simulations. These calculations were performed using the Adagio and Aria codes, and using constitutive models developed from tests performed in the laboratory at the Waste Isolation Pilot Plant and elsewhere. They show that based on these inputs, sinking would be limited to 0.1 m or possibly much less over 10^6 years, even for a large, heavy waste package.

Finally, the technical details and safety analysis for a heavy shaft hoist with payload capacity of 85 MT are discussed, based on previous work done in Germany at the Gorleben site. Such a capacity would facilitate transport of packages weighing about 60 MT (e.g., 12 pressurized water reactor fuel assemblies, canister, disposal overpack, and shielding). For larger packages (e.g., containing 32 fuel assemblies) the hoist design concept could be extended to 175 MT. Costs for hoist hardware would be approximately $20 to $30 million, plus shaft construction, hoist installation, and other costs associated with management, engineering, procurement, and construction.

1. Introduction

The FY11/FY12 summary report for the Thermal Load Management/Disposal Concepts R&D work package (Hardin et al. 2012) developed and analyzed a set of reference concepts for geologic disposal of spent nuclear fuel (SNF) and high-level waste (HLW). This report supplements that one, offering updated concept development, thermal analysis, salt rock mechanics, and conceptual information for heavy shaft hoists. Some of these topics stem from questions that were raised in the earlier report but not analyzed, such as the feasibility of transporting large waste packages in vertical shafts. Other topics are related to ongoing work to evaluate the feasibility of direct disposal of SNF in dual-purpose canisters (DPCs), because they are especially relevant for larger, heavier waste packages that contain more SNF and may contain fuel with higher burnup (Hardin et al. 2013).

This supplemental report documents additional studies performed after the major deliverable of the previous R&D (Hardin et al. 2012). The focus of work in this area is transitioning to the DPC direct disposal evaluation, and the results documented here support that transition.

References for Section 1

Hardin, E., T. Hadgu, D. Clayton, R. Howard, H. Greenberg, J. Blink, M. Sharma, M. Sutton, J. Carter, M. Dupont and P. Rodwell 2012. *Disposal Concepts/Thermal Load Management (FY11/12 Summary Report).* FCRD-USED-2012-000219, Rev.1. U.S. Department of Energy, Used Fuel Disposition R&D Campaign.

Hardin, E., D. Clayton, R. Howard, J. Scaglione, E. Pierce, K. Banerjee, M.D. Voegele, H. Greenberg, J. Wen, T. Buscheck, J. Carter and T. Severynse 2013. *Preliminary Report on Dual-Purpose Canister Disposal Alternatives.* FCRD-UFD-2013-000171 Rev. 0. U.S. Department of Energy, Used Fuel Disposition R&D Campaign. August, 2013.

2. Disposal Concept Update

This section updates the disposal concepts described in the FY11/12 summary report (Hardin et al. 2012). The more recent information describes additional concepts and measures that would accommodate larger, hotter waste packages up to and including direct disposal of dual-purpose canisters (32-PWR size or larger).

Background – Geologic disposal concepts are readily divided into "enclosed" and "open" modes of waste package emplacement (Hardin et al. 2012). The enclosed modes involve emplacing packages directly into contact with engineered material or host rock with temperature limits. The open modes maintain air space around each package that can be ventilated to remove heat prior to permanent closure of the repository. These spaces may remain open and continue to enhance heat dissipation after closure. Open emplacement concepts combine the functions of surface decay storage (i.e., in fuel pools or dry storage) with geologic disposal in the same underground facility. An open-concept repository can be constructed and operated much sooner than enclosed concepts that require surface decay storage of 100 years or longer (Hardin et al. 2012). Earlier emplacement of spent nuclear fuel (SNF) waste would allow much of the disposal cost to be incurred at the same time that currently operating nuclear power plants are being shut down.

Most international high-level waste (HLW) and SNF disposal programs are focused on enclosed modes in crystalline or clay-based host rock types, with inherent limits on heat generation and SNF capacity for waste packages. As shown previously, with the exception of the salt repository, these enclosed concepts have low waste package power limits (or long aging requirements) (Hardin et al. 2012, Section 3).

Among the alternatives investigated in this multi-year study, the salt repository concept and the open emplacement modes discussed below are best suited for larger waste packages with higher heat output. A disposal solution using larger packages is attractive for the U.S. which currently faces the disposal of more than twice as much SNF as any other nation. This was demonstrated for reference open mode concepts (Hardin et al. 2012, Section 3.2) and for larger packages (e.g., up 32-PWR size) that would be used to dispose of dual-purpose canisters (Hardin and Voegele 2013). For thermal management more flexibility is obtained with host rock that has both high thermal conductivity and tolerance for higher peak temperatures. This illustrated in Figure 2-1, which shows the power limits per assembly, for 32-PWR size packages that meet peak temperature targets for salt, hard rock sedimentary rock and backfill. It shows that substantial additional aging (decay storage and/or repository ventilation) is needed to accommodate higher burnup SNF in sedimentary rock. For backfill the 100°C target could be difficult to meet with 32-PWR size packages, although higher temperature backfill materials or designs could be effective.

This section reviews the recent developments for larger, hotter packages. The focus is on thermal management, and the assumption for this discussion is that SNF in existing canisters would be re-packaged for disposal. Postclosure criticality is addressed elsewhere (Clarity and Scaglione 2013; EPRI 2008a) and would be facilitated by purpose-built packages. The updated list of reference concepts (Table 2-1) is numbered consistently with the previous list (Hardin et al. 2012). Changes (with numbers from the table) include:

- Added the horizontal borehole and in-drift enclosed emplacement modes for crystalline rock (1.2 and 1.3). The horizontal mode was added to accommodate larger packages.

Waste packages would likely be transported underground in the horizontal orientation (Hardin et al. 2012, Section 1.4.4) and up-ending would not be needed for horizontal emplacement. In-drift emplacement would also not require pushing packages into boreholes (but would create a radiation environment in the drift).

- Added horizontal and vertical borehole emplacement modes for salt (2.1 and 2.2). These borehole modes maximize heat transfer from packages to the intact salt, and they are shielded by rock, facilitating repository operations.
- Generalized shale media to sedimentary (claystone, mudstone, shale, etc.) and separated the unbackfilled alternative to include both low- and high-temperature modes (4.1 and 4.2). Including a range of argillaceous media descriptors is consistent with international practice. Low- and high-temperature modes indicate whether the near-field host rock peak temperature is greater than 100°C, which was identified in the "design test case" (Hardin et al. 2012) and is even more important for larger, hotter packages.
- Added the hard rock backfilled open concept (6.2). With backfill at closure, open-mode emplacement is extended to saturated (as well as unsaturated) settings. This increases the range of workable concepts. The waste package outer layer would be of corrosion resistant material to provide redundant engineered barriers as well as the geologic setting.
- Added cavern-retrievable modes using surface storage casks (7.1) or purpose-built underground vaults (7.2). These concepts have been considered for use in Japan and Korea, and have unique advantages such as physical security of the waste, and small repository footprints. They may also have economic advantages from combining storage and disposal functions in the same facility, and minimizing waste transport.

The remainder of this section discusses changes considered for the salt repository; hard rock disposal concepts; backfill thermal behavior; and the cavern-retrievable concepts. In addition, Section 3 of this report includes a parametric study of spacings for the sedimentary open concepts.

2.1 Salt Repository Concept Update

For disposal of large waste packages in salt the lateral spacings between waste packages are increased from 20 m to 30 m based on finite-element analysis of peak salt temperature (Hardin et al. 2013, Section 5). The larger spacings have the effect of reducing contributions to peak temperature from adjacent drifts, which causes the peak to occur earlier in time, within a few years after emplacement.

The original generic salt repository concept (Carter et al. 2011) called for placing heat-generating HLW canisters into individual alcoves mined from access drifts. The main purpose of the arrangement is to spread the packages out on a grid for heat dissipation. The alcove mode also allows worker entry into the access drifts, once all the waste packages are covered with crushed salt. The equipment that would emplace these packages would be articulated to maneuver into the alcoves, and capable of picking up a package with cantilevered arms and depositing it against the back wall.

For heavy waste packages (e.g., up to 100 MT plus shielding for transport) a different kind of transport-emplacement vehicle could be used with in-drift emplacement (see Figure 2-2 and discussion below). The in-drift mode can also spread packages out on a grid, and do so with a

lower extraction ratio than with alcoves. The emplacement drift would be excavated first, then waste packages would be emplaced starting at the farthest extent and retreating back to the access. The drift would be backfilled with crushed salt as the packages are emplace, so no worker access would be possible after emplacement.

Thermal calculations for in-drift emplacement yield peak salt temperatures approximately 25 C° hotter than alcove emplacement (Hardin et al. 2013, Figures 5-1 and 5-5) because the packages are farther from the drift walls instead of immediately adjacent to the back wall of the alcove. The original thermal analysis of the salt repository incorporated semi-cylindrical cavities in the alcove floor, into which packages were placed to facilitate heat transfer to the intact salt (Hardin et al. 2012). For in-drift emplacement these features are more important than for alcove emplacement, and decrease the peak salt temperature by more than 50 C° (Hardin et al. 2013, Figures 5-3 and 5-5). Accordingly, the transport-emplacement vehicle should be designed to straddle these cavities (Figure 2-2).

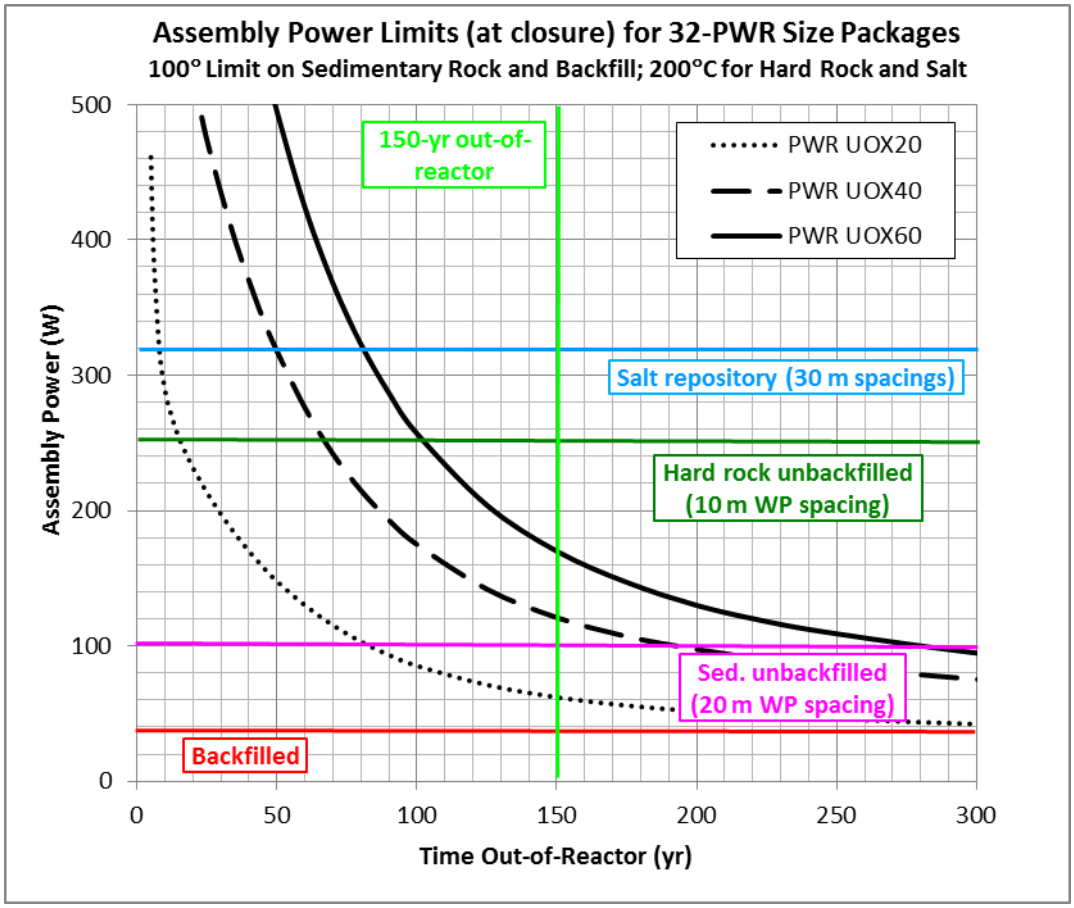

Note: Assembly power limits are shown for 32-PWR size packages in the salt repository, hard rock unbackfilled repository, and sedimentary unbackfilled repository. Where assembly power is less than these limits, before the assumed time limit for repository closure (150 yr is shown) the temperature targets can be met. Use of backfill poses the most restrictive power limits for both hard rock and sedimentary concepts.

Figure 2-1. Heat output per PWR fuel assembly, for three values of burnup showing approximate power limits (at closure) for disposal in 32-PWR size packages

Table 2-1. Reference concepts for small and large waste packages

Concept	Long-Term Ventilation Required
Crystalline rock, enclosed, swelling clay-based buffer	
1.1 Crystalline enclosed (vertical borehole emplacement)	(enclosed)
1.2 Crystalline enclosed (horizontal borehole emplacement)	
1.3 Crystalline enclosed (in-drift emplacement)	
Salt repository	
2.1 Horizontal in-alcove transverse or in-drift axial emplacement	(enclosed)
2.2 Borehole emplacement	
Clay/shale, enclosed	
3. Clay/shale enclosed	(enclosed)
Sedimentary, unbackfilled open	
4.1 Sedimentary unbackfilled, low-temperature	✓
4.2 Sedimentary unbackfilled, high-temperature	✓
Sedimentary backfilled open	
5.1 Sedimentary backfilled open	✓
Hard-rock, open emplacement	
6.1 Hard-rock, unsaturated, unbackfilled open	✓
6.2 Hard-rock, backfilled open	✓
Cavern-retrievable	
7.1 Surface storage systems (shielded) in underground galleries	✓
7.2 Purpose-built, shielded, ventilated storage/disposal casks (vaults)	✓

The transport-emplacement vehicle (TEV) for in-drift emplacement in salt would resemble a rubber-tire version of rail-mounted TEV proposed previously (DOE 2008). A rubber tired version was also proposed previously during conceptual design, but rail was selected. The TEV for salt would consist of a round shield with a shield door on the front, and a retractable shield plate on the bottom (Figure 2-2). The shields would be supported by a chassis with hydraulic wheel trucks, each truck consisting of two wheels on a short axle supported from the center (e.g., described at *www.wheelift.com*). Each wheel truck is independently steered and driven, with vertical travel of 25 cm or more for transit over rough surfaces. Tires are solid urethane. The chassis would be forked at the front, allowing it to drive over a large waste package, close the shield door, latch the package, hoist the package into the shield, and close the lower shield plate. The steps would be reversed to deposit the package into a prepared cavity in the emplacement drift floor. The "kneeling" capability of the chassis could be used to assist with latching, hoisting and depositing the package. Hoisting capacity of approximately 1.5 m would allow clearance for the lower shield during transport, and lowering into a 1-m deep cavity. The same TEV concept could be used for rubber-tire conveyance in other host media and with other disposal concepts.

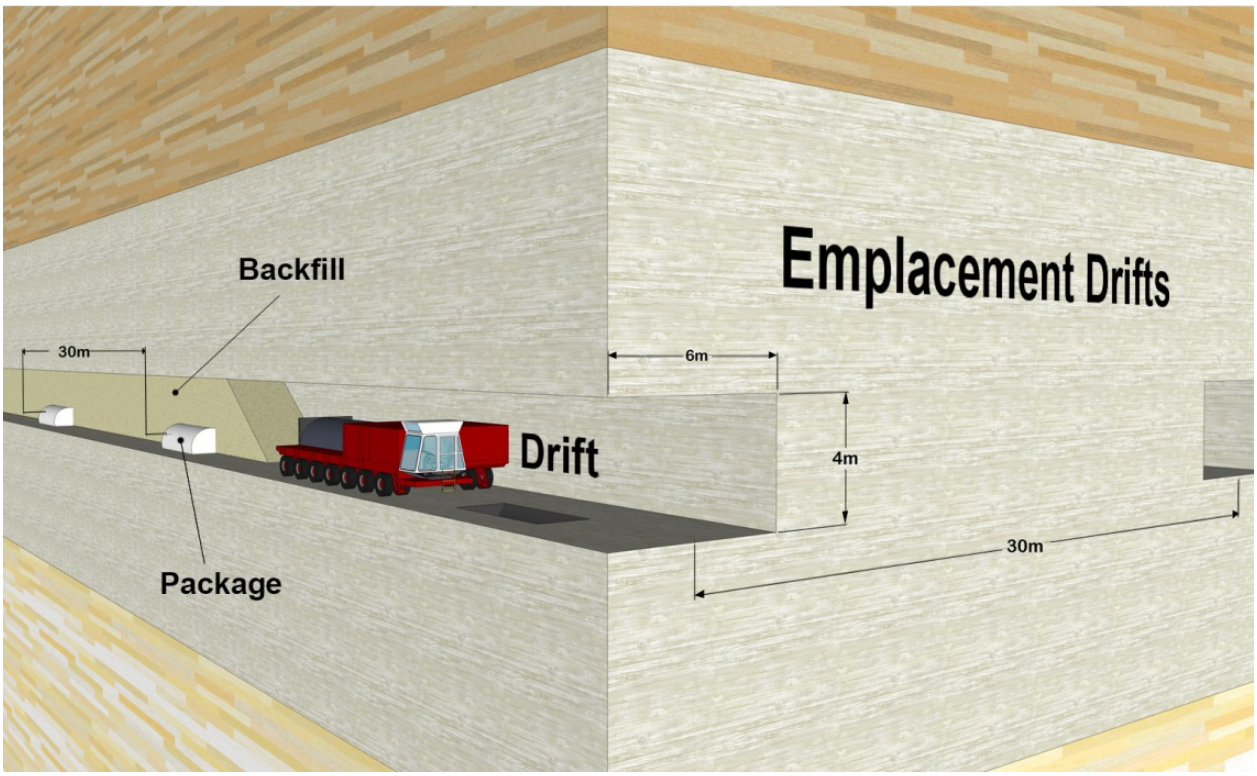

Figure 2-2. Concept drawing for in-drift emplacement of large waste packages in a salt repository

2.2 Hard Rock (Crystalline) Open Repository Concepts

Hard rock (e.g., competent rock, generally igneous or metamorphic, including indurated tuff) offers long opening stand-up times, and typically has greater thermal conductivity and higher temperature tolerance (e.g., to 200°C as recommended by Hardin et al. 1997) than rock types containing significant clay or other hydrous minerals. Virtually all hard rock types have some fracturing, so mitigating rock permeability is important.

In the hard rock open concepts, waste packages would be emplaced axially in open drifts, and ventilated for decades (e.g., up to 100 years) to remove heat. The concepts would use corrosion resistant packaging and other engineered barriers as needed for defense-in-depth. For the unsaturated, unbackfilled case, other engineered barriers could include water diversion features (e.g., drip shields), multiple corrosion resistant packaging materials (e.g., Ti and Hastelloy). The presence of sufficient permeability will make the host rock free-draining. With drainage there is little possibility of focused groundwater flow along repository openings, so plugging and sealing of emplacement and access drifts may not be needed. This concept is similar to previous work (DOE 2008) and to a previous proposal for direct disposal of DPCs (EPRI 2008b).

For the saturated case low-permeability backfill would be added prior to repository closure, to prevent groundwater movement along repository openings, and limit transport of water and oxygen to the package (and radionuclide release from the package).

Thermal calculations show that a 200°C drift wall temperature target could be readily met for SNF with high burnup, with fuel age less than 150 years out-of-reactor at repository closure,

even for waste packages as large as 32-PWR size (Hardin 2013; Hardin and Voegele 2013). If drift wall temperature is the controlling variable, there is significant margin to optimize the repository layout and durations for storage and ventilation, for the hard rock (crystalline) open concepts. With backfill, for waste package sizes 21-PWR and greater, waste package and backfill peak temperatures would be well above 200°C, except that for low burnup (e.g., 20 GW-d/MT) the peak backfill temperature could be on the order of 150°C (Hardin and Voegele 2013, Figure 8; Hardin et al. 2012, Section 3.3).

2.3 Backfill Thermal Behavior

Granular backfill materials generally have relatively low thermal conductivity (e.g., 0.42 W/m-K for dehydrated, compacted bentonite; see Hardin et al. 2012) which subjects those materials and the waste package to higher temperatures in disposal applications. The thermal resistance from layers of granular backfill/buffer material is such that peak EBS temperatures are dominated by the backfill/buffer contribution, in any rock type (sedimentary or hard rock), wherever a backfill or buffer is used. Accordingly, the peak temperature results for hard rock discussed above apply to sedimentary media as well.

Elevated temperature at the waste package contact with backfill/buffer materials is generally not a problem for stability of the package or its contents. SNF can withstand temperature of 350°C without significant damage to zirconium-alloy cladding (BSC 2008a). The relationship of package surface temperature to SNF temperature depends on the package size, construction and heat output. Previous analysis found the difference to be less than 50 C° after closure (BSC 2008b) but some additional margin may be needed for larger packages (e.g., 32-PWR size) and to account for convective temperature differences on the package wall. Some waste package materials such as stainless steel and corrosion-resistant nickel alloys are subject to sensitization or de-alloying processes that can occur over decades to hundreds of years, at 300°C or cooler (Fox and McCright 1983; BSC 2008a). Hence there is a need for waste package peak surface temperatures to be limited to approximately 250 to 300°C.

Installation of backfill is not likely to significantly affect temperature in the host rock. However, elevated temperature in the backfill could impact the properties of the backfill itself, and in particular, alter clays that are used to produce swelling behavior and low permeability. Scoping calculations show that backfill material capable of withstanding 150°C peak temperature could make the use of backfill a more viable option disposal of large waste packages (Hardin and Voegele 2013). This possibility is the objective of ongoing materials research in the Used Fuel Disposition (UFD) program.

2.4 Cavern-Retrievable Concepts

This concept is close to that proposed by the original authors (see Apted and McKinley 2013). It would use existing dry cask storage systems, relocated from the surface to large galleries or caverns underground (Table 2-1, item 7.1). Ramp access would be needed to move the heavy shielded casks underground. Initial construction would provide the means to limit groundwater contact with the casks after closure, e.g., by emplacing storage casks on engineered pads of low-permeability material with sufficient shear strength for long-term stability. Hydraulic containment liners for landfill disposal applications are typically constructed in such a manner using mixtures of sand and clay (Kenney et al.1992). Reliance on low-permeability clay-based buffer/backfill materials could be effective for saturated groundwater conditions, or in the

unsaturated zone where pore pressures and groundwater flow velocities are minimal (e.g., Hardin and Sassani 2011).

Shielded surface storage casks for DPCs cool by natural convection into the surrounding air. Emplacement galleries would be ventilated using a combination of forced and natural convection to remove this heat. Conditions would be dry during ventilation, especially for host rock of sufficiently low permeability, or in the unsaturated zone. Operations to close the facility would consist of removing services such as electrical conductors, and backfilling with engineered material (e.g., granular dehydrated compacted bentonite). Closure operations could proceed when heat output had decayed sufficiently to maintain backfill temperature (in dehydrated and hydrated regions) below 100°C.

This concept would use the storage casks already deployed wherever DPCs exist, and the casks would be transported to the repository separately from waste. It could also be used for self-shielded containers such as CASTOR casks. Use of existing hardware could limit disposal cost. The concept is similar in principle to in-drift disposal in crystalline rock with reliance on the low-permeability backfill/buffer and natural barrier performance. This concept has not been thoroughly evaluated in the technical literature and presents opportunities for R&D (Hardin and Voegele 2013).

An alternative concept would use specially built vaults in an underground facility to store, and eventually dispose of SNF in the same canisters used for dry storage and transportation (Table 2-1, item 7.2). Emplacement could be horizontal or vertical; in either case vaults would be constructed with low-permeability material to maintain waste isolation after closure, while also providing for cooling by natural convection prior to closure. Vaults would be similar to surface storage concepts such as the NUHOMS systems from TransNuclear (horizontal) or the subterranean Hi-Storm 100 system from Holtec International (vertical), optimized for postclosure waste isolation. This concept is similar to that originally proposed (see above) but with vaults pre-constructed for postclosure waste isolation. It also presents opportunities for R&D, for example, developing a configuration for the subterranean storage system that accepts a range of existing canister types, and optimizing heat transfer.

References for Section 2

Apted, M.J. and I.G. McKinley 2013. “Optimizing Back-end Flexibility With The Care Concept.” *Proceedings: 14th International High-Level Radioactive Waste Management Conference*. Albuquerque, NM. April 28 – May 2, 2013. American Nuclear Society. Paper #6913.

BSC (Bechtel-SAIC Co.) 2008a. *Postclosure Analysis of the Range of Design Thermal Loadings*. ANL-NBS-HS-000057 REV 00. U.S. Department of Energy, Office of Civilian Radioactive Waste Management. January, 2008.

BSC (Bechtel-SAIC Co.) 2008b. *Basis of Design for the TAD Canister-Based Repository Design Concept*. 000-3DR-MGRO-00300-000-003. U.S. Department of Energy, Office of Civilian Radioactive Waste Management. October, 2008.

Carter, J.T., F. Hansen, R. Kehrman and T. Hayes 2011. *A generic salt repository for disposal of waste from a spent nuclear fuel recycle facility*. SRNL-RP-2011-00149 Rev. 0. Aiken, SC: Savannah River National Laboratory.

Carter, J., A. Luptak, J. Gastelum, C. Stockman and A. Miller 2012. *Fuel Cycle Potential Waste Inventory for Disposition.* FCR&D-USED-2010-000031 Rev. 5. U.S. Department of Energy, Used Fuel Disposition R&D Campaign. July, 2012.

Clarity, J.B. and J.M Scaglione 2013. *Feasibility of Direct Disposal of Dual-Purpose Canisters-Criticality Evaluations*. ORNL/LTR-2013/213. Oak Ridge National Laboratory, Oak Ridge, TN. June, 2013.

DOE (U.S. Department of Energy) 2008. *Yucca Mountain Repository License Application for Construction Authorization*. DOE/RW-0573. Washington, D.C.: U.S. Department of Energy.

EPRI (Electric Power Research Institute) 2008a. *Feasibility of Direct Disposal of Dual-Purpose Canisters: Options for Assuring Criticality Control,* Electric Power Research Institute. Palo Alto, CA. #1016629.

EPRI (Electric Power Research Institute) 2008b. *Feasibility of Direct Disposal of Dual-Purpose Canisters in a High-Level Waste Repository.* Electric Power Research Institute. Palo Alto, CA. #1018051.

Fox, M.J. and R.D. McCright 1983. *An Overview of Low Temperature Sensitization*. UCRL-15619. Lawrence Livermore National Laboratory. Livermore, CA.

Hardin, E.L., D.A. Chesnut, T.J. Kneafsey, K. Pruess, J.J. Roberts and W. Lin 1997. *Synthesis report on thermally driven coupled processes.* UCRL-ID-128495. Livermore, CA: Lawrence Livermore National Laboratory. October 15, 1997. OSTI ID: 16624.

Hardin, E. and D. Sassani 2011. "Application of the Prefabricated EBS Concept in Unsaturated, Oxidizing Host Media." *Proceedings: 13th International High-Level Radioactive Waste Management Conference*. Albuquerque, NM. April, 2011. American Nuclear Society. Paper #3380.

Hardin, E., T. Hadgu, D. Clayton, R. Howard, H. Greenberg, J. Blink, M. Sharma, M. Sutton, J. Carter, M. Dupont and P. Rodwell 2012. *Disposal Concepts/Thermal Load Management (FY11/12 Summary Report).* FCRD-USED-2012-000219, Rev.1. U.S. Department of Energy, Used Fuel Disposition R&D Campaign.

Hardin, E. 2013. *Temperature-Package Power Correlations for Open-Mode Geologic Disposal Concepts*. SAND2013-1425. Sandia National Laboratories. Albuquerque, NM. February, 2013.

Hardin, E. and M. Voegele 2013. *Alternative Concepts for Direct Disposal of Dual Purpose Canisters*. FCRD-UFD-2013-000102, Rev.0. U.S. Department of Energy, Used Fuel Disposition R&D Campaign.

Hardin, E., D. Clayton, R. Howard, J. Scaglione, E. Pierce, K. Banerjee, M.D. Voegele, H. Greenberg, J. Wen, T. Buscheck, J. Carter and T. Severynse 2013. *Preliminary Report on Dual-Purpose Canister Disposal Alternatives.* FCRD-UFD-2013-000171 Rev. 0. U.S. Department of Energy, Used Fuel Disposition R&D Campaign. August, 2013.

Kenney, T.C., W.A. Van Veen, M.A. Swallow and M.A. Sungaila 1992. "Hydraulic conductivity of compacted bentonite-sand mixtures." *Canadian Geotechnical Journal*. V. 29, N. 3, pp. 364-374.

3. Thermal Analysis Update

3.1 Parametric Thermal Analysis for Sedimentary Open-Mode Concepts

Argillaceous (containing clay) sedimentary host media typically have lower thermal conductivity than salt or hard rock (crystalline) which presents an additional challenge for repository thermal management. This section focuses on parametric studies of repository spacings and storage/ventilation time, and peak host rock temperature, for 32-PWR size packages, in argillaceous media. The challenge of thermal management for large waste packages with backfill is discussed in a previous section; whereas peak backfill temperature occurs close to waste packages, the peak host rock temperature occurs a short distance away which allows some flexibility to select repository spacings to limit temperature.

The trade studies presented in this section result from a series of thermal sensitivity studies developed over a two-year period (Sutton et al. 2011; Greenberg et al. 2012a and 2012b; Hardin et al. 2011 and 2012) that evaluated both "enclosed" and "open" repository design concepts. Two recent studies are presented here: an extension of FY12 thermal analysis to larger packages, and additional trade studies on repository spacings. Specifically, this report extends the analyzed maximum waste package spacing from 20 to 30 m, and the maximum drift spacing from 60 to 90 m.

The inputs to thermal analyses presented here are:

- Clay/shale host rock with thermal conductivity of 1.75 W/m-K (see Hardin et al. 2012, Appendix D)
- 32-PWR size waste packages
- SNF with burnup of 40 GWd/MT (typical of current inventory; Carter et al. 2012)
- 50 year surface decay storage
- Repository ventilation time (after the end of surface storage) of 150 years for the first study, while the second study calculates ventilation time as a function of other variables.
- Three alternative temperature targets for clay/shale media: 100°C, 120°C and 140°C at the drift wall.

The semi-analytical modeling approach was developed previously (Hardin et al. 2012, Appendix A). A variation is used to solve iteratively for ventilation time (Greenberg et al. 2013a).

Temperature at a given time and waste package location is the result of contributions from three sources: the waste package itself; 2) adjacent packages in the same drift; and 3) adjacent drifts. The superposition solution used in the semi-analytical model calculation is well suited for separating these contributions, to study how the relative contributions at the time of peak temperature are related to system parameters such as ventilation time.

The approach is used by Greenberg et al. (2013b) to demonstrate a particular approach to repository design optimization that might be used in future repository conceptual design studies. The approach seeks to balance contributions to peak temperature from the three sources listed above; using ad hoc optimality criteria (as surrogates for excavation volume, construction cost, etc.) for choosing spacings. This optimization approach may be useful in the future but is beyond

the scope of this report, which evaluates feasibility of thermal management in a generic sense with particular attention to peak temperature targets and ventilation time. Optimization becomes important when site-specific data are available, such as host rock thermal conductivity, anisotropy, spatial variability, and uncertainty.

It should be noted that other parameters may also be used in this type of analysis, including SNF burnup, drift diameter, location of the temperature compliance point, and waste package capacity. For EBS thermal analysis, the thermal conductivity of backfill has a major influence as discussed above. For parametric studies in this report large (32-PWR size) waste packages and moderate SNF burnup (40 GW-d/MT) are selected, and the temperature compliance point is the drift wall.

3.1.1 Initial Parameter Study for Open Modes in Sedimentary Media

Table 3-1 shows the required ventilation time results from the initial parameter study, for combinations of waste package size, drift spacing, waste package spacing, and peak temperature target. Blank cells represent cases that were not analyzed because more favorable solutions were found (i.e., ventilation time less than 150 yr, with smaller spacings). Similarly, because workable cases were identified with 50 years of surface storage, additional cases based on 100 years of surface storage were not evaluated. The same results are shown graphically in Figure 3-1.

Table 3-1. Ventilation time solutions for cases analyzed (initial parameter study)

Required Ventilation Time (yr) to meet Temperature Criterion Open mode concepts in clay/shale 40-GWd/MT			12-PWR waste package			21-PWR waste package			32-PWR waste package		
			Waste Package Spacing, m			Waste Package Spacing, m			Waste Package Spacing, m		
TC[A]	Dr Sp[B], m	t-store[C], yr	10	15	20	10	15	20	10	15	20
100	30	50	116			683	310	125	1450	800	500
100	30	100	40			600			1350		
100	45	50	19			235	100	42	950	490	275
100	45	100	0			186			850		
100	60	50	11			160	53	35	660	300	145
100	60	100	0			82			560		
120	30	50	20			400	108	30	950	485	270
120	30	100	0			320			800		
120	45	50	0			135	27	12	590	240	90
120	45	100	0			60			500		
120	60	50	0			53	20	9	347	100	62
120	60	100	0			0			250		
140	30	50	0			210	30	3	660	285	115
140	30	100	0			130			574		
140	45	50				40	3	0	350	90	40
140	45	100				0			265		
140	60	50				24	0	0	150	50	34
140	60	100				0			75		

Notes: [A] Temperature criterion (°C). [B] Drift spacing (m). [C] Surface decay storage duration (yr). Blank boxes were not analyzed because more favorable solutions were found.

THIS PAGE INTENTIONALLY LEFT BLANK

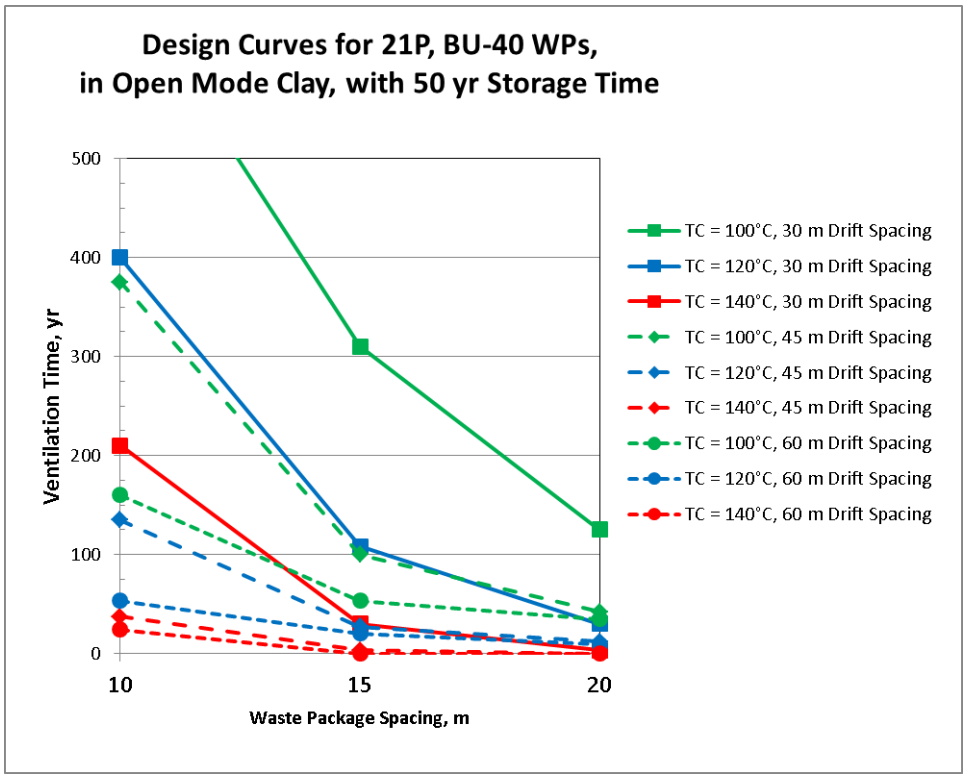

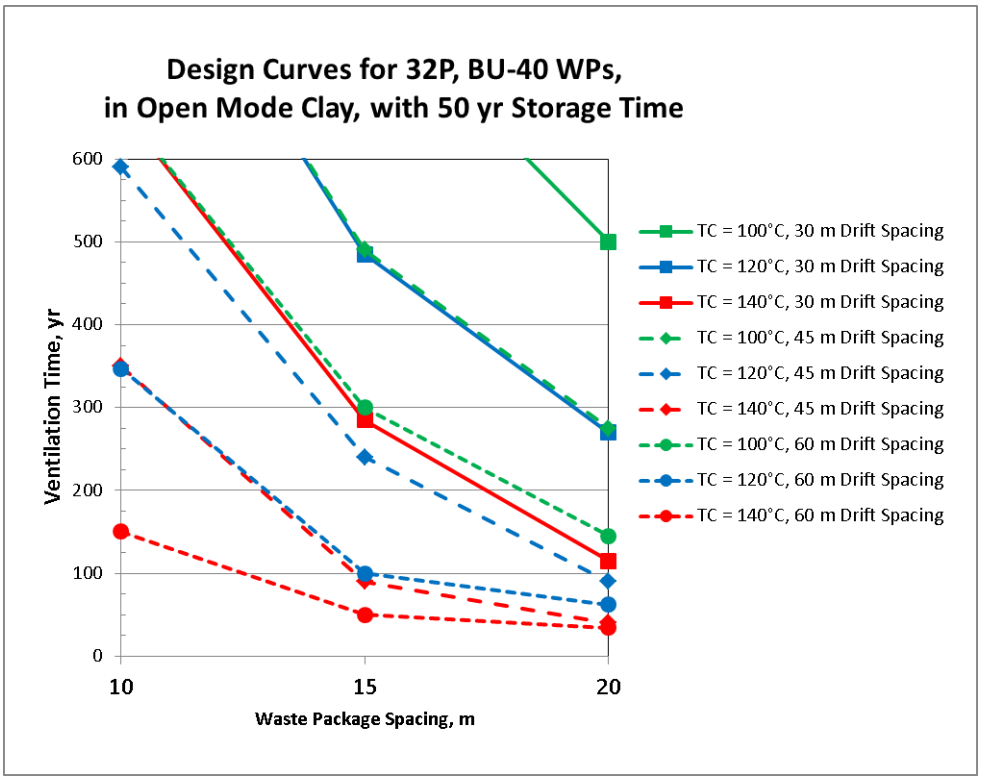

Figure 3-1. Graphical results for 21-PWR and 32-PWR waste packages (initial parameter study)

3.1.2 Additional Parameter Study Cases – Required Ventilation Time

The largest waste package spacing analyzed is extended from 20 to 30 m, and the largest drift spacing from 60 to 90 m. These calculations use the same modification of the semi-analytical model to find the ventilation time needed to meet a given peak temperature target (Greenberg 2013a). The needed ventilation times for these additional cases are summarized in Table 3-2.

The contributions to drift wall temperature from the three sources listed above, are shown in Table 3-3. Considering the results in Tables 3-2 and 3-3, the following trends are evident:

- Waste package spacing is more sensitive than drift spacing, for limiting peak temperatures (and produces a more direct increase in excavation volume)
- The drift wall peak temperature target (over the range investigated, 100°C to 140°C) is about as effective as waste package spacing (with no increase in excavation volume)
- The largest spacings (with lowest temperatures) tend to isolate waste packages so that for the lowest peak temperatures, the major contributions are from the central waste packages.

The final point is true for any temperature target and any ventilation time, but with increased ventilation time (not investigated in this study) the magnitudes of the temperature contributions decrease so that packages can be closer together.

Table 3-2. Ventilation time results for additional cases

50 yr Decay Storage 32-PWR Size Package 40 GW-d/MT Burnup			Needed Ventilation Time (yr)*		
			Waste Package Spacing (m)		
	Drift Wall Peak Temp. Target (C)	Drift Spacing (m)	10	20	30
Sedimentary (Clay/Shale)	100	30	1450	513	236
	100	60	660	146	86
	100	90	335	106	80
	120	30	950	270	81
	120	60	347	63	46
	120	90	148	57	44
	140	30	662	116	35
	140	60	156	34	24
	140	90	83	32	23

* Ventilation times longer than 150 yr are shaded.

Table 3-3. Percentage contributions to peak wall temperature from the central package, adjacent packages, and adjacent drifts

Drift Wall Peak Temperature Contribution Summary	Drift Wall Peak Temp. Target (°C)	Drift Spacing (m)	Drift Wall Peak Temperature Contributions (%) (50 yr decay storage, 32-PWR size packages, 40 GW-d/MT burnup; cases from Table 3-3)								
			WP Spacing = 10 m			WP Spacing = 20 m			WP Spacing = 30 m		
			Central Package	Adjacent Drifts	Adjacent Packages	Central Package	Adjacent Drifts	Adjacent Packages	Central Package	Adjacent Drifts	Adjacent Packages
Clay/shale (sedimentary)	100	30	12	76	12	28	60	13	42	48	10
	100	60	21	57	22	53	25	21	87	5	8
	100	90	39	24	37	76	4	20	90	2	8
	120	30	14	73	14	30	57	13	50	39	11
	120	60	24	52	24	76	6	18	93	2	5
	120	90	49	9	42	83	1	16	94	0	6
	140	30	14	71	15	32	54	14	73	19	8
	140	60	27	46	27	85	2	13	96	1	3
	140	90	55	4	42	85	0	14	96	0	4

* Ventilation times longer than 150 yr are shaded.

THIS PAGE INTENTIONALLY LEFT BLANK

3.1.3 Additional Parameter Study Cases – Host Rock Thermal Gradients

This parametric study of repository drift and waste package spacings was developed by Greenberg et al. (2013b). The objectives were to explore repository layout alternatives (i.e., spacings) for DPC direct disposal, to determine: 1) what spacings could be used to meet temperature targets (100°C for argillaceous host media and backfill); and 2) how to minimize the extent of host rock around the emplacement drifts where temperature exceeds these targets.

- Host rock peak temperature targets of 100°C and 120°C were used in this study.
- Parametric analysis was done for waste package and drift spacings, assuming:
- 32-PWR size waste packages
- SNF burnup of 40 or 60 GW-d/MT
- Decay storage 50 years before disposal
- Ventilation time 25, 50, 75, and 100 years (after decay storage) for the 40 GW-d/MT analysis, and 150 years for the 60 GW-d/MT analysis
- Ventilation system heat removal efficiency 75%
- Drift diameter 4.5 m
- Drift spacing of 70 m for the 40 GW-d/MT analysis; 70 m and 90 m for the 60 GW-d/MT analysis
- Host rock thermal conductivity 1.75 W/m-K

Figure 3-2 shows the relationship between waste package spacing and peak temperature, for several values of depth into the drift wall for the parametric spacing study for 40 GW-d/MT cases, and ventilation time of 100 years. The plot shows that package spacing of 23 m would ensure the peak drift wall temperature is at or below 100°C.

Figure 3-3 shows the relationship between waste package spacing and peak temperature, for several values of depth into the drift wall for the parametric spacing study for 60 GW-d/MT cases, and ventilation time of 150 years for drift spacing of 70 m and 90 m. The plot shows that with a drift spacing of 90 m, a package spacing of 34 m would ensure the peak drift wall temperature is at or below 100°C, and with a drift spacing of 70 m, a package spacing of around 38 m would be required.

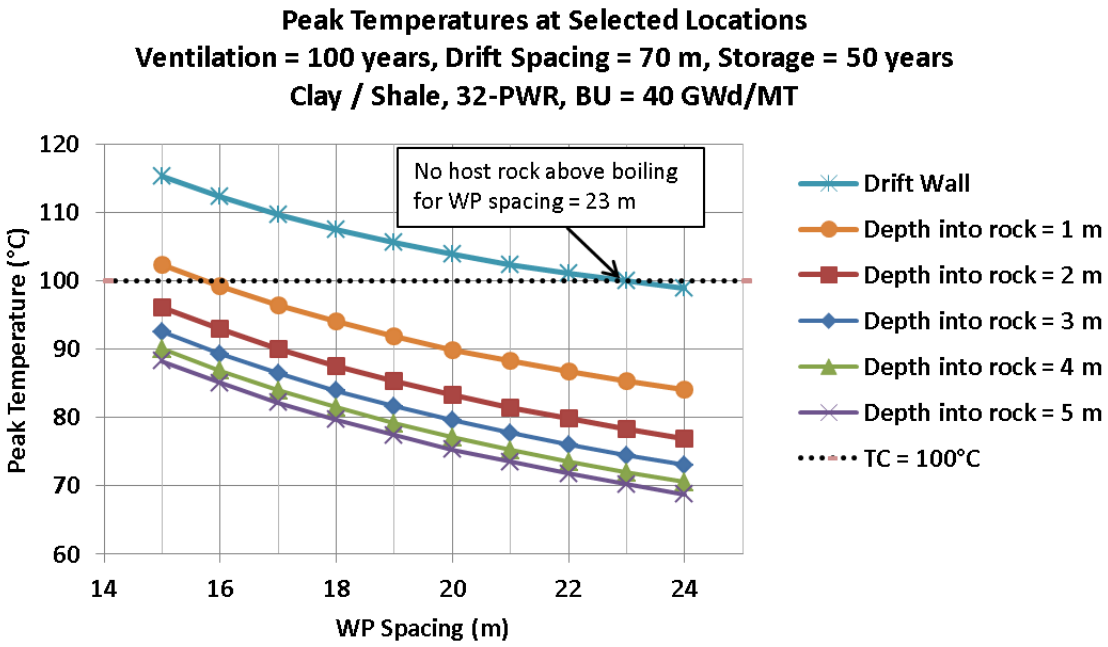

Figure 3-2. Peak temperature vs. package spacing for values of depth into the rock (32-PWR size packages, 40 GW-d/MT burnup)

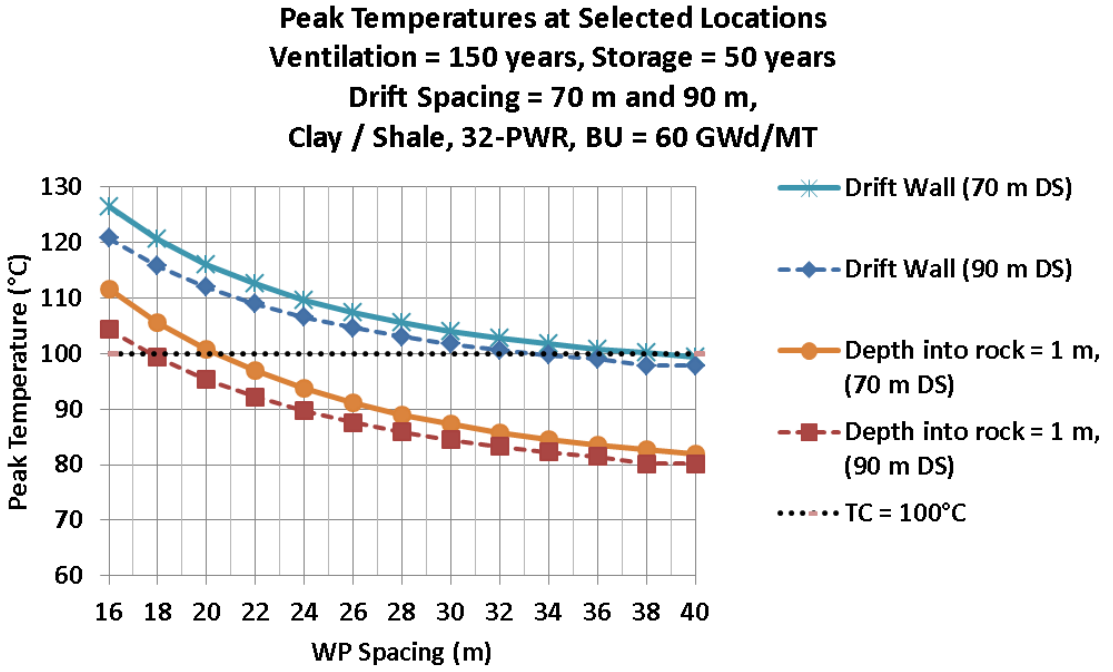

Figure 3-3. Peak temperature vs. package spacing for values of depth into the rock (32-PWR size packages, 60 GW-d/MT burnup, 90 m drift spacing)

Another look at the same calculations is provided in Tables 3-4 and 3-5, which present the depth into the drift wall of the 100°C and 120°C peak temperature isotherms for the 40 GW-d/MT burnup case, and the 100°C isotherm for the 60 GW-d/MT burnup case, as a function of ventilation time and waste package spacing. This is a measure of the extent of the host rock that would be affected by temperatures above the target. The table also indicates that package spacing of 23 m would ensure the peak drift wall temperature is at or below 100°C.

Table 3-4. Depth into the drift wall for which peak temperature equals the target value (40 GW-d/MT)

	Package Spacing (m) [B]				
	16	**18**	**20**	**22**	**24**
Ventilation Time (yr) [A]	**Depth (into drift wall) to Meet T=100°C**				
100	0.9	0.6	0.3	0.1	0.0
75	1.5	0.9	0.7	0.5	0.4
50	2.2	1.7	1.3	1.1	0.9
25	3.6	2.8	2.3	1.9	1.8
	Depth (into drift wall) to Meet T=120°C				
100	0.0	0.0	0.0	0.0	0.0
75	0.0	0.0	0.0	0.0	0.0
50	0.7	0.4	0.3	0.1	0.0
25	1.6	1.2	1.0	0.8	0.8
[A] After 50 years decay storage. [B] Drift spacing 70 m; SNF burnup 40 GW-d/MT.					

Table 3-5. Depth into the drift wall for which peak temperature equals the target value (60 GW-d/MT)

	Package Spacing (m) [B]						
	26	**28**	**30**	**32**	**34**	**36**	**38**
Ventilation Time (yr) and Drift Spacing (m) [A]	**Depth (into drift wall) to Meet T=100°C**						
150 yr / 90 m	0.27	0.18	0.10	0.04	0.00	0.00	0.00
150 yr / 70 m	0.46	0.34	0.24	0.17	0.10	0.05	0.01
[A] After 50 years decay storage. [B] SNF burnup 60 GW-d/MT.							

3.1.4 Summary of Parameter Studies for Sedimentary Open-Mode Concepts

Section 3.1.1 analyzed the thermal performance for 12-PWR, 21-PWR, and 32-PWR size waste packages with moderate SNF burnup of (40 GW-d/MT). The results show that even a 32-PWR size waste package can be emplaced with fewer than 150 years of ventilation if the temperature target is imposed at the drift wall (and not in buffer or backfill material). Section 3.1.2 extended the analysis to larger waste package and drift spacings, with similar results. Section 3.1.3 provided new information on thermal gradients into the host rock, and determined spacing requirements to keep the host rock temperature below 100°C. These studies also show that allowing slightly higher peak host rock temperature targets can significantly reduce the repository layout. Similar conclusions were reached in thermal analysis for disposal of dual-purpose canisters (Hardin and Voegele 2013). The allowable thermal exposure for potential argillaceous host media is an area of ongoing research in the UFD program.

3.2 Package Power Limit Calculations for Open-Mode Concepts

Logistical simulation of used nuclear fuel (UNF) management in the U.S. combines storage, transportation and disposal elements to evaluate schedule, cost and other resources needed for all major operations leading to final geologic disposal. In such simulations, disposal of UNF is controlled (at least in part) by imposing emplacement thermal power limits, in order to meet limits on peak temperature for key engineered and natural barrier components. These package power limits are used in software models such as CALVIN (Nutt et al. 2012) as threshold requirements that must be met by means of decay storage or SNF blending in waste packages, before emplacement in a repository.

Enclosed and open mode disposal concepts were described and analyzed previously (Hardin et al. 2012) and are tabulated above (Table 2-1). This section develops emplacement thermal power limit estimates for open-mode disposal concepts, for use in logistical simulations. The approach is to simulate peak temperature for a range of waste package sizes, spent nuclear fuel (SNF) burnups, and repository spacings, then correlate peak temperature with emplacement power. The approach works for a range of waste package sizes because peak temperature depends to first order on the package thermal power and not the diameter. Peak temperature occurs within only a few years after emplacement for these concepts, so it is strongly correlated with power at emplacement. The emplacement power limit is defined by where the correlation line intercepts the temperature target, and statistical analysis is used to account for scatter in the results used to generate the fit. The analysis is repeated for each disposal concept, with drift spacing fixed at 70 m (from Hardin et al. 2012), and waste package spacing fixed at 10 m or 20 m.

3.2.1 Analysis Method and Results

For this study the open modes were simplified according to sedimentary or hard rock, and backfilled or unbackfilled (remains open after closure, at least through the period of peak temperature). Thermal properties assumed for sedimentary and hard rock concepts are summarized in Table 3-6.

Table 3-6. Thermal properties for geologic settings

Setting	Thermal Conductivity (W/m-K)	Thermal Diffusivity (m^2/sec)
Sedimentary	1.75	6.45E-7
Hard Rock	2.5	1.13E-6

For each open-mode disposal concept the duration of surface decay storage and repository ventilation must be specified, and for this study the following timing cases are presented:

- **10/40/10 Case** – Ten years of surface decay storage, 40 years of repository ventilation, and 10 years (unventilated, but unbackfilled) for closure operations prior to final closure.
- **10/90/10 Case** – Ten years of surface decay storage, 90 years of repository ventilation, and 10 years (unventilated, but unbackfilled) for closure operations prior to final closure.
- **50/100/10 Case** – Fifty years of surface decay storage, 100 years of repository ventilation, and 10 years (unventilated, but unbackfilled) for closure operations prior to final closure. This case corresponds to the longest durations of decay storage and

ventilation prior to closure, that are being considered in an ongoing evaluation of direct disposal of dual-purpose canisters (Miller et al. 2012).

- **50/150/10 Case** – Fifty years of surface decay storage, 150 years of repository ventilation, and 10 years (unventilated, but unbackfilled) for closure operations prior to final closure.
- **100/200/10 Case** – One hundred years of surface decay storage, 200 years of repository ventilation, and 10 years (unventilated, but unbackfilled) for closure operations prior to final closure.

The 10-year repository closure operations period included with each case would be used for construction of plugs and seals, removal of any items or materials, backfilling of non-emplacement areas, and backfilling of emplacement openings or access drifts as required.

Thermal history simulations are conducted for each timing case, for three fuel burnup characteristics, and four waste package sizes. Heat generation by SNF with 20, 40 and 60 GW-d/MTHM burnup was produced from isotopic calculations (based on Carter et al. 2012). Waste dimensions were taken from Hardin et al. (2012) and are described in terms of how many PWR assemblies they contain (i.e., 4-PWR, 12-PWR, 21-PWR and 32-PWR sizes).

Thermal analysis was conducted by superposing analytical solutions for thermal conduction in an infinite medium around a finite line source (representing the central package), point sources (adjacent packages in the same drift or alignment), and line sources (adjacent drifts or alignments). The approach is described elsewhere (Hardin et al. 2012, Section 3 and Appendix A). For air gaps a gray-body, thermal radiation solution for concentric surfaces is used (Hardin 2013). Radii and thermal conductivity values for the annular layers representing the EBS, emissivity values used for thermal radiation calculations, and ventilation heat removal efficiency are summarized in Table 3-7.

Thermal calculations were performed to investigate the sensitivity of peak drift wall temperature to drift spacing, for 21-PWR and 32-PWR size waste packages in a sedimentary unbackfilled repository. A spacing value of 70 m is selected because it incorporates much of the peak temperature reduction possible using drift spacing (Hardin et al. 2012). The characteristic time for a given temperature rise in diffusive systems is proportional to the square of the distance from a heat source, but the decreasing SNF heat output in repository analyses overwhelms the effect from distance, after decay of short-lived fission products that generate most of the heat in the first hundred years. Note that drift spacing has a greater effect in later time (e.g., after 300 years) when the entire repository heats up and the contribution from adjacent drifts dominates contributions from the package itself, or adjacent packages in the same drift.

Waste package spacing is more effective than drift diameter at lowering peak EBS temperatures outside the waste package, and slightly more effective than drift spacing. Hence two values of waste package spacing are used in this study (Table 3-7). The two values 10 m and 20 m represent a reasonably achievable range; spacings smaller than 10 m could significantly increase peak temperatures, while spacings greater than 20 m could greatly increase the repository layout.

Table 3-7. Geometrical and emissivity parameters

Concept	Drift Diameter (m)	Drift Spacing (m)	Package Spacing (m)	Backfill Thermal Cond. (W/m-K)	Package Emissivity	Wall Emissivity	Preclosure Ventilation Efficiency
Sedimentary Unbackfilled	4.5	70	10 & 20	–	0.6	0.9	75%
Sedimentary Backfilled	4.5	70	10 & 20	0.6	–	–	75%
Hard rock Unbackfilled	5.5	70	10 & 20	–	0.8	0.9	75%
Hard rock Backfilled	5.5	70	20	0.6	–	–	75%

Once temperature histories were obtained for each run, selecting disposal concept, timing case, SNF burnup, and package size, a statistical procedure was used to evaluate the correlation of peak temperature (drift wall, or waste package for backfilled concepts) with waste package power at emplacement. The procedure also includes confidence interval analysis to estimate the maximum package power at emplacement consistent with meeting prescribed temperature limits. For the sedimentary concepts (unbackfilled or backfilled) a limit of 100°C was assigned (protecting the host rock, or the backfill and host rock, respectively). For the hard rock unbackfilled concept a wall temperature limit of 200°C is used, and for the hard rock backfilled concept a package temperature of 100°C. These limits are reasonably consistent with current international practice and previous work in the U.S. (Hardin et al. 2012), although they could be modified in the future based on findings from ongoing research, which may include site-specific information.

Correlation plots were generated for each disposal concept and timing case, combining burnup and package size data (Figures 3-4 through 3-9). Correlation is generally good, and could be improved using package power at repository closure instead of waste emplacement, because less time would intervene until peak temperature. However, package power limits at closure are inconsistent with use of the results with the CALVIN simulation tool (Nutt et al. 2012).

A confidence interval analysis was used for each concept and timing case (i.e., for each correlation plot) to estimate the maximum package power at emplacement, to achieve the assigned temperature limit. The procedure is based on the t-statistic (Bowker and Lieberman 1972, Section 9.9). According to this source, a confidence interval for the value of package power p corresponding to a given (limit) value of temperature T, say T', with confidence level 1-α, is given approximately by

$$Interval \approx \frac{T'}{b} \pm \frac{t_{\alpha/2;\,n-1} S_{T/p}}{b} \sqrt{1 + \frac{\left(T'/b\right)^2}{\sum_{i=1}^{n} p_i^2}} \tag{3-1}$$

$$b = \frac{\sum_{i=1}^{n} p_i T_i}{\sum_{i=1}^{n} p_i^2} \tag{3-2}$$

$$S_{T/P} = \sqrt{\frac{\sum_{i=1}^{n} T_i^2 - \left(\left(\sum_{i=1}^{n} p_i T_i \right)^2 \Big/ \sum_{i=1}^{n} p_i^2 \right)}{n-1}} \tag{3-3}$$

where $t_{\alpha/2;\, n-1}$ is the $\alpha/2$ percentage point of the t-distribution for n-1 degrees of freedom, and n is the number of observations (p_i ,T_i). Thus, the maximum power is at the lower limit of this interval:

$$p_{max} \approx \frac{T'}{b} - \frac{t_{\alpha/2;\, n-1} S_{T/p}}{b} \sqrt{1 + \frac{(T'/b)^2}{\sum_{i=1}^{n} p_i^2}} \tag{3-4}$$

which is used in the compilation of confidence interval data for all concepts and timing cases. Correlation plots for each concept are presented as follows:

- **Sedimentary Unbackfilled (10 m Drift Spacing)** – Correlation plot (Figure 3-4) and peak wall and package temperature summary (Table 3-8).
- **Sedimentary Unbackfilled (20 m Drift Spacing)** – Correlation plot (Figure 3-5) and peak wall and package temperature summary (Table 3-9).
- **Sedimentary Backfilled (20 m Drift Spacing)** – Correlation plot (Figure 3-6) and peak wall and package temperature summary (Table 3-10).
- **Hard rock Unbackfilled (10 m Drift Spacing)** – Correlation plot (Figure 3-7) and peak wall and package temperature summary (Table 3-11).
- **Hard rock Unbackfilled (20 m Drift Spacing)** – Correlation plot (Figure 3-8) and peak wall and package temperature summary (Table 3-12).
- **Hard rock Backfilled (20 m Drift Spacing)** – Correlation plot (Figure 3-7) and peak wall and package temperature summary (Table 3-13).

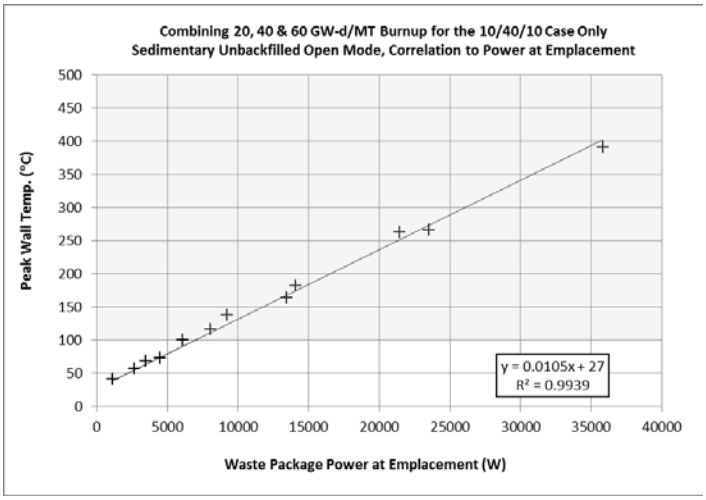

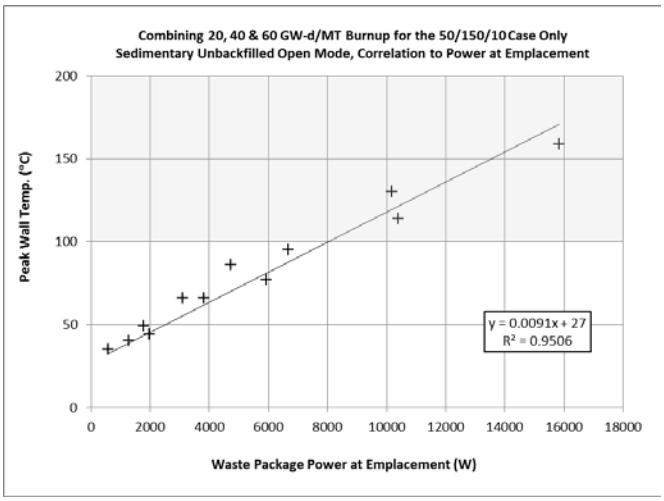

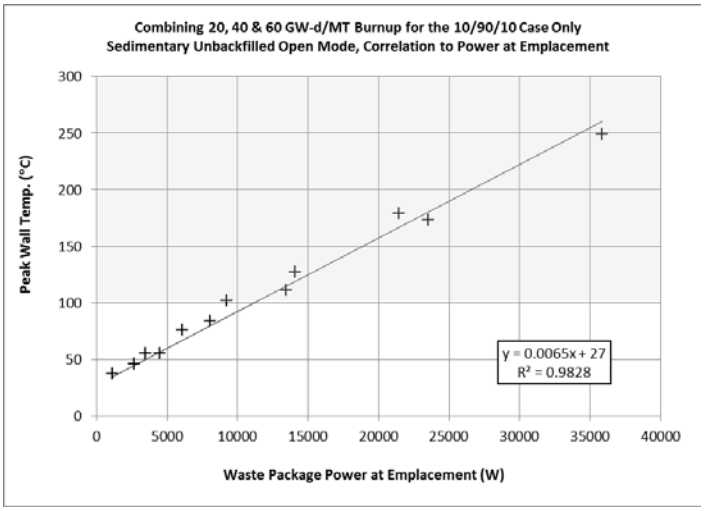

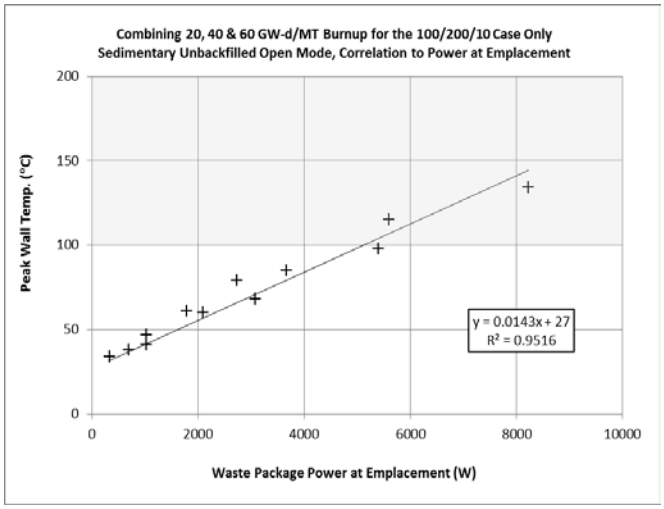

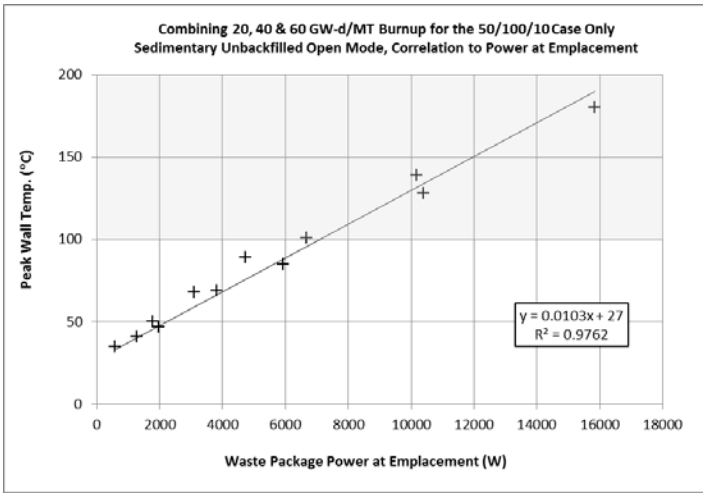

Figure 3-4. Correlation plots for the sedimentary unbackfilled open mode with 10 m drift spacing (timing cases as indicated).

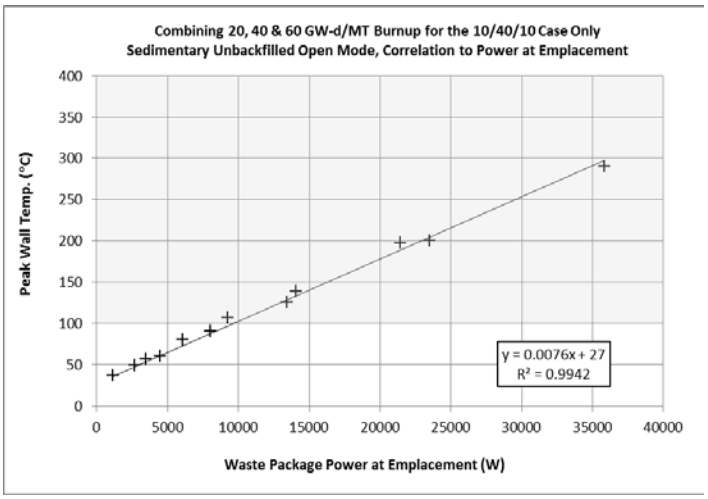

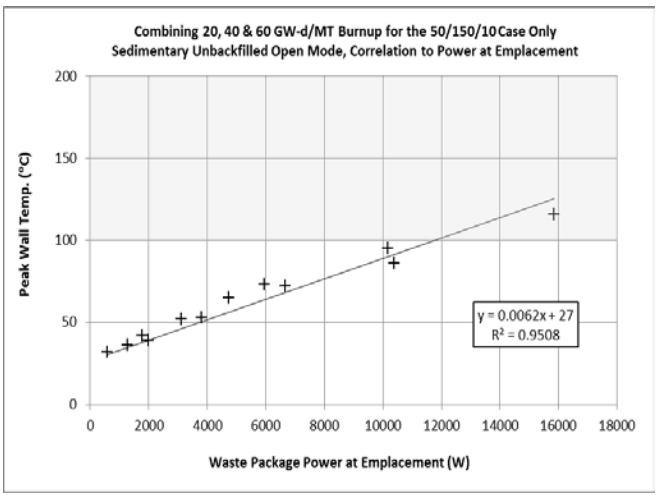

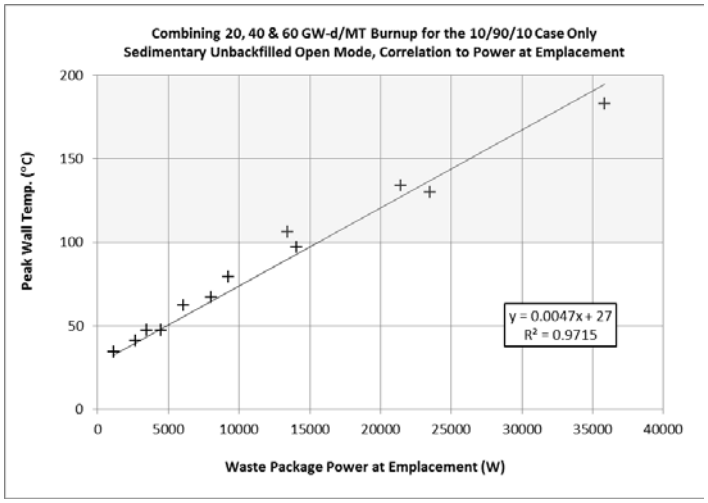

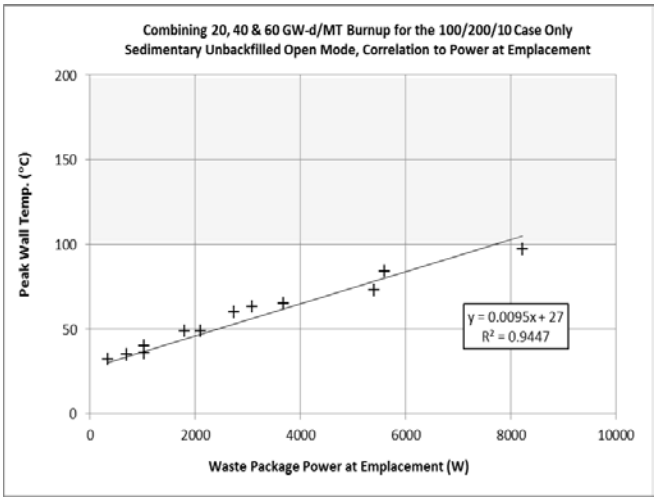

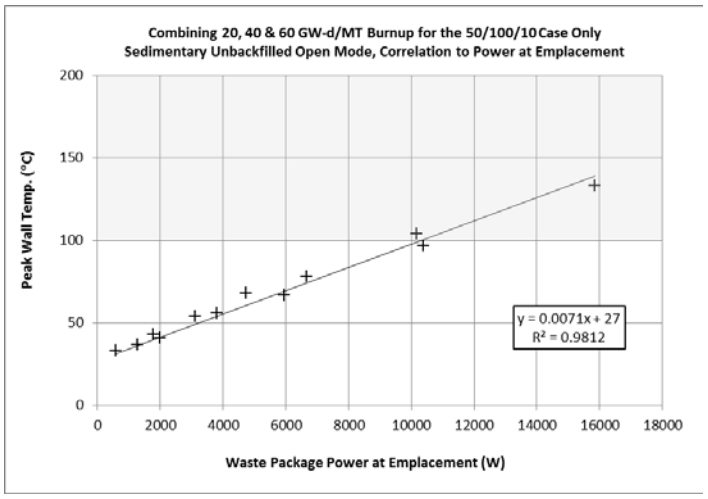

Figure 3-5. Correlation plots for the sedimentary unbackfilled open mode with 20 m drift spacing (timing cases as indicated).

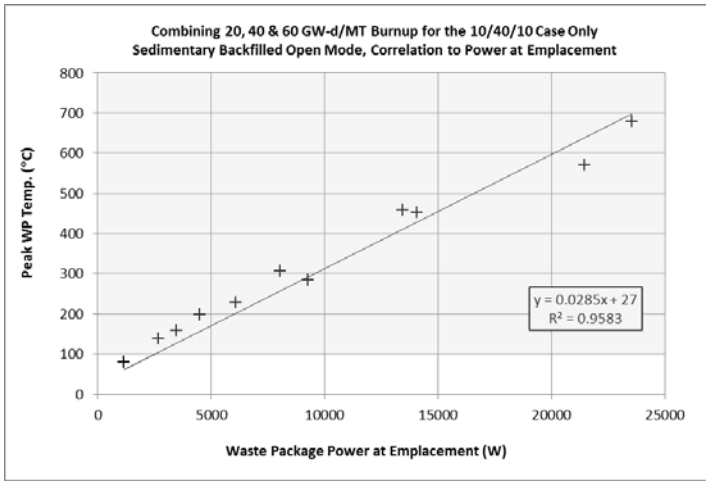

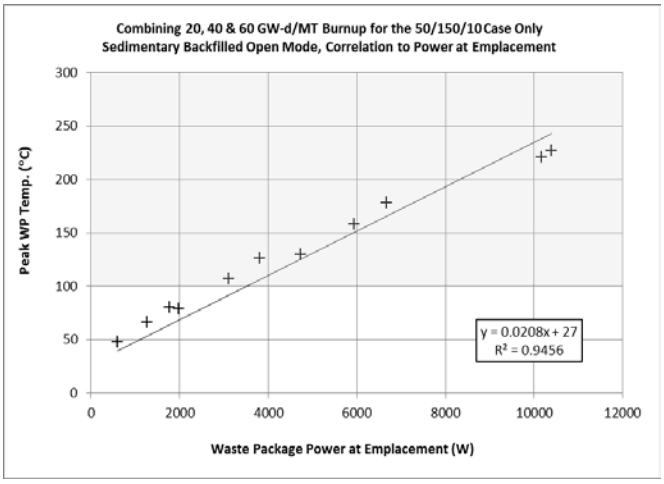

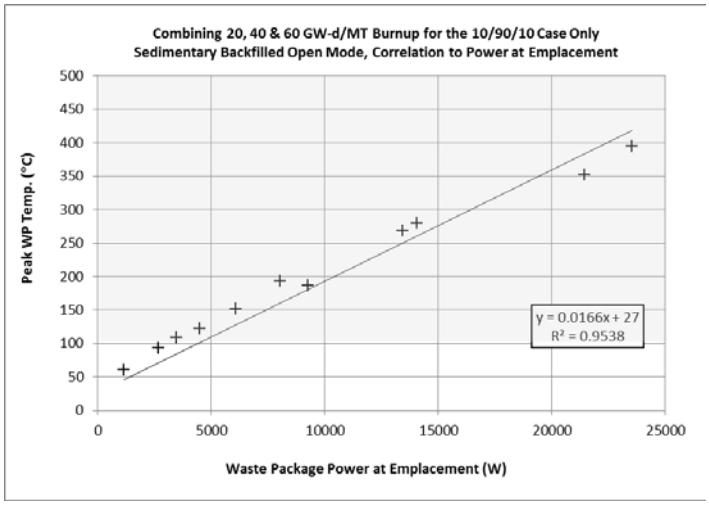

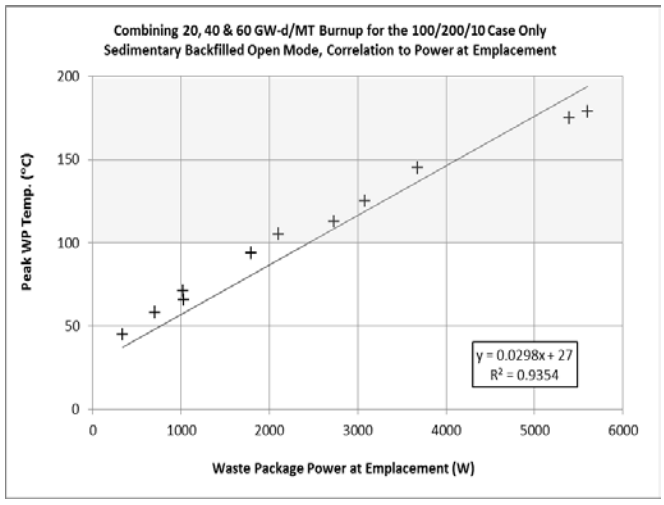

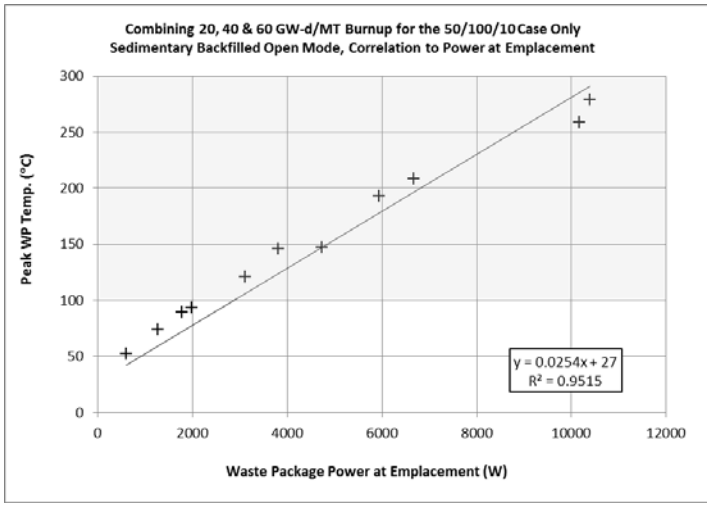

Figure 3-6. Correlation plots for the sedimentary backfilled open mode with 20 m drift spacing (timing cases as indicated).

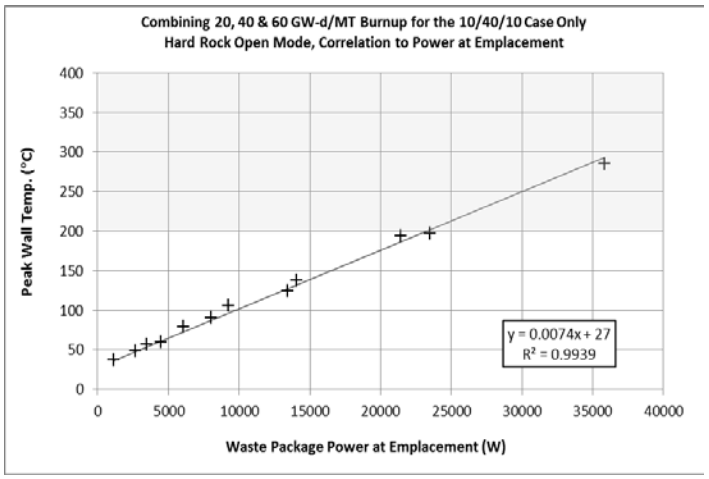

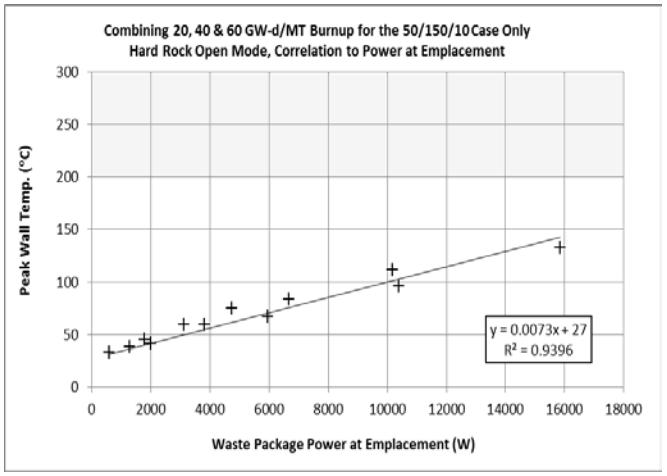

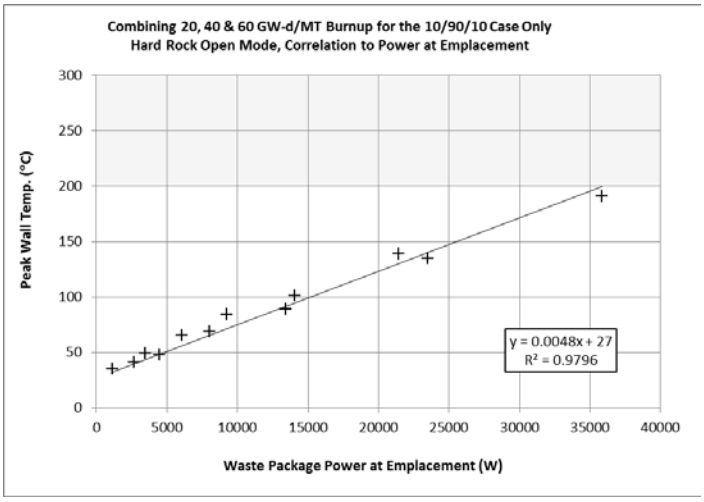

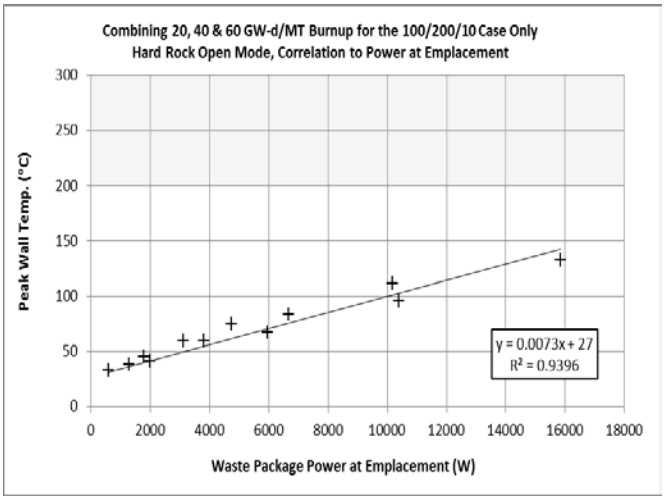

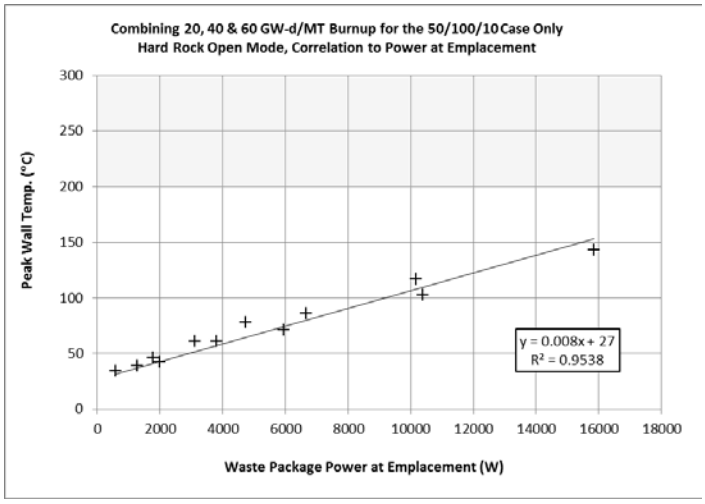

Figure 3-7. Correlation plots for the hard rock unbackfilled open mode with 10 m drift spacing (timing cases as indicated).

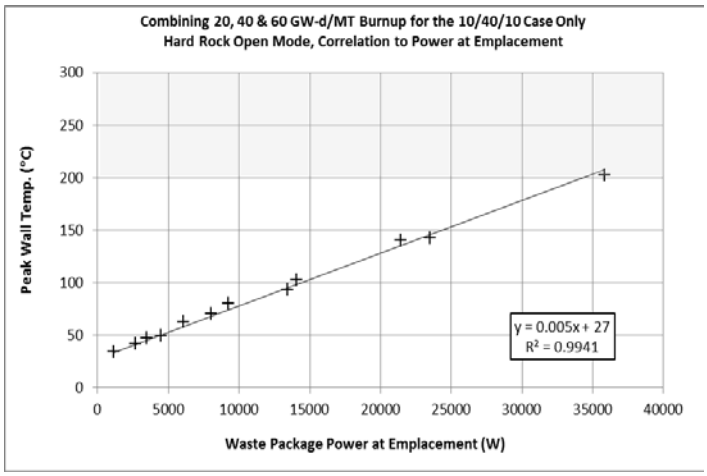

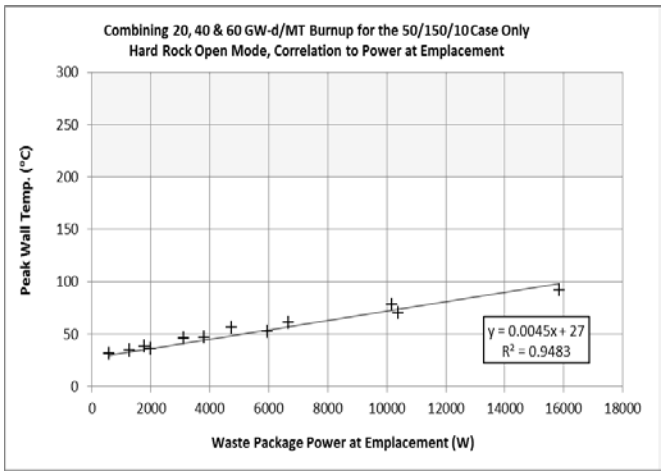

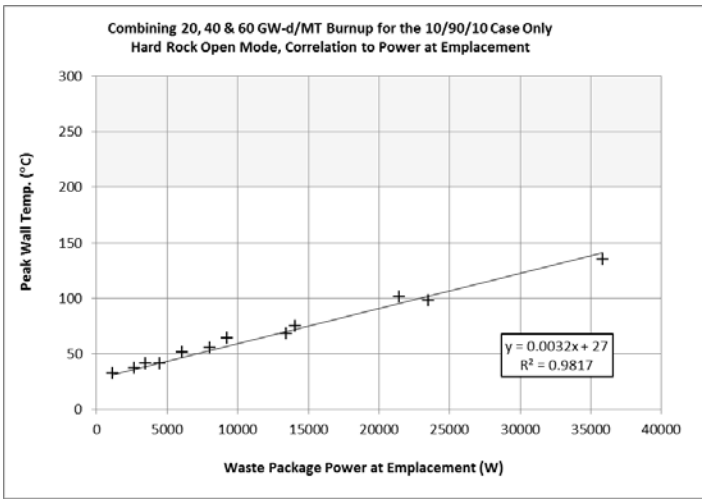

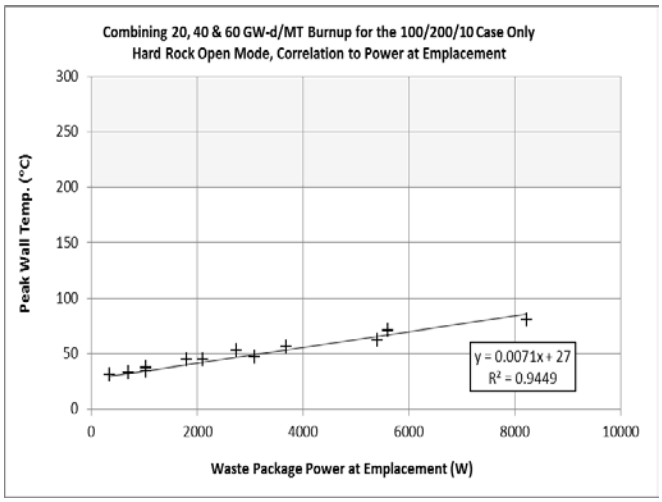

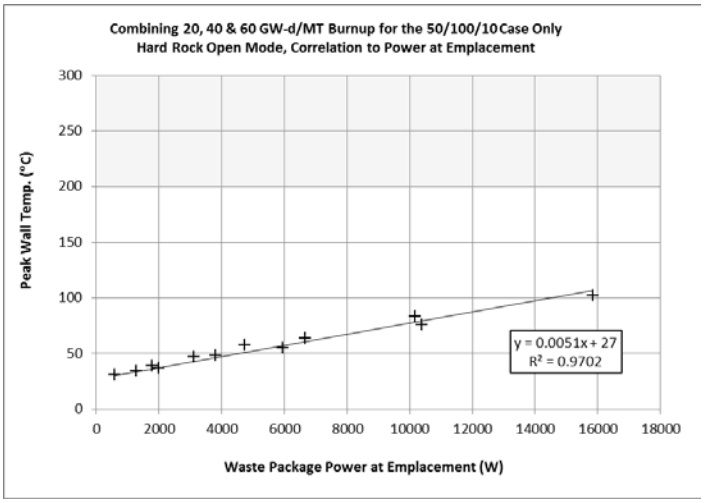

Figure 3-8. Correlation plots for the hard rock unbackfilled open mode with 20 m drift spacing (timing cases as indicated).

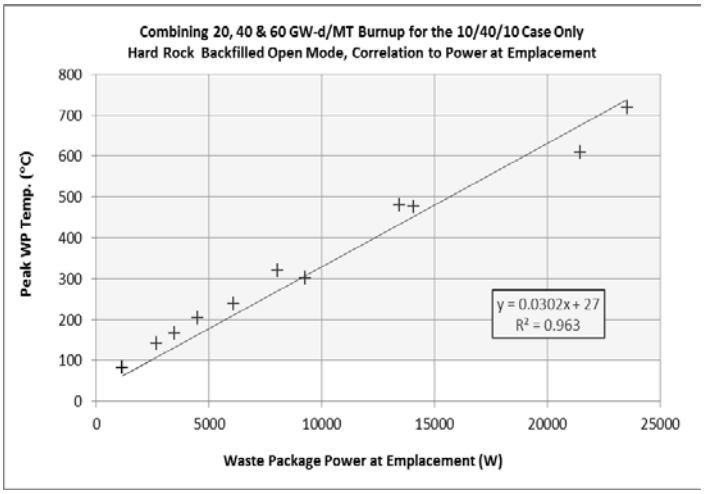

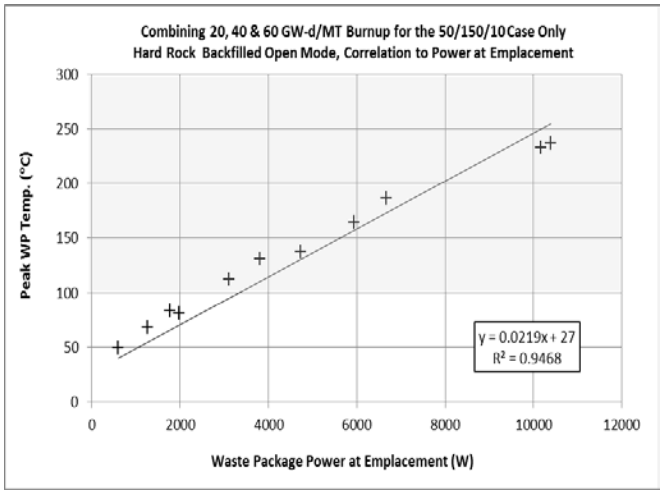

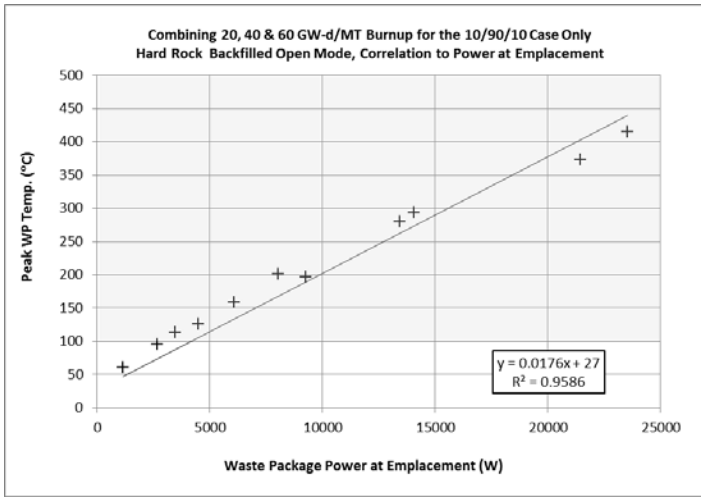

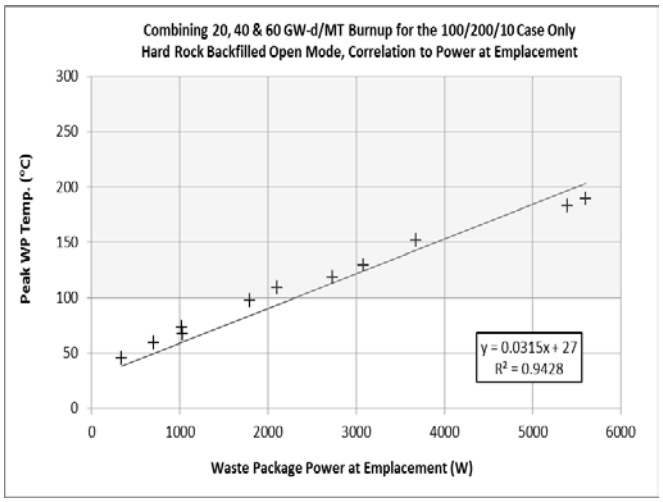

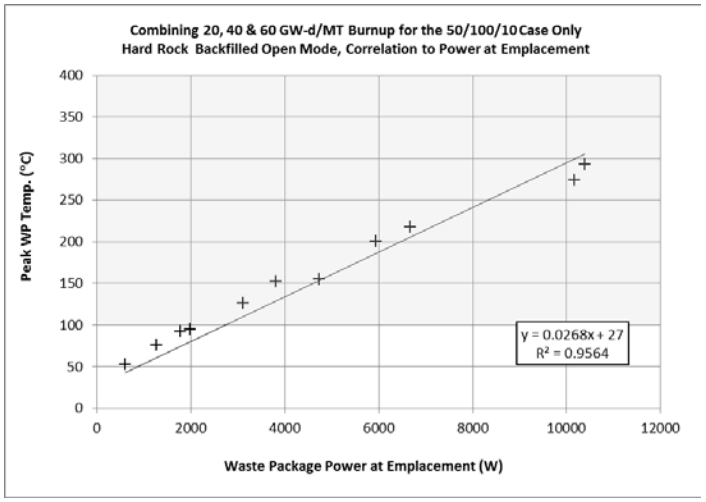

Figure 3-9. Correlation plots for the hard rock backfilled open mode with 20 m drift spacing (timing cases as indicated).

Table 3-8. Peak wall and package temperature results for the sedimentary open unbackfilled (10 m package spacing) concept.

UOX20, Clay, 70-m drift spacing, unbackfilled (assume drifts stay open)

	~50 yr (store/vent/close = 10/40/10 total=60 yr)					~100 yr (store/vent/close = 10/90/10 total=110 yr)					~150 yr (store/vent/close = 50/100/10 total=160 yr)					~200 yr (store/vent/close = 50/150/10 total=210 yr)					~300 yr (store/vent/close = 100/200/10 total=310 yr)				
	Peak Wall T	Time of Peak	Power at Empl.	Power at Closure	Power at Peak T	Peak Wall T	Time of Peak	Power at Empl.	Power at Closure	Power at Peak T	Peak Wall T	Time of Peak	Power at Empl.	Power at Closure	Power at Peak T	Peak Wall T	Time of Peak	Power at Empl.	Power at Closure	Power at Peak T	Peak Wall T	Time of Peak	Power at Empl.	Power at Closure	Power at Peak T
WP size	(°C)	(yr OoR)	(W)	(W)	(W)	(°C)	(yr OoR)	(W)	(W)	(W)	(°C)	(yr OoR)	(W)	(W)	(W)	(°C)	(yr OoR)	(W)	(W)	(W)	(°C)	(yr OoR)	(W)	(W)	(W)
4	41	63	1156	520	501	37	123	1156	319	289	35	421	592	238	142	35	498	592	202	128	34	628	341	164	110
12	69	63	3468	1560	1502	55	123	3468	956	866	50	419	1776	715	427	49	498	1776	606	385	47	628	1024	492	330
21	100	63	6069	2730	2628	76	123	6069	1674	1516	68	419	3108	1252	747	66	498	3108	1061	674	61	628	1791	861	577
32	138	63	9248	4160	4005	102	125	9248	2550	2282	89	419	4736	1907	1138	86	498	4736	1616	1027	79	628	2730	1312	879
	Peak WP T	Time of Peak	Power at Empl.	Power at Closure	Power at Peak T	Peak WP T	Time of Peak	Power at Empl.	Power at Closure	Power at Peak T	Peak WP T	Time of Peak	Power at Empl.	Power at Closure	Power at Peak T	Peak WP T	Time of Peak	Power at Empl.	Power at Closure	Power at Peak T	Peak WP T	Time of Peak	Power at Empl.	Power at Closure	Power at Peak T
WP size	(°C)	(yr OoR)	(W)	(W)	(W)	(°C)	(yr OoR)	(W)	(W)	(W)	(°C)	(yr OoR)	(W)	(W)	(W)	(°C)	(yr OoR)	(W)	(W)	(W)	(°C)	(yr OoR)	(W)	(W)	(W)
4	49	58	1156	520	534	42	113	1156	319	308	38	177	592	238	222	37	288	592	202	172	36	432	341	164	140
12	82	59	3468	1560	1580	64	115	3468	956	913	56	190	1776	715	639	54	380	1776	606	450	50	482	1024	492	393
21	114	61	6069	2730	2695	86	117	6069	1674	1576	73	241	3108	1252	986	71	380	3108	1061	788	65	532	1791	861	646
32	150	62	9248	4160	4056	112	119	9248	2550	2370	94	314	4736	1907	1321	91	415	4736	1616	1144	83	585	2730	1312	925

UOX40, Clay, 70-m drift spacing, unbackfilled (assume drifts stay open)

	~50 yr (store/vent/close = 10/40/10 total=60 yr)					~100 yr (store/vent/close = 10/90/10 total=110 yr)					~150 yr (store/vent/close = 50/100/10 total=160 yr)					~200 yr (store/vent/close = 50/150/10 total=210 yr)					~300 yr (store/vent/close = 100/200/10 total=310 yr)				
	Peak Wall T	Time of Peak	Power at Empl.	Power at Closure	Power at Peak T	Peak Wall T	Time of Peak	Power at Empl.	Power at Closure	Power at Peak T	Peak Wall T	Time of Peak	Power at Empl.	Power at Closure	Power at Peak T	Peak Wall T	Time of Peak	Power at Empl.	Power at Closure	Power at Peak T	Peak Wall T	Time of Peak	Power at Empl.	Power at Closure	Power at Peak T
WP size	(°C)	(yr OoR)	(W)	(W)	(W)	(°C)	(yr OoR)	(W)	(W)	(W)	(°C)	(yr OoR)	(W)	(W)	(W)	(°C)	(yr OoR)	(W)	(W)	(W)	(°C)	(yr OoR)	(W)	(W)	(W)
4	57	62	2680	1104	1074	46	119	2680	648	594	41	216	1272	462	370	40	380	1272	378	261	38	628	700	296	186
12	116	62	8040	3312	3223	84	119	8040	1944	1783	69	216	3816	1385	1111	66	380	3816	1134	784	60	628	2100	889	557
21	182	62	14070	5796	5639	127	119	14070	3402	3121	101	216	6678	2423	1944	95	380	6678	1985	1372	85	628	3675	1556	974
32	263	62	21440	8832	8593	179	119	21440	5184	4755	139	216	10176	3693	2962	130	380	10176	3024	2091	115	628	5600	2371	1485
	Peak WP T	Time of Peak	Power at Empl.	Power at Closure	Power at Peak T	Peak WP T	Time of Peak	Power at Empl.	Power at Closure	Power at Peak T	Peak WP T	Time of Peak	Power at Empl.	Power at Closure	Power at Peak T	Peak WP T	Time of Peak	Power at Empl.	Power at Closure	Power at Peak T	Peak WP T	Time of Peak	Power at Empl.	Power at Closure	Power at Peak T
WP size	(°C)	(yr OoR)	(W)	(W)	(W)	(°C)	(yr OoR)	(W)	(W)	(W)	(°C)	(yr OoR)	(W)	(W)	(W)	(°C)	(yr OoR)	(W)	(W)	(W)	(°C)	(yr OoR)	(W)	(W)	(W)
4	71	58	2680	1104	1135	55	111	2680	648	635	48	171	1272	462	436	45	236	1272	378	350	42	406	700	296	251
12	134	60	8040	3312	3312	98	113	8040	1944	1872	79	177	3816	1385	1273	74	270	3816	1134	965	66	454	2100	889	700
21	198	61	14070	5796	5717	140	115	14070	3402	3222	111	190	6678	2423	2120	103	304	6678	1985	1571	92	489	3675	1556	1166
32	275	61	21440	8832	8711	190	117	21440	5184	4831	148	201	10176	3693	3110	137	340	10176	3024	2237	121	544	5600	2371	1650

UOX60, Clay, 70-m drift spacing, unbackfilled (assume drifts stay open)

	~50 yr (store/vent/close = 10/40/10 total=60 yr)					~100 yr (store/vent/close = 10/90/10 total=110 yr)					~150 yr (store/vent/close = 50/100/10 total=160 yr)					~200 yr (store/vent/close = 50/150/10 total=210 yr)					~300 yr (store/vent/close = 100/200/10 total=310 yr)				
	Peak Wall T	Time of Peak	Power at Empl.	Power at Closure	Power at Peak T	Peak Wall T	Time of Peak	Power at Empl.	Power at Closure	Power at Peak T	Peak Wall T	Time of Peak	Power at Empl.	Power at Closure	Power at Peak T	Peak Wall T	Time of Peak	Power at Empl.	Power at Closure	Power at Peak T	Peak Wall T	Time of Peak	Power at Empl.	Power at Closure	Power at Peak T
WP size	(°C)	(yr OoR)	(W)	(W)	(W)	(°C)	(yr OoR)	(W)	(W)	(W)	(°C)	(yr OoR)	(W)	(W)	(W)	(°C)	(yr OoR)	(W)	(W)	(W)	(°C)	(yr OoR)	(W)	(W)	(W)
4	73	61	4480	1696	1671	55	117	4480	944	873	47	181	1980	643	570	44	277	1980	500	403	41	628	1028	371	222
12	164	61	13440	5088	5013	111	117	13440	2832	2618	85	181	5940	1930	1709	77	277	5940	1500	1209	68	629	3084	1114	666
21	266	61	23520	8904	8773	173	117	23520	4956	4582	128	181	10395	3377	2991	114	277	10395	2625	2116	98	629	5397	1949	1166
32	391	61	35840	13568	13370	249	117	35840	7552	6982	180	181	15840	5146	4558	159	277	15840	4000	3225	134	629	8224	2970	1777
	Peak WP T	Time of Peak	Power at Empl.	Power at Closure	Power at Peak T	Peak WP T	Time of Peak	Power at Empl.	Power at Closure	Power at Peak T	Peak WP T	Time of Peak	Power at Empl.	Power at Closure	Power at Peak T	Peak WP T	Time of Peak	Power at Empl.	Power at Closure	Power at Peak T	Peak WP T	Time of Peak	Power at Empl.	Power at Closure	Power at Peak T
WP size	(°C)	(yr OoR)	(W)	(W)	(W)	(°C)	(yr OoR)	(W)	(W)	(W)	(°C)	(yr OoR)	(W)	(W)	(W)	(°C)	(yr OoR)	(W)	(W)	(W)	(°C)	(yr OoR)	(W)	(W)	(W)
4	91	57	4480	1696	1775	67	111	4480	944	921	55	166	1980	643	618	50	226	1980	500	470	45	366	1028	371	328
12	184	59	13440	5088	5165	126	113	13440	2832	2714	98	171	5940	1930	1802	87	239	5940	1500	1353	75	410	3084	1114	907
21	281	61	23520	8904	8773	187	115	23520	4956	4664	140	177	10395	3377	3055	124	251	10395	2625	2282	105	496	5397	1949	1386
32	401	61	35840	13568	13370	260	115	35840	7552	7107	191	177	15840	5146	4654	168	262	15840	4000	3366	141	496	8224	2970	2111

Table 3-9. Peak wall and package temperature results for the sedimentary open unbackfilled (20 m package spacing) concept.

UOX20, Clay, 70-m drift spacing, unbackfilled (assume drifts stay open)

	~50 yr (store/vent/close = 10/40/10 total=60 yr)					~100 yr (store/vent/close = 10/90/10 total=110 yr)					~150 yr (store/vent/close = 50/100/10 total=160 yr)					~200 yr (store/vent/close = 50/150/10 total=210 yr)					~300 yr (store/vent/close = 100/200/10 total=310 yr)				
	Peak Wall T	Time of Peak	Power at Empl.	Power at Closure	Power at Peak T	Peak Wall T	Time of Peak	Power at Empl.	Power at Closure	Power at Peak T	Peak Wall T	Time of Peak	Power at Empl.	Power at Closure	Power at Peak T	Peak Wall T	Time of Peak	Power at Empl.	Power at Closure	Power at Peak T	Peak Wall T	Time of Peak	Power at Empl.	Power at Closure	Power at Peak T
WP size	(°C)	(yr OoR)	(W)	(W)	(W)	(°C)	(yr OoR)	(W)	(W)	(W)	(°C)	(yr OoR)	(W)	(W)	(W)	(°C)	(yr OoR)	(W)	(W)	(W)	(°C)	(yr OoR)	(W)	(W)	(W)
4	37	59	1156	520	527	34	115	1156	319	304	33	241	592	238	188	32	380	592	202	150	32	515	341	164	126
12	57	59	3468	1560	1580	47	116	3468	956	907	43	244	1776	715	560	42	380	1776	606	450	40	532	1024	492	369
21	80	59	6069	2730	2765	62	116	6069	1674	1587	54	257	3108	1252	955	52	380	3108	1061	788	49	532	1791	861	646
32	107	59	9248	4160	4214	79	116	9248	2550	2418	68	257	4736	1907	1455	65	380	4736	1616	1200	60	532	2730	1312	985
	Peak WP T	Time of Peak	Power at Empl.	Power at Closure	Power at Peak T	Peak WP T	Time of Peak	Power at Empl.	Power at Closure	Power at Peak T	Peak WP T	Time of Peak	Power at Empl.	Power at Closure	Power at Peak T	Peak WP T	Time of Peak	Power at Empl.	Power at Closure	Power at Peak T	Peak WP T	Time of Peak	Power at Empl.	Power at Closure	Power at Peak T
WP size	(°C)	(yr OoR)	(W)	(W)	(W)	(°C)	(yr OoR)	(W)	(W)	(W)	(°C)	(yr OoR)	(W)	(W)	(W)	(°C)	(yr OoR)	(W)	(W)	(W)	(°C)	(yr OoR)	(W)	(W)	(W)
4	46	54	1156	520	562	39	107	1156	319	322	36	164	592	238	233	35	236	592	202	190	34	358	341	164	155
12	72	55	3468	1560	1665	57	108	3468	956	960	50	168	1776	715	689	47	247	1776	606	557	45	387	1024	492	446
21	97	57	6069	2730	2838	73	111	6069	1674	1643	63	172	3108	1252	1189	59	261	3108	1061	948	55	410	1791	861	756
32	124	57	9248	4160	4325	92	111	9248	2550	2503	77	177	4736	1907	1779	72	288	4736	1616	1377	67	423	2730	1312	1132

UOX40, Clay, 70-m drift spacing, unbackfilled (assume drifts stay open)

	~50 yr (store/vent/close = 10/40/10 total=60 yr)					~100 yr (store/vent/close = 10/90/10 total=110 yr)					~150 yr (store/vent/close = 50/100/10 total=160 yr)					~200 yr (store/vent/close = 50/150/10 total=210 yr)					~300 yr (store/vent/close = 100/200/10 total=310 yr)				
	Peak Wall T	Time of Peak	Power at Empl.	Power at Closure	Power at Peak T	Peak Wall T	Time of Peak	Power at Empl.	Power at Closure	Power at Peak T	Peak Wall T	Time of Peak	Power at Empl.	Power at Closure	Power at Peak T	Peak Wall T	Time of Peak	Power at Empl.	Power at Closure	Power at Peak T	Peak Wall T	Time of Peak	Power at Empl.	Power at Closure	Power at Peak T
WP size	(°C)	(yr OoR)	(W)	(W)	(W)	(°C)	(yr OoR)	(W)	(W)	(W)	(°C)	(yr OoR)	(W)	(W)	(W)	(°C)	(yr OoR)	(W)	(W)	(W)	(°C)	(yr OoR)	(W)	(W)	(W)
4	49	58	2680	1104	1135	41	113	2680	648	624	37	190	1272	462	404	36	288	1272	378	309	35	470	700	296	228
12	91	58	8040	3312	3406	67	113	8040	1944	1872	56	187	3816	1385	1225	53	288	3816	1134	927	49	470	2100	889	684
21	139	58	14070	5796	5960	97	113	14070	3402	3276	78	187	6678	2423	2143	72	288	6678	1985	1623	65	470	3675	1556	1198
32	197	58	21440	8832	9082	134	113	21440	5184	4992	104	189	10176	3693	3242	95	288	10176	3024	2473	84	470	5600	2371	1825
	Peak WP T	Time of Peak	Power at Empl.	Power at Closure	Power at Peak T	Peak WP T	Time of Peak	Power at Empl.	Power at Closure	Power at Peak T	Peak WP T	Time of Peak	Power at Empl.	Power at Closure	Power at Peak T	Peak WP T	Time of Peak	Power at Empl.	Power at Closure	Power at Peak T	Peak WP T	Time of Peak	Power at Empl.	Power at Closure	Power at Peak T
WP size	(°C)	(yr OoR)	(W)	(W)	(W)	(°C)	(yr OoR)	(W)	(W)	(W)	(°C)	(yr OoR)	(W)	(W)	(W)	(°C)	(yr OoR)	(W)	(W)	(W)	(°C)	(yr OoR)	(W)	(W)	(W)
4	64	54	2680	1104	1201	50	106	2680	648	663	44	161	1272	462	457	41	220	1272	378	366	39	345	700	296	277
12	114	55	8040	3312	3553	83	108	8040	1944	1953	68	164	3816	1385	1350	63	226	3816	1134	1078	57	370	2100	889	797
21	161	57	14070	5796	6044	115	109	14070	3402	3389	92	168	6678	2423	2318	83	239	6678	1985	1820	74	382	3675	1556	1368
32	216	57	21440	8832	9211	150	111	21440	5184	5076	117	171	10176	3693	3484	107	247	10176	3024	2718	94	410	5600	2371	1994

UOX60, Clay, 70-m drift spacing, unbackfilled (assume drifts stay open)

	~50 yr (store/vent/close = 10/40/10 total=60 yr)					~100 yr (store/vent/close = 10/90/10 total=110 yr)					~150 yr (store/vent/close = 50/100/10 total=160 yr)					~200 yr (store/vent/close = 50/150/10 total=210 yr)					~300 yr (store/vent/close = 100/200/10 total=310 yr)				
	Peak Wall T	Time of Peak	Power at Empl.	Power at Closure	Power at Peak T	Peak Wall T	Time of Peak	Power at Empl.	Power at Closure	Power at Peak T	Peak Wall T	Time of Peak	Power at Empl.	Power at Closure	Power at Peak T	Peak Wall T	Time of Peak	Power at Empl.	Power at Closure	Power at Peak T	Peak Wall T	Time of Peak	Power at Empl.	Power at Closure	Power at Peak T
WP size	(°C)	(yr OoR)	(W)	(W)	(W)	(°C)	(yr OoR)	(W)	(W)	(W)	(°C)	(yr OoR)	(W)	(W)	(W)	(°C)	(yr OoR)	(W)	(W)	(W)	(°C)	(yr OoR)	(W)	(W)	(W)
4	60	58	4480	1696	1748	47	111	4480	944	921	41	172	1980	643	598	39	255	1980	500	430	36	423	1028	371	296
12	126	58	13440	5088	5244	106	108	13440	2832	2844	67	171	5940	1930	1802	73	221	5940	1500	1436	63	337	3084	1114	1044
21	200	58	23520	8904	9187	130	111	23520	4956	4837	97	170	10395	3377	3171	86	249	10395	2625	2296	73	423	5397	1949	1551
32	290	58	35840	13568	13990	183	111	35840	7552	7371	133	170	15840	5146	4832	116	249	15840	4000	3498	97	423	8224	2970	2364
	Peak WP T	Time of Peak	Power at Empl.	Power at Closure	Power at Peak T	Peak WP T	Time of Peak	Power at Empl.	Power at Closure	Power at Peak T	Peak WP T	Time of Peak	Power at Empl.	Power at Closure	Power at Peak T	Peak WP T	Time of Peak	Power at Empl.	Power at Closure	Power at Peak T	Peak WP T	Time of Peak	Power at Empl.	Power at Closure	Power at Peak T
WP size	(°C)	(yr OoR)	(W)	(W)	(W)	(°C)	(yr OoR)	(W)	(W)	(W)	(°C)	(yr OoR)	(W)	(W)	(W)	(°C)	(yr OoR)	(W)	(W)	(W)	(°C)	(yr OoR)	(W)	(W)	(W)
4	82	54	4480	1696	1860	60	106	4480	944	967	50	159	1980	643	643	46	215	1980	500	489	41	337	1028	371	348
12	153	55	13440	5088	5493	86	111	13440	2832	2764	83	162	5940	1930	1895	61	249	5940	1500	1312	54	423	3084	1114	887
21	223	57	23520	8904	9320	149	109	23520	4956	4930	114	164	10395	3377	3279	100	226	10395	2625	2470	84	358	5397	1949	1750
32	307	57	35840	13568	14200	200	110	35840	7552	7441	149	166	15840	5146	4941	129	231	15840	4000	3701	108	374	8224	2970	2584

Table 3-10. Peak wall and package temperature results for the sedimentary open backfilled (20 m package spacing) concept.

UOX20, Clay, 70-m drift spacing, backfilled

	~50 yr (store/vent/close = 10/40/10 total=60 yr)					~100 yr (store/vent/close = 10/90/10 total=110 yr)					~150 yr (store/vent/close = 50/100/10 total=160 yr)					~200 yr (store/vent/close = 50/150/10 total=210 yr)					~300 yr (store/vent/close = 100/200/10 total=310 yr)				
	Peak Wall T	Time of Peak	Power at Empl.	Power at Closure	Power at Peak T	Peak Wall T	Time of Peak	Power at Empl.	Power at Closure	Power at Peak T	Peak Wall T	Time of Peak	Power at Empl.	Power at Closure	Power at Peak T	Peak Wall T	Time of Peak	Power at Empl.	Power at Closure	Power at Peak T	Peak Wall T	Time of Peak	Power at Empl.	Power at Closure	Power at Peak T
WP size	(°C)	(yr OoR)	(W)	(W)	(W)	(°C)	(yr OoR)	(W)	(W)	(W)	(°C)	(yr OoR)	(W)	(W)	(W)	(°C)	(yr OoR)	(W)	(W)	(W)	(°C)	(yr OoR)	(W)	(W)	(W)
4	37	59	1156	520	527	34	115	1156	319	304	33	241	592	238	188	32	280	592	202	150	32	515	341	164	126
12	57	59	3468	1560	1580	47	116	3468	956	907	43	244	1776	715	560	42	380	1776	606	450	40	532	1024	492	369
21	80	59	6069	2730	2765	62	116	6069	1674	1587	54	257	3108	1252	955	52	380	3108	1061	788	49	532	1791	861	646
32	107	59	9248	4160	4214	79	116	9248	2550	2418	68	257	4736	1907	1455	65	380	4736	1616	1200	60	532	2730	1312	985
	Peak WP T	Time of Peak	Power at Empl.	Power at Closure	Power at Peak T	Peak WP T	Time of Peak	Power at Empl.	Power at Closure	Power at Peak T	Peak WP T	Time of Peak	Power at Empl.	Power at Closure	Power at Peak T	Peak WP T	Time of Peak	Power at Empl.	Power at Closure	Power at Peak T	Peak WP T	Time of Peak	Power at Empl.	Power at Closure	Power at Peak T
WP size	(°C)	(yr OoR)	(W)	(W)	(W)	(°C)	(yr OoR)	(W)	(W)	(W)	(°C)	(yr OoR)	(W)	(W)	(W)	(°C)	(yr OoR)	(W)	(W)	(W)	(°C)	(yr OoR)	(W)	(W)	(W)
4	79	61	1156	520	513	60	111	1156	319	313	52	161	592	238	236	48	211	592	202	201	45	312	341	164	166
12	159	61	3468	1560	1540	109	111	3468	956	939	89	161	1776	715	709	80	211	1776	606	603	71	313	1024	492	496
21	227	61	6069	2730	2695	152	111	6069	1674	1643	121	161	3108	1252	1240	107	211	3108	1061	1055	94	317	1791	861	863
32	284	61	9248	4160	4107	187	111	9248	2550	2503	147	161	4736	1907	1889	130	212	4736	1616	1603	113	322	2730	1312	1304

UOX40, Clay, 70-m drift spacing, backfilled

	~50 yr (store/vent/close = 10/40/10 total=60 yr)					~100 yr (store/vent/close = 10/90/10 total=110 yr)					~150 yr (store/vent/close = 50/100/10 total=160 yr)					~200 yr (store/vent/close = 50/150/10 total=210 yr)					~300 yr (store/vent/close = 100/200/10 total=310 yr)				
	Peak Wall T	Time of Peak	Power at Empl.	Power at Closure	Power at Peak T	Peak Wall T	Time of Peak	Power at Empl.	Power at Closure	Power at Peak T	Peak Wall T	Time of Peak	Power at Empl.	Power at Closure	Power at Peak T	Peak Wall T	Time of Peak	Power at Empl.	Power at Closure	Power at Peak T	Peak Wall T	Time of Peak	Power at Empl.	Power at Closure	Power at Peak T
WP size	(°C)	(yr OoR)	(W)	(W)	(W)	(°C)	(yr OoR)	(W)	(W)	(W)	(°C)	(yr OoR)	(W)	(W)	(W)	(°C)	(yr OoR)	(W)	(W)	(W)	(°C)	(yr OoR)	(W)	(W)	(W)
4	49	58	2680	1104	1135	41	113	2680	648	624	37	190	1272	462	404	36	288	1272	378	309	35	470	700	296	228
12	91	58	8040	3312	3406	67	113	8040	1944	1872	56	187	3816	1385	1225	53	288	3816	1134	927	49	470	2100	889	684
21	139	58	14070	5796	5960	97	113	14070	3402	3276	78	187	6678	2423	2143	72	288	6678	1985	1623	65	470	3675	1556	1198
32	197	58	21440	8832	9082	134	113	21440	5184	4992	104	198	10176	3693	3242	95	288	10176	3024	2473	84	470	5600	2371	1825
	Peak WP T	Time of Peak	Power at Empl.	Power at Closure	Power at Peak T	Peak WP T	Time of Peak	Power at Empl.	Power at Closure	Power at Peak T	Peak WP T	Time of Peak	Power at Empl.	Power at Closure	Power at Peak T	Peak WP T	Time of Peak	Power at Empl.	Power at Closure	Power at Peak T	Peak WP T	Time of Peak	Power at Empl.	Power at Closure	Power at Peak T
WP size	(°C)	(yr OoR)	(W)	(W)	(W)	(°C)	(yr OoR)	(W)	(W)	(W)	(°C)	(yr OoR)	(W)	(W)	(W)	(°C)	(yr OoR)	(W)	(W)	(W)	(°C)	(yr OoR)	(W)	(W)	(W)
4	138	61	2680	1104	1089	93	111	2680	648	635	74	161	1272	462	457	66	211	1272	378	376	58	311	700	296	295
12	307	61	8040	3312	3267	193	111	8040	1944	1904	146	161	3816	1385	1370	126	211	3816	1134	1128	105	311	2100	889	885
21	452	61	14070	5796	5717	280	111	14070	3402	3331	208	161	6678	2423	2397	178	211	6678	1985	1975	145	313	3675	1556	1543
32	571	61	21440	8832	8711	352	111	21440	5184	5076	259	161	10176	3693	3653	221	211	10176	3024	3009	179	316	5600	2371	2338

UOX60, Clay, 70-m drift spacing, backfilled

	~50 yr (store/vent/close = 10/40/10 total=60 yr)					~100 yr (store/vent/close = 10/90/10 total=110 yr)					~150 yr (store/vent/close = 50/100/10 total=160 yr)					~200 yr (store/vent/close = 50/150/10 total=210 yr)					~300 yr (store/vent/close = 100/200/10 total=310 yr)				
	Peak Wall T	Time of Peak	Power at Empl.	Power at Closure	Power at Peak T	Peak Wall T	Time of Peak	Power at Empl.	Power at Closure	Power at Peak T	Peak Wall T	Time of Peak	Power at Empl.	Power at Closure	Power at Peak T	Peak Wall T	Time of Peak	Power at Empl.	Power at Closure	Power at Peak T	Peak Wall T	Time of Peak	Power at Empl.	Power at Closure	Power at Peak T
WP size	(°C)	(yr OoR)	(W)	(W)	(W)	(°C)	(yr OoR)	(W)	(W)	(W)	(°C)	(yr OoR)	(W)	(W)	(W)	(°C)	(yr OoR)	(W)	(W)	(W)	(°C)	(yr OoR)	(W)	(W)	(W)
4	60	58	4480	1696	1748	47	111	4480	944	921	41	172	1980	643	598	39	255	1980	500	430	36	423	1028	371	296
12	126	58	13440	5088	5244	86	111	13440	2832	2764	67	171	5940	1930	1802	61	249	5940	1500	1312	54	423	3084	1114	887
21	200	58	23520	8904	9178	130	111	23520	4956	4837	97	170	10395	3377	3171	86	249	10395	2625	2296	73	423	5397	1949	1551
32	290	58	35840	13568	13990	183	111	35840	7552	7371	133	170	15840	5146	4832	116	249	15840	4000	3498	97	423	8224	2970	2364
	Peak WP T	Time of Peak	Power at Empl.	Power at Closure	Power at Peak T	Peak WP T	Time of Peak	Power at Empl.	Power at Closure	Power at Peak T	Peak WP T	Time of Peak	Power at Empl.	Power at Closure	Power at Peak T	Peak WP T	Time of Peak	Power at Empl.	Power at Closure	Power at Peak T	Peak WP T	Time of Peak	Power at Empl.	Power at Closure	Power at Peak T
WP size	(°C)	(yr OoR)	(W)	(W)	(W)	(°C)	(yr OoR)	(W)	(W)	(W)	(°C)	(yr OoR)	(W)	(W)	(W)	(°C)	(yr OoR)	(W)	(W)	(W)	(°C)	(yr OoR)	(W)	(W)	(W)
4	197	61	4480	1696	1671	122	111	4480	944	921	93	161	1980	643	636	79	211	1980	500	497	66	311	1028	371	369
12	458	61	13440	5088	5013	269	111	13440	2832	2764	193	161	5940	1930	1907	158	211	5940	1500	1490	125	311	3084	1114	1107
21	680	61	23520	8904	8773	395	111	23520	4956	4837	279	161	10395	3377	3336	227	211	10395	2625	2608	175	311	5397	1949	1938
32	864	61	35840	13568	13370	500	111	35840	7552	7371	351	161	15840	5146	5084	284	211	15840	4000	3974	218	313	8224	2970	2939

Table 3-11. Peak wall and package temperature results for the hard rock open unbackfilled (10 m package spacing) concept.

UOX20, Hard Rock, 70-m drift spacing, unbackfilled (assume drifts stay open)

	~50 yr (store/vent/close = 10/40/10 total=60 yr)					~100 yr (store/vent/close = 10/90/10 total=110 yr)					~150 yr (store/vent/close = 50/100/10 total=160 yr)					~200 yr (store/vent/close = 50/150/10 total=210 yr)					~300 yr (store/vent/close = 100/200/10 total=310 yr)				
	Peak Wall T	Time of Peak	Power at Empl.	Power at Closure	Power at Peak T	Peak Wall T	Time of Peak	Power at Empl.	Power at Closure	Power at Peak T	Peak Wall T	Time of Peak	Power at Empl.	Power at Closure	Power at Peak T	Peak Wall T	Time of Peak	Power at Empl.	Power at Closure	Power at Peak T	Peak Wall T	Time of Peak	Power at Empl.	Power at Closure	Power at Peak T
WP size	(°C)	(yr OoR)	(W)	(W)	(W)	(°C)	(yr OoR)	(W)	(W)	(W)	(°C)	(yr OoR)	(W)	(W)	(W)	(°C)	(yr OoR)	(W)	(W)	(W)	(°C)	(yr OoR)	(W)	(W)	(W)
4	37	65	1156	520	488	35	414	1156	319	143	34	523	592	238	488	33	582	592	202	116	33	721	341	164	99
12	57	65	3468	1560	1465	49	402	3468	956	437	46	525	1776	715	372	45	582	1776	606	348	43	721	1024	492	297
21	79	65	6069	2730	2564	65	417	6069	1674	749	61	525	3108	1252	652	59	582	3108	1061	609	55	721	1791	861	519
32	106	65	9248	4160	3907	84	417	9248	2550	1141	78	536	4736	1907	980	75	582	4736	1616	928	70	721	2730	1312	791
	Peak WP T	Time of Peak	Power at Empl.	Power at Closure	Power at Peak T	Peak WP T	Time of Peak	Power at Empl.	Power at Closure	Power at Peak T	Peak WP T	Time of Peak	Power at Empl.	Power at Closure	Power at Peak T	Peak WP T	Time of Peak	Power at Empl.	Power at Closure	Power at Peak T	Peak WP T	Time of Peak	Power at Empl.	Power at Closure	Power at Peak T
WP size	(°C)	(yr OoR)	(W)	(W)	(W)	(°C)	(yr OoR)	(W)	(W)	(W)	(°C)	(yr OoR)	(W)	(W)	(W)	(°C)	(yr OoR)	(W)	(W)	(W)	(°C)	(yr OoR)	(W)	(W)	(W)
4	43	57	1156	520	541	38	113	1156	319	308	36	314	592	238	165	35	380	592	202	150	34	557	341	164	119
12	68	59	3468	1560	1580	55	117	3468	956	901	50	406	1776	715	1580	48	477	1776	606	395	46	628	1024	492	330
21	91	61	6069	2730	2695	72	233	6069	1674	1526	65	421	3108	1252	745	63	512	3108	1061	662	58	628	1791	861	577
32	118	61	9248	4160	4107	91	126	9248	2550	2268	82	468	4736	1907	1066	79	540	4736	1616	976	73	628	2730	1312	879

UOX40, Hard Rock, 70-m drift spacing, unbackfilled (assume drifts stay open)

	~50 yr (store/vent/close = 10/40/10 total=60 yr)					~100 yr (store/vent/close = 10/90/10 total=110 yr)					~150 yr (store/vent/close = 50/100/10 total=160 yr)					~200 yr (store/vent/close = 50/150/10 total=210 yr)					~300 yr (store/vent/close = 100/200/10 total=310 yr)				
	Peak Wall T	Time of Peak	Power at Empl.	Power at Closure	Power at Peak T	Peak Wall T	Time of Peak	Power at Empl.	Power at Closure	Power at Peak T	Peak Wall T	Time of Peak	Power at Empl.	Power at Closure	Power at Peak T	Peak Wall T	Time of Peak	Power at Empl.	Power at Closure	Power at Peak T	Peak Wall T	Time of Peak	Power at Empl.	Power at Closure	Power at Peak T
WP size	(°C)	(yr OoR)	(W)	(W)	(W)	(°C)	(yr OoR)	(W)	(W)	(W)	(°C)	(yr OoR)	(W)	(W)	(W)	(°C)	(yr OoR)	(W)	(W)	(W)	(°C)	(yr OoR)	(W)	(W)	(W)
4	48	63	2680	1104	1060	41	126	2680	648	564	39	468	1272	462	229	38	512	1272	378	215	37	721	700	296	167
12	90	63	8040	3312	3179	69	126	8040	1944	1692	61	469	3816	1385	685	59	512	3816	1134	646	55	687	2100	889	520
21	137	63	14070	5796	5564	101	126	14070	3402	2960	86	469	6678	2423	1199	83	537	6678	1985	1093	75	687	3675	1556	910
32	194	63	21440	8832	8478	139	126	21440	5184	4511	117	469	10176	3693	8478	111	537	10176	3024	1665	100	687	5600	2371	1387
	Peak WP T	Time of Peak	Power at Empl.	Power at Closure	Power at Peak T	Peak WP T	Time of Peak	Power at Empl.	Power at Closure	Power at Peak T	Peak WP T	Time of Peak	Power at Empl.	Power at Closure	Power at Peak T	Peak WP T	Time of Peak	Power at Empl.	Power at Closure	Power at Peak T	Peak WP T	Time of Peak	Power at Empl.	Power at Closure	Power at Peak T
WP size	(°C)	(yr OoR)	(W)	(W)	(W)	(°C)	(yr OoR)	(W)	(W)	(W)	(°C)	(yr OoR)	(W)	(W)	(W)	(°C)	(yr OoR)	(W)	(W)	(W)	(°C)	(yr OoR)	(W)	(W)	(W)
4	60	57	2680	1104	1151	48	111	2680	648	635	43	177	1272	462	424	41	303	1272	378	300	39	489	700	296	222
12	107	59	8040	3312	3358	80	113	8040	1944	1872	67	211	3816	1385	1128	64	380	3816	1134	784	59	569	2100	889	599
21	154	61	14070	5796	5717	112	117	14070	3402	3171	92	314	6678	2423	1540	88	458	6678	1985	1219	80	628	3675	1556	974
32	208	61	21440	8832	8711	149	118	21440	5184	4793	123	380	10176	3693	2091	117	477	10176	3024	1807	105	628	5600	2371	1485

UOX60, Hard Rock, 70-m drift spacing, unbackfilled (assume drifts stay open)

	~50 yr (store/vent/close = 10/40/10 total=60 yr)					~100 yr (store/vent/close = 10/90/10 total=110 yr)					~150 yr (store/vent/close = 50/100/10 total=160 yr)					~200 yr (store/vent/close = 50/150/10 total=210 yr)					~300 yr (store/vent/close = 100/200/10 total=310 yr)				
	Peak Wall T	Time of Peak	Power at Empl.	Power at Closure	Power at Peak T	Peak Wall T	Time of Peak	Power at Empl.	Power at Closure	Power at Peak T	Peak Wall T	Time of Peak	Power at Empl.	Power at Closure	Power at Peak T	Peak Wall T	Time of Peak	Power at Empl.	Power at Closure	Power at Peak T	Peak Wall T	Time of Peak	Power at Empl.	Power at Closure	Power at Peak T
WP size	(°C)	(yr OoR)	(W)	(W)	(W)	(°C)	(yr OoR)	(W)	(W)	(W)	(°C)	(yr OoR)	(W)	(W)	(W)	(°C)	(yr OoR)	(W)	(W)	(W)	(°C)	(yr OoR)	(W)	(W)	(W)
4	60	61	4480	1696	1671	48	122	4480	944	836	42	263	1980	643	420	41	477	1980	500	271	39	690	1028	371	207
12	124	61	13440	5088	5013	89	122	13440	2832	2509	71	264	5940	1930	1255	67	473	5940	1500	819	61	687	3084	1114	632
21	197	61	23520	8904	8773	135	122	23520	4956	4391	103	264	10395	3377	2196	96	474	10395	2625	1431	85	687	5397	1949	1091
32	285	61	35840	13568	13370	191	122	35840	7552	6691	143	264	15840	5146	3347	132	474	15840	4000	2180	116	687	8224	2970	1662
	Peak WP T	Time of Peak	Power at Empl.	Power at Closure	Power at Peak T	Peak WP T	Time of Peak	Power at Empl.	Power at Closure	Power at Peak T	Peak WP T	Time of Peak	Power at Empl.	Power at Closure	Power at Peak T	Peak WP T	Time of Peak	Power at Empl.	Power at Closure	Power at Peak T	Peak WP T	Time of Peak	Power at Empl.	Power at Closure	Power at Peak T
WP size	(°C)	(yr OoR)	(W)	(W)	(W)	(°C)	(yr OoR)	(W)	(W)	(W)	(°C)	(yr OoR)	(W)	(W)	(W)	(°C)	(yr OoR)	(W)	(W)	(W)	(°C)	(yr OoR)	(W)	(W)	(W)
4	75	57	4480	1696	1775	57	110	4480	944	930	48	169	1980	643	607	45	239	1980	500	451	41	470	1028	371	274
12	144	59	13440	5088	5165	103	113	13440	2832	2714	81	177	5940	1930	1745	74	270	5940	1500	1234	65	536	3084	1114	749
21	214	61	23520	8904	8773	148	117	23520	4956	4582	113	186	10395	3377	2917	103	311	10395	2625	1938	91	628	5397	1949	1167
32	298	61	35840	13568	13370	202	118	35840	7552	6922	151	195	15840	5146	4255	138	380	15840	4000	2554	121	628	8224	2970	1779

Table 3-12. Peak wall and package temperature results for the hard rock open unbackfilled (20 m package spacing) concept.

UOX20, Hard Rock, 70-m drift spacing, unbackfilled (assume drifts stay open)

	~50 yr (store/vent/close = 10/40/10 total=60 yr)					~100 yr (store/vent/close = 10/90/10 total=110 yr)					~150 yr (store/vent/close = 50/100/10 total=160 yr)					~200 yr (store/vent/close = 50/150/10 total=210 yr)					~300 yr (store/vent/close = 100/200/10 total=310 yr)				
	Peak Wall T	Time of Peak	Power at Empl.	Power at Closure	Power at Peak T	Peak Wall T	Time of Peak	Power at Empl.	Power at Closure	Power at Peak T	Peak Wall T	Time of Peak	Power at Empl.	Power at Closure	Power at Peak T	Peak Wall T	Time of Peak	Power at Empl.	Power at Closure	Power at Peak T	Peak Wall T	Time of Peak	Power at Empl.	Power at Closure	Power at Peak T
WP size	(°C)	(yr OoR)	(W)	(W)	(W)	(°C)	(yr OoR)	(W)	(W)	(W)	(°C)	(yr OoR)	(W)	(W)	(W)	(°C)	(yr OoR)	(W)	(W)	(W)	(°C)	(yr OoR)	(W)	(W)	(W)
4	34	61	1156	520	513	32	129	1156	319	278	31	387	592	238	149	31	477	592	202	132	31	628	341	164	110
12	47	61	3468	1560	1540	41	128	3468	956	840	39	406	1776	715	434	38	477	1776	606	395	37	628	1024	492	330
21	62	61	6069	2730	2695	51	128	6069	1674	1470	47	406	3108	1252	760	46	477	3108	1061	692	44	628	1791	861	577
32	80	61	9248	4160	4107	64	129	9248	2550	2226	58	406	4736	1907	1158	56	477	4736	1616	1054	53	628	2730	1312	879
	Peak WP T	Time of Peak	Power at Empl.	Power at Closure	Power at Peak T	Peak WP T	Time of Peak	Power at Empl.	Power at Closure	Power at Peak T	Peak WP T	Time of Peak	Power at Empl.	Power at Closure	Power at Peak T	Peak WP T	Time of Peak	Power at Empl.	Power at Closure	Power at Peak T	Peak WP T	Time of Peak	Power at Empl.	Power at Closure	Power at Peak T
WP size	(°C)	(yr OoR)	(W)	(W)	(W)	(°C)	(yr OoR)	(W)	(W)	(W)	(°C)	(yr OoR)	(W)	(W)	(W)	(°C)	(yr OoR)	(W)	(W)	(W)	(°C)	(yr OoR)	(W)	(W)	(W)
4	41	54	1156	520	562	36	107	1156	319	322	34	169	592	238	229	33	255	592	202	183	32	406	341	164	145
12	60	56	3468	1560	1643	49	109	3468	956	953	44	185	1776	715	649	42	295	1776	606	511	40	432	1024	492	419
21	77	56	6069	2730	2875	61	111	6069	1674	1643	53	185	3108	1252	1137	51	332	3108	1061	843	48	482	1791	861	687
32	96	57	9248	4160	4325	74	113	9248	2550	2468	64	248	4736	1907	1481	62	380	4736	1616	1200	57	511	2730	1312	1010

UOX40, Hard Rock, 70-m drift spacing, unbackfilled (assume drifts stay open)

	~50 yr (store/vent/close = 10/40/10 total=60 yr)					~100 yr (store/vent/close = 10/90/10 total=110 yr)					~150 yr (store/vent/close = 50/100/10 total=160 yr)					~200 yr (store/vent/close = 50/150/10 total=210 yr)					~300 yr (store/vent/close = 100/200/10 total=310 yr)				
	Peak Wall T	Time of Peak	Power at Empl.	Power at Closure	Power at Peak T	Peak Wall T	Time of Peak	Power at Empl.	Power at Closure	Power at Peak T	Peak Wall T	Time of Peak	Power at Empl.	Power at Closure	Power at Peak T	Peak Wall T	Time of Peak	Power at Empl.	Power at Closure	Power at Peak T	Peak Wall T	Time of Peak	Power at Empl.	Power at Closure	Power at Peak T
WP size	(°C)	(yr OoR)	(W)	(W)	(W)	(°C)	(yr OoR)	(W)	(W)	(W)	(°C)	(yr OoR)	(W)	(W)	(W)	(°C)	(yr OoR)	(W)	(W)	(W)	(°C)	(yr OoR)	(W)	(W)	(W)
4	42	60	2680	1104	1104	37	118	2680	648	599	34	314	1272	462	293	34	380	1272	378	261	33	577	700	296	198
12	70	60	8040	3312	3312	55	119	8040	1944	1783	48	289	3816	1385	926	47	380	3816	1134	784	44	569	2100	889	599
21	102	60	14070	5796	5796	75	119	14070	3402	3121	64	289	6678	2423	1620	61	380	6678	1985	1372	56	569	3675	1556	1048
32	140	60	21440	8832	8832	101	119	21440	5184	4755	83	289	10176	3693	2468	78	380	10176	3024	2091	71	569	5600	2371	1597
	Peak WP T	Time of Peak	Power at Empl.	Power at Closure	Power at Peak T	Peak WP T	Time of Peak	Power at Empl.	Power at Closure	Power at Peak T	Peak WP T	Time of Peak	Power at Empl.	Power at Closure	Power at Peak T	Peak WP T	Time of Peak	Power at Empl.	Power at Closure	Power at Peak T	Peak WP T	Time of Peak	Power at Empl.	Power at Closure	Power at Peak T
WP size	(°C)	(yr OoR)	(W)	(W)	(W)	(°C)	(yr OoR)	(W)	(W)	(W)	(°C)	(yr OoR)	(W)	(W)	(W)	(°C)	(yr OoR)	(W)	(W)	(W)	(°C)	(yr OoR)	(W)	(W)	(W)
4	54	54	2680	1104	1201	44	106	2680	648	663	39	162	1272	462	454	38	239	1272	378	347	36	374	700	296	264
12	91	56	8040	3312	3503	68	108	8040	1944	1953	57	169	3816	1385	1318	54	239	3816	1134	1040	49	410	2100	889	748
21	124	57	14070	5796	6044	91	110	14070	3402	3360	74	179	6678	2423	2210	69	277	6678	1985	1662	63	442	3675	1556	1247
32	161	58	21440	8832	9082	116	112	21440	5184	5034	93	195	10176	3693	3174	87	295	10176	3024	2438	78	482	5600	2371	1795

UOX60, Hard Rock, 70-m drift spacing, unbackfilled (assume drifts stay open)

	~50 yr (store/vent/close = 10/40/10 total=60 yr)					~100 yr (store/vent/close = 10/90/10 total=110 yr)					~150 yr (store/vent/close = 50/100/10 total=160 yr)					~200 yr (store/vent/close = 50/150/10 total=210 yr)					~300 yr (store/vent/close = 100/200/10 total=310 yr)				
	Peak Wall T	Time of Peak	Power at Empl.	Power at Closure	Power at Peak T	Peak Wall T	Time of Peak	Power at Empl.	Power at Closure	Power at Peak T	Peak Wall T	Time of Peak	Power at Empl.	Power at Closure	Power at Peak T	Peak Wall T	Time of Peak	Power at Empl.	Power at Closure	Power at Peak T	Peak Wall T	Time of Peak	Power at Empl.	Power at Closure	Power at Peak T
WP size	(°C)	(yr OoR)	(W)	(W)	(W)	(°C)	(yr OoR)	(W)	(W)	(W)	(°C)	(yr OoR)	(W)	(W)	(W)	(°C)	(yr OoR)	(W)	(W)	(W)	(°C)	(yr OoR)	(W)	(W)	(W)
4	49	59	4480	1696	1722	41	115	4480	944	888	37	186	1980	643	556	36	303	1980	500	376	34	536	1028	371	250
12	93	59	13440	5088	5165	68	115	13440	2832	2665	55	186	5940	1930	1667	52	295	5940	1500	1152	47	536	3084	1114	749
21	142	59	23520	8904	9039	98	115	23520	4956	4664	76	186	10395	3377	2917	70	295	10395	2625	2016	62	536	5397	1949	1311
32	202	59	35840	13568	13770	135	115	35840	7552	7107	102	186	15840	5146	4444	92	295	15840	4000	3073	80	536	8224	2970	1997
	Peak WP T	Time of Peak	Power at Empl.	Power at Closure	Power at Peak T	Peak WP T	Time of Peak	Power at Empl.	Power at Closure	Power at Peak T	Peak WP T	Time of Peak	Power at Empl.	Power at Closure	Power at Peak T	Peak WP T	Time of Peak	Power at Empl.	Power at Closure	Power at Peak T	Peak WP T	Time of Peak	Power at Empl.	Power at Closure	Power at Peak T
WP size	(°C)	(yr OoR)	(W)	(W)	(W)	(°C)	(yr OoR)	(W)	(W)	(W)	(°C)	(yr OoR)	(W)	(W)	(W)	(°C)	(yr OoR)	(W)	(W)	(W)	(°C)	(yr OoR)	(W)	(W)	(W)
4	67	54	4480	1696	1860	51	106	4480	944	967	44	160	1980	643	639	41	218	1980	500	484	38	354	1028	371	336
12	119	55	13440	5088	5493	85	108	13440	2832	2844	68	164	5940	1930	1874	61	239	5940	1500	1353	54	380	3084	1114	958
21	167	57	23520	8904	9320	117	109	23520	4956	4930	90	169	10395	3377	3189	81	239	10395	2625	2367	70	406	5397	1949	1598
32	223	58	35840	13568	13990	152	111	35840	7552	7371	116	177	15840	5146	4654	103	255	15840	4000	3436	88	442	8224	2970	2291

Table 3-13. Peak wall and package temperature results for the hard rock open backfilled (20 m package spacing) concept.

UOX20, Hard Rock, 70-m drift spacing, backfilled

	~50 yr (store/vent/close = 10/40/10 total=60 yr)					~100 yr (store/vent/close = 10/90/10 total=110 yr)					~150 yr (store/vent/close = 50/100/10 total=160 yr)					~200 yr (store/vent/close = 50/150/10 total=210 yr)					~300 yr (store/vent/close = 100/200/10 total=310 yr)				
	Peak Wall T	Time of Peak	Power at Empl.	Power at Closure	Power at Peak T	Peak Wall T	Time of Peak	Power at Empl.	Power at Closure	Power at Peak T	Peak Wall T	Time of Peak	Power at Empl.	Power at Closure	Power at Peak T	Peak Wall T	Time of Peak	Power at Empl.	Power at Closure	Power at Peak T	Peak Wall T	Time of Peak	Power at Empl.	Power at Closure	Power at Peak T
WP size	(°C)	(yr OoR)	(W)	(W)	(W)	(°C)	(yr OoR)	(W)	(W)	(W)	(°C)	(yr OoR)	(W)	(W)	(W)	(°C)	(yr OoR)	(W)	(W)	(W)	(°C)	(yr OoR)	(W)	(W)	(W)
4	34	61	1156	520	513	32	129	1156	319	278	31	387	592	238	149	31	477	592	202	132	31	628	341	164	110
12	47	61	3468	1560	1540	41	128	3468	956	840	39	406	1776	715	434	38	477	1776	606	395	37	628	1024	492	330
21	62	61	6069	2730	2695	51	128	6069	1674	1470	47	406	3108	1252	760	46	477	3108	1061	692	44	628	1791	861	577
32	80	61	9248	4160	4107	64	129	9248	2550	2226	58	406	4736	1907	1158	56	477	4736	1616	1054	53	628	2730	1312	879
	Peak WP T	Time of Peak	Power at Empl.	Power at Closure	Power at Peak T	Peak WP T	Time of Peak	Power at Empl.	Power at Closure	Power at Peak T	Peak WP T	Time of Peak	Power at Empl.	Power at Closure	Power at Peak T	Peak WP T	Time of Peak	Power at Empl.	Power at Closure	Power at Peak T	Peak WP T	Time of Peak	Power at Empl.	Power at Closure	Power at Peak T
WP size	(°C)	(yr OoR)	(W)	(W)	(W)	(°C)	(yr OoR)	(W)	(W)	(W)	(°C)	(yr OoR)	(W)	(W)	(W)	(°C)	(yr OoR)	(W)	(W)	(W)	(°C)	(yr OoR)	(W)	(W)	(W)
4	82	61	1156	520	513	61	111	1156	319	313	53	161	592	238	236	49	211	592	202	201	45	311	341	164	166
12	166	61	3468	1560	1540	113	111	3468	956	939	92	161	1776	715	709	83	211	1776	606	603	73	311	1024	492	498
21	239	61	6069	2730	2695	158	111	6069	1674	1643	126	161	3108	1252	1240	112	211	3108	1061	1055	97	312	1791	861	869
32	301	61	9248	4160	4107	197	111	9248	2550	2503	155	161	4736	1907	1889	137	211	4736	1616	1607	118	314	2730	1312	1321

UOX40, Hard Rock, 70-m drift spacing, backfilled

	~50 yr (store/vent/close = 10/40/10 total=60 yr)					~100 yr (store/vent/close = 10/90/10 total=110 yr)					~150 yr (store/vent/close = 50/100/10 total=160 yr)					~200 yr (store/vent/close = 50/150/10 total=210 yr)					~300 yr (store/vent/close = 100/200/10 total=310 yr)				
	Peak Wall T	Time of Peak	Power at Empl.	Power at Closure	Power at Peak T	Peak Wall T	Time of Peak	Power at Empl.	Power at Closure	Power at Peak T	Peak Wall T	Time of Peak	Power at Empl.	Power at Closure	Power at Peak T	Peak Wall T	Time of Peak	Power at Empl.	Power at Closure	Power at Peak T	Peak Wall T	Time of Peak	Power at Empl.	Power at Closure	Power at Peak T
WP size	(°C)	(yr OoR)	(W)	(W)	(W)	(°C)	(yr OoR)	(W)	(W)	(W)	(°C)	(yr OoR)	(W)	(W)	(W)	(°C)	(yr OoR)	(W)	(W)	(W)	(°C)	(yr OoR)	(W)	(W)	(W)
4	42	60	2680	1104	1104	37	118	2680	648	599	34	314	1272	462	293	34	380	1272	378	261	33	577	700	296	198
12	70	60	8040	3312	3312	55	119	8040	1944	1783	48	289	3816	1385	926	47	380	3816	1134	784	44	569	2100	889	599
21	102	60	14070	5796	5796	75	119	14070	3402	3121	64	289	6678	2423	1620	61	380	6678	1985	1372	56	569	3675	1556	1048
32	140	60	21440	8832	8832	101	119	21440	5184	4755	83	289	10176	3693	2468	87	380	10176	3024	2091	71	569	5600	2371	1597
	Peak WP T	Time of Peak	Power at Empl.	Power at Closure	Power at Peak T	Peak WP T	Time of Peak	Power at Empl.	Power at Closure	Power at Peak T	Peak WP T	Time of Peak	Power at Empl.	Power at Closure	Power at Peak T	Peak WP T	Time of Peak	Power at Empl.	Power at Closure	Power at Peak T	Peak WP T	Time of Peak	Power at Empl.	Power at Closure	Power at Peak T
WP size	(°C)	(yr OoR)	(W)	(W)	(W)	(°C)	(yr OoR)	(W)	(W)	(W)	(°C)	(yr OoR)	(W)	(W)	(W)	(°C)	(yr OoR)	(W)	(W)	(W)	(°C)	(yr OoR)	(W)	(W)	(W)
4	142	61	2680	1104	1089	95	111	2680	648	635	76	161	1272	462	457	68	211	1272	378	376	59	311	700	296	295
12	321	61	8040	3312	3267	201	111	8040	1944	1904	152	161	3816	1385	1370	131	211	3816	1134	1128	109	311	2100	889	885
21	476	61	14070	5796	5717	293	111	14070	3402	3331	218	161	6678	2423	2397	186	211	6678	1985	1975	152	311	3675	1556	1549
32	608	61	21440	8832	8711	373	111	21440	5184	5076	274	161	10176	3693	3653	233	211	10176	3024	3009	189	311	5600	2371	2361

UOX60, Hard Rock, 70-m drift spacing, backfilled

	~50 yr (store/vent/close = 10/40/10 total=60 yr)					~100 yr (store/vent/close = 10/90/10 total=110 yr)					~150 yr (store/vent/close = 50/100/10 total=160 yr)					~200 yr (store/vent/close = 50/150/10 total=210 yr)					~300 yr (store/vent/close = 100/200/10 total=310 yr)				
	Peak Wall T	Time of Peak	Power at Empl.	Power at Closure	Power at Peak T	Peak Wall T	Time of Peak	Power at Empl.	Power at Closure	Power at Peak T	Peak Wall T	Time of Peak	Power at Empl.	Power at Closure	Power at Peak T	Peak Wall T	Time of Peak	Power at Empl.	Power at Closure	Power at Peak T	Peak Wall T	Time of Peak	Power at Empl.	Power at Closure	Power at Peak T
WP size	(°C)	(yr OoR)	(W)	(W)	(W)	(°C)	(yr OoR)	(W)	(W)	(W)	(°C)	(yr OoR)	(W)	(W)	(W)	(°C)	(yr OoR)	(W)	(W)	(W)	(°C)	(yr OoR)	(W)	(W)	(W)
4	49	59	4480	1696	1722	41	115	4480	944	888	37	186	1980	643	556	36	303	1980	500	376	34	536	1028	371	250
12	93	59	13440	5088	5165	68	115	13440	2832	2665	55	196	5940	1930	1667	52	295	5940	1500	1152	47	536	3084	1114	749
21	142	59	23520	8904	9039	98	115	23520	4956	4664	76	186	10395	3377	2917	70	295	10395	2625	2016	62	536	5397	1949	1311
32	202	59	35840	13568	13770	135	115	35840	7552	7107	102	186	15840	5146	4444	92	295	15840	4000	3073	80	536	8224	2970	1997
	Peak WP T	Time of Peak	Power at Empl.	Power at Closure	Power at Peak T	Peak WP T	Time of Peak	Power at Empl.	Power at Closure	Power at Peak T	Peak WP T	Time of Peak	Power at Empl.	Power at Closure	Power at Peak T	Peak WP T	Time of Peak	Power at Empl.	Power at Closure	Power at Peak T	Peak WP T	Time of Peak	Power at Empl.	Power at Closure	Power at Peak T
WP size	(°C)	(yr OoR)	(W)	(W)	(W)	(°C)	(yr OoR)	(W)	(W)	(W)	(°C)	(yr OoR)	(W)	(W)	(W)	(°C)	(yr OoR)	(W)	(W)	(W)	(°C)	(yr OoR)	(W)	(W)	(W)
4	204	61	4480	1696	1671	126	111	4480	944	921	95	161	1980	643	636	81	211	1980	500	497	67	311	1028	371	369
12	479	61	13440	5088	5013	280	111	13440	2832	2764	201	161	5940	1930	1907	164	211	5940	1500	1490	129	311	3084	1114	1107
21	717	61	23520	8904	8773	415	111	23520	4956	4837	293	161	10395	3377	3336	237	211	10395	2625	2608	183	311	5397	1949	1938
32	919	61	35840	13568	13370	530	111	35840	7552	7371	372	161	15840	5146	5084	300	211	15840	4000	3974	230	311	8224	2970	2953

3.3 Summary

The timing cases have different emphasis on decay storage vs. ventilation time, which causes the maximum power for the 10/90/10 case to be greater than for the others (Table 3-14). With 90 years of ventilation for decay of short-lived fission products, relatively high power can be tolerated at emplacement, for the unbackfilled cases.

The backfilled cases present a special challenge with the 100°C backfill temperature limit. Thermal resistance through the annular backfill element dominates the other aspects of heat transfer in these cases. The hard rock backfilled maximum power values are slightly less than the sedimentary backfilled case, because the drift diameter is greater so the backfill annulus is thicker (drift diameter 5.5 m vs. 4.5 m).

The confidence interval analysis for the backfilled cases was repeated with temperature limits of 120°C, 150°C and 200°C. These cases represent situations where: 1) backfill material is demonstrated to have temperature tolerance; and/or 2) the innermost and hottest part of the backfill annulus is impacted by temperature. The results (Table 3-15) indicate that some improvement is possible although the maximum power values for these backfilled cases are still much less than for the unbackfilled cases.

Table 3-14. Summary of confidence interval statistics (maximum package power to meet temperature limits) for open mode disposal concepts and timing cases.

Timing Case	b	Confidence			CALVIN Limit (W at emplacement)
		Level	Mean	± C.I.	
Sedimentary Unbackfilled Open Concept (Drift Spacing 10 m, Temperature Limit 100°C)					
10/40/10	0.010464	0.95	6976	2916	5238
10/90/10	0.006516	0.95	11203	3706	8287
50/100/10	0.010260	0.95	7115	1532	5583
50/150/10	0.009092	0.95	8029	2189	5840
100/200/10	0.014283	0.95	5111	1154	3957
Sedimentary Unbackfilled Open Concept (Drift Spacing 20 m, Temperature Limit 100°C)					
10/40/10	0.007558	0.95	9659	3778	7943
10/90/10	0.004675	0.95	15615	3706	11838
50/100/10	0.007072	0.95	10323	1419	8904
50/150/10	0.006204	0.95	11767	2276	9491
100/200/10	0.009468	0.95	7710	1308	6401
Sedimentary Backfilled Open Concept (Drift Spacing 20 m, Temperature Limit 100°C)					
10/40/10	0.026247	0.95	2781	5284	-1997 [A]
10/90/10	0.015114	0.95	4830	3706	-454 [A]
50/100/10	0.023303	0.95	3133	2302	831
50/150/10	0.018867	0.95	3869	2560	1309
100/200/10	0.027162	0.95	2688	1407	1280
Hard Rock Unbackfilled Open Concept (Drift Spacing 10 m, Temperature Limit 200°C)					
10/40/10	0.007422	0.95	23310	3706	21427
10/90/10	0.004824	0.95	35864	3706	32158
50/100/10	0.007956	0.95	21744	2692	19052
50/150/10	0.007312	0.95	23661	3180	20481
100/200/10	0.011835	0.95	14618	1619	12999
Hard Rock Unbackfilled Open Concept (Drift Spacing 20 m, Temperature Limit 200°C)					
10/40/10	0.005030	0.95	34391	4166	32381
10/90/10	0.003172	0.95	54538	3706	50373
50/100/10	0.005053	0.95	34237	2816	31421
50/150/10	0.004502	0.95	38429	3923	34506
100/200/10	0.007101	0.95	24362	2413	21949
Hard Rock Backfilled Open Concept (Drift Spacing 20 m, Temperature Limit 100°C)					
10/40/10	0.030208	0.95	2417	5068	-491 [A]
10/90/10	0.015995	0.95	4564	3706	-504 [A]
50/100/10	0.024697	0.95	2956	2205	751
50/150/10	0.019951	0.95	3659	2502	1157
100/200/10	0.028743	0.95	2540	1353	1186
Notes: [A] Negative values indicate thermal limit is not likely to be achieved.					

Table 3-15. Summary of confidence interval statistics for backfilled open mode concepts with different backfill temperature limits (120°C, 150°C and 200°C)

Timing Case	b	Confidence			CALVIN Limit (W at emplacement)
		Level	Mean	± C.I.	
Sedimentary Backfilled Open Concept (Drift Spacing 20 m, Temperature Limit 120°C)					
10/40/10	0.028543	0.95	3258	3187	177
10/90/10	0.016635	0.95	5591	3706	2403
50/100/10	0.025362	0.95	3667	1489	2178
50/150/10	0.020776	0.95	4476	1570	2907
100/200/10	0.029791	0.95	3122	912	2210
Sedimentary Backfilled Open Concept (Drift Spacing 20 m, Temperature Limit 150°C)					
10/40/10	0.028543	0.95	4309	3210	1221
10/90/10	0.016635	0.95	7394	3706	4184
50/100/10	0.025362	0.95	4850	1509	3341
50/150/10	0.020776	0.95	5920	1601	4319
100/200/10	0.029791	0.95	4129	941	3187
Sedimentary Backfilled Open Concept (Drift Spacing 20 m, Temperature Limit 200°C)					
10/40/10	0.028543	0.95	6061	3261	2955
10/90/10	0.016635	0.95	10400	3706	7139
50/100/10	0.025362	0.95	6821	1555	5266
50/150/10	0.020776	0.95	8327	1672	6655
100/200/10	0.029791	0.95	5807	1006	4801
Hard Rock Backfilled Open Concept (Drift Spacing 20 m, Temperature Limit 120°C)					
10/40/10	0.030208	0.95	3079	3031	167
10/90/10	0.017551	0.95	5299	3706	2268
50/100/10	0.026805	0.95	3469	1415	2055
50/150/10	0.021915	0.95	4244	1550	2694
100/200/10	0.028743	0.95	3236	1369	1867
Hard Rock Backfilled Open Concept (Drift Spacing 20 m, Temperature Limit 150°C)					
10/40/10	0.030208	0.95	4072	3050	1154
10/90/10	0.017551	0.95	7008	3706	3958
50/100/10	0.026805	0.95	4589	1432	3156
50/150/10	0.021915	0.95	5613	1578	4034
100/200/10	0.028743	0.95	4279	1399	2881
Hard Rock Backfilled Open Concept (Drift Spacing 20 m, Temperature Limit 200°C)					
10/40/10	0.030208	0.95	5727	3094	2795
10/90/10	0.017551	0.95	9857	3706	6763
50/100/10	0.026805	0.95	6454	1472	4982
50/150/10	0.021915	0.95	7894	1641	6253
100/200/10	0.028743	0.95	6019	1464	4555

References for Section 3

Bowker, A.H. and G.J. Lieberman 1972. *Engineering Statistics*. Prentice-Hall Inc., Englewood Cliffs, NJ.

Carter, J., A. Luptak, J. Gastelum, C. Stockman and A. Miller 2012. *Fuel Cycle Potential Waste Inventory for Disposition.* FCR&D-USED-2010-000031 Rev. 5. U.S. Department of Energy, Used Fuel Disposition R&D Campaign. July, 2012.

Greenberg, H.R., M. Sharma and M. Sutton 2012a. *Investigations on Repository Near-Field Thermal Modeling*. LLNL-TR-491099 Rev. 2. Lawrence Livermore National Laboratory. November, 2012.

Greenberg, H.R., M. Sharma, M. Sutton and A.V. Barnwell 2012b. *Repository Near-Field Thermal Modeling Update Including Analysis of Open Mode Design Concepts,* LLNL-TR-572252. Lawrence Livermore National Laboratory. August, 2012.

Greenberg, H.R., J. Blink and T.A. Buscheck 2013a. *Repository Layout and Required Ventilation Trade Studies in Clay/Shale Using the DSEF Thermal Analytical Model*. Milestone Report M4FT-13LL0804012. U.S. Department of Energy, Used Fuel Disposition R&D Campaign. June, 2013.

Greenberg, H.R., J. Wen and T.A. Buscheck 2013b. *Scoping Thermal Analysis of Alternative Dual-Purpose Canister Disposal Concepts*. LLNL-TR-639869. Lawrence Livermore National Laboratory. June, 2013.

Hardin, E., J. Blink, H. Greenberg, M. Sutton, M. Fratoni, J. Carter, M. Dupont and R. Howard 2011. *Generic Repository Design Concepts and Thermal Analysis (FY11).* FCRD-USED-2011-000143 Rev. 2. U.S. Department of Energy, Used Fuel Disposition R&D Campaign. December, 2011.

Hardin, E., T. Hadgu, D. Clayton, R. Howard, H. Greenberg, J. Blink, M. Sharma, M. Sutton, J. Carter, M. Dupont and P. Rodwell 2012. *Repository Reference Disposal Concepts and Thermal Load Management Analysis*. FCRD-UFD-2012-00219 Rev. 2. U.S. Department of Energy, Used Fuel Disposition R&D Campaign. November, 2012.

Hardin, E. 2013. *Temperature-Package Power Correlations for Open-Mode Geologic Disposal Concepts.* SAND13-1425. Sandia National Laboratories. Albuquerque, NM. February, 2013.

Hardin, E. and M. Voegele 2013. *Alternative Concepts for Direct Disposal of Dual Purpose Canisters*. FCRD-UFD-2013-000102, Rev.0. U.S. Department of Energy, Used Fuel Disposition R&D Campaign.

Miller, A., R. Rechard, E. Hardin and R. Howard 2012. *Assumptions for Evaluating Feasibility of Direct Geologic Disposal of Existing Dual-Purpose Canisters*. FCRD-UFD-2012-000352 Rev. 0. September, 2012. U.S. Department of Energy, Used Fuel Disposition R&D Campaign.

Nutt, M., E. Morris, F. Puig, J. Carter, P. Rodwell, A. Delley, R. Howard and D. Giuliano 2012. *Used Fuel Management System Architecture Evaluation, Fiscal Year 2012*. FCRD-NFST-2013-000020 Rev. 0. October, 2012. U.S. Department of Energy, Nuclear Fuel Storage and Transportation Planning Campaign.

Sutton, M., J.A. Blink, M. Fratoni, H.R. Greenberg and A. D. Ross 2011. *Investigations on Repository Near-Field Thermal Modeling.* LLNL-TR-491099 Rev. 1. Lawrence Livermore National Laboratory. December, 2011.

4. Vertical Waste Package Movement in a Salt Repository

While salt does creep, it does so under stress conditions imparted by overburden pressure, but not from the much smaller weight of waste packages. Stresses from reaction loads near emplaced waste packages are small compared to stress redistribution caused by excavation. Even thermally activated salt deformation in response to waste package weight is minor, as demonstrated by coupled thermal-mechanical simulations (Clayton et al. 2013) using constitutive laws for salt that are validated against laboratory and field-scale observations (Hansen and Leigh 2011).

With renewed interest in disposal of heat generating waste in salt, feasibility studies for disposal of large packages in a generic salt repository are underway. One aspect of these studies is to investigate the potential vertical movement of the waste packages. Intact salt creeps at a rate that depends on shear stress and temperature. Given that large packages could weigh up to 130 tons (depending on capacity and shielding requirements) and generate near-field temperatures up to 200 °C, it is possible that the waste packages could move over thousands of years.

4.1 Analysis Method

A two-pronged approach was used in this investigation. Potential vertical movement was analyzed using coupled thermal-mechanical modeling and coupled thermal-viscous flow modeling. The thermal-mechanical modeling used salt constitutive models, while the thermal-viscous flow modeling assumed that the salt acts like a highly viscous fluid. Both approaches simulated a three-dimensional, 5-m long, 2-m diameter waste package embedded in intact salt (Figure 4-1).

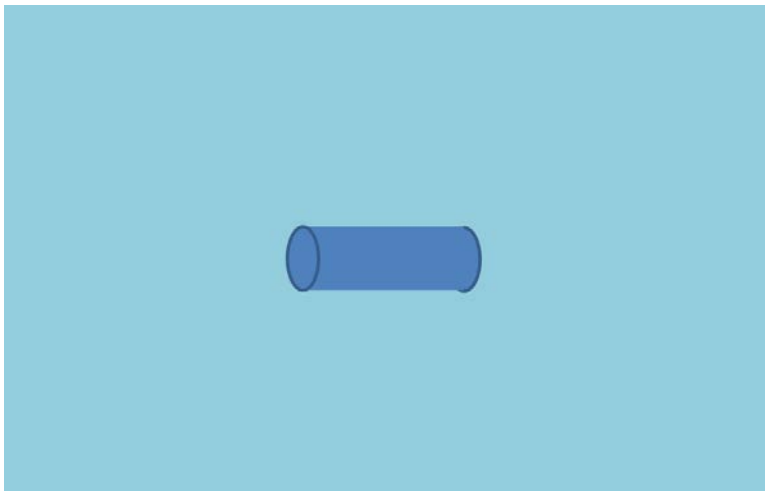

Figure 4-1. Schematic of waste package embedded in intact salt

The grid was constructed using 3-D hexagonal elements. A slice of the grid is shown below in Figure 4-2. The green portion represents the cylindrical waste package, while the blue portion represents the intact salt. The intact salt was modeled as a bed 60 m by 60 m by 100 m with the

waste package in the center. Symmetry conditions were used on the four sides of the model and boundary conditions were used on the top and bottom of the domain to simulate a waste package depth of ~600 m.

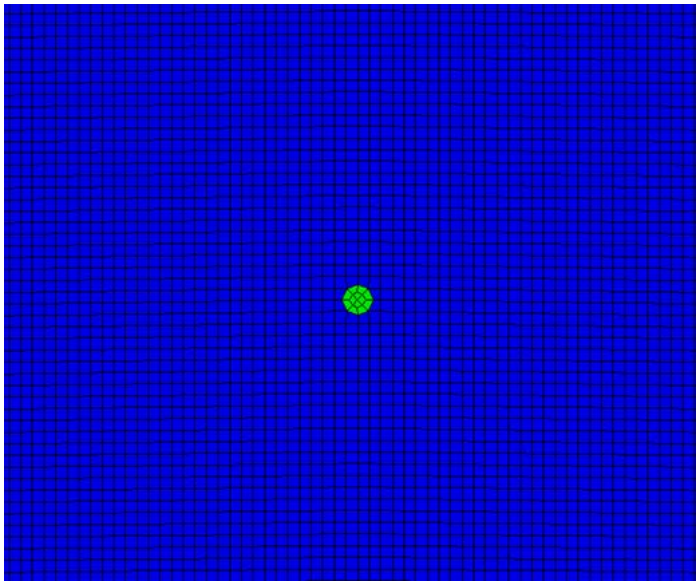

Figure 4-2. Near-field grid

4.1.1 Thermal-Mechanical

Coupled thermal-mechanical calculations were carried out by coupling thermal and mechanical codes through an interface that allows state variables such as temperature and displacement to be passed from one code to the other. The combined code is executed using output from the thermal code as input to the mechanical code, and vice versa. To do this, we used two available codes in the Sierra tool set: Aria (a Galerkin finite element based program for solving coupled-physics problems described by systems of partial differential equations) and Adagio (a Lagrangian mechanical modeling program with special provisions for modeling salt deformation). A third code, Arpeggio, was used to couple the two codes together and control the simulations.

For the thermal analysis, a convective-type boundary condition was applied to the top and bottom of the model to simulate conductive heat transport into the host rock above and below the repository. All materials were assumed to be initially at 25 °C. A thermal load of 13 kW was applied at time zero uniformly throughout the waste package, with a decay response specified as a function of time (Figure 4-3). The decay curve used was chosen to simulate 40 GW-d/MT burnup, pressurized water reactor waste with age of 50 years out-of-reactor at the time of emplacement.

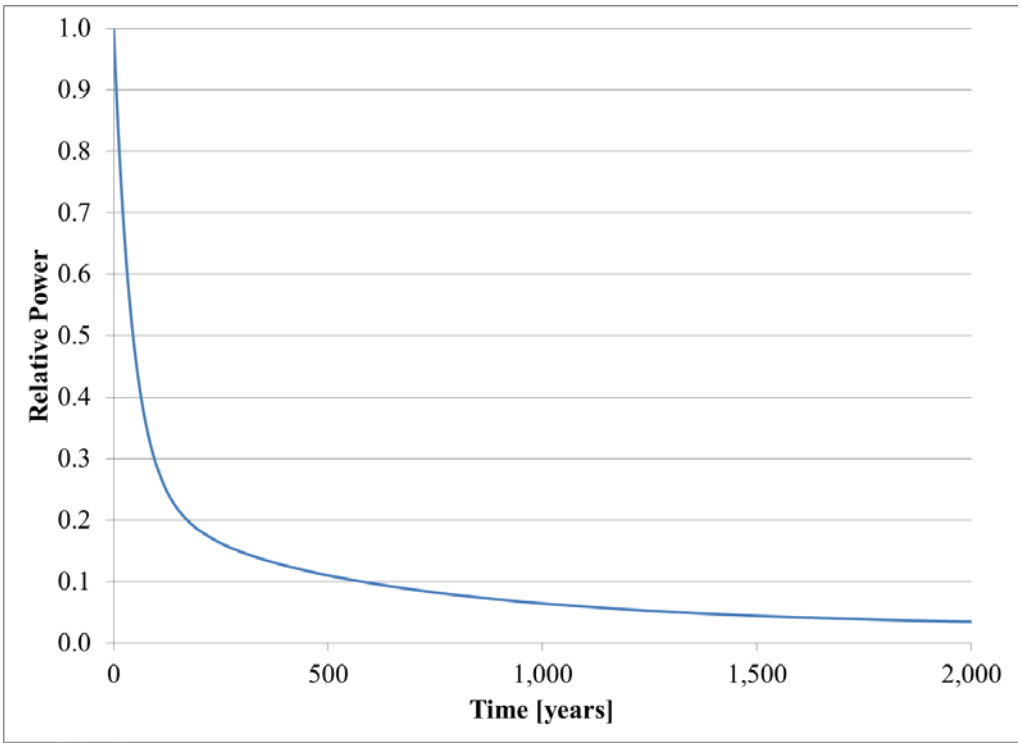

Figure 4-3. Decay curve used in the thermal analysis

The temperature dependent thermal conductivity of intact salt used in the analysis is given in the following equation

$$\lambda_{salt}(T) = \lambda_{300}\left(\frac{300}{T}\right)^{\gamma} \tag{4-1}$$

where:

λ_{300} = material constant, 5.4 W/m/K
γ = material constant = 1.14
T = temperature [K].

A summary of the thermal material properties assumed for the waste and intact salt are shown in Table 4-1.

Table 4-1. Thermal properties for the waste and salt

Material	Thermal Conductivity (W/m/K)	Specific Heat (J/kg/K)	Density (kg/m^3)
Waste	53	500	7,854
Intact Salt	Equation (4-1)	931	2,160

For the mechanical analysis, boundary conditions were set so that horizontal displacements were zero along the vertical boundaries, and both horizontal and vertical displacements were zero along the bottom. Mechanical loads acting on the model consisted of an overburden pressure applied to the top representing an alcove depth of ~600 m. The domain was initialized with lithostatic stresses corresponding to depth. The intact salt was modeled using the multimechanism-deformation (M-D) creep model (Munson 1997) and the waste package was assumed to respond elastically using the properties of steel shown in Table 4-2.

Table 4-2. Mechanical properties used for the waste

Material	Young's Modulus (Pa)	Poisson's Ratio	Thermal Expansion (K^{-1})
Heater	2.0E11	0.3	1.0E-5

4.1.2 Thermal-Viscous Flow

Coupled thermal-viscous flow calculations were carried out using Aria (a Galerkin finite element based program for solving coupled-physics problems described by systems of partial differential equations). Aria incorporates both the thermal and viscous flow models, and was the only code needed for these calculations. For the purposes of this analysis, the salt is treated as a viscous fluid with temperature-dependent viscosity. For the thermal part of the calculations, the same boundary conditions and thermal properties used in the thermal-mechanical modeling were used in the thermal-viscous flow modeling. The viscosity was derived from the salt constitutive models used in the mechanical calculations.

The viscosity of a fluid can be defined by the relationship

$$\tau = \mu \frac{du}{dy} \tag{4-2}$$

where τ is the shear stress and u is the velocity in the x-direction. The quantity du/dy is a velocity gradient and can be interpreted as a strain rate. Salt constitutive models give a relationship between applied stress and strain rate. Using the M-D creep model stress/strain rate relationship and solving for viscosity gives the following relationship

$$\mu = \frac{\tau}{A_1 e^{\left(\frac{-Q_1}{RT}\right)}\left(\frac{\sigma}{G}\right)^{n_1} + A_2 e^{\left(\frac{-Q_2}{RT}\right)}\left(\frac{\sigma}{G}\right)^{n_2} + H(\sigma-\sigma_0)\left[B_1 e^{\left(\frac{-Q_1}{RT}\right)} + B_2 e^{\left(\frac{-Q_2}{RT}\right)}\right] \times sinh\left[\frac{q(\sigma-\sigma_0)}{G}\right]} \tag{4-3}$$

where the *A*s and *B*s are constants, *Q*s are activation energies, *T* is the absolute temperature, *R* is the universal gas constant, *G* is the shear modulus, σ is the generalized stress, *n*s are the stress exponents, *H* is the Heaviside step function with the argument $(\sigma - \sigma_0)$, q is the stress constant and σ_0 is the stress limit of the dislocation slip mechanism. The force on the waste package due to buoyancy can be calculated by multiplying the waste package volume by the difference in density between the waste package and the salt, and the gravitational constant. The shear stress is then calculated by dividing the buoyant force of the waste package by the surface area of the waste package. The mean applied stress was calculated by dividing the force of the waste package by the projected area. For these calculations, the smallest projected area, with the waste

package in the vertical position, was used so as not to underestimate the mean applied stress. The applied stress was then assumed to be three times the mean applied stress. For the 5-m long, 2-m diameter waste package with 7,854 kg/m^3 density (density of solid steel), the shear and applied stresses were calculated to be 3.21E4 Pa and 1.15E6 Pa, respectively. Using these stress values and salt constitutive model parameters from Munson (1997), the effective viscosity of the intact salt as a function temperature is

$$\mu = 4.74E11/[8.37E7 \cdot e\text{^}(-1.26E4/T) + e\text{^}(-5.03E3/T)] \quad (4\text{-}4)$$

where T is the temperature in Kelvin. A plot of effective viscosity versus temperature is shown in Figure 4-4.

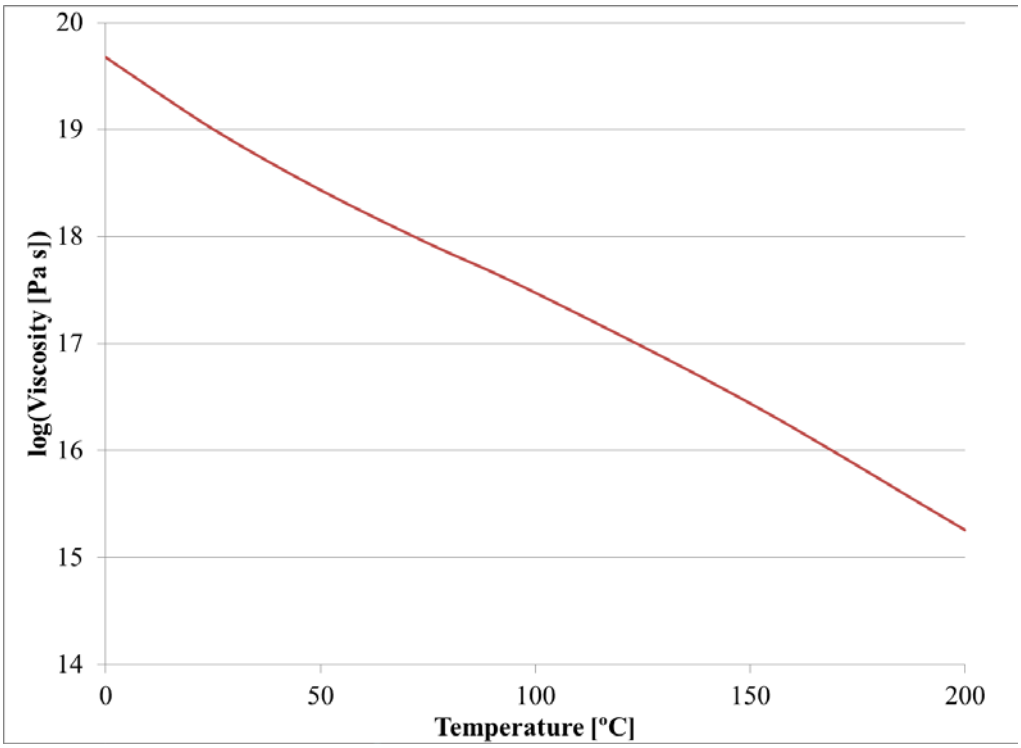

Figure 4-4. Effective viscosity versus temperature for intact salt calculated using the M-D creep model (Munson 1997).

An initial estimate of the settling velocity of the waste package in the absence of heating is useful to establish the scale of the motion and also for verification of numerical calculations of the heated problem to follow. The slow (creeping flow) settling velocity of a fluid sphere of radius a, density ρ_{can}, viscosity μ_{can} in a fluid of density ρ and viscosity μ, can be determined based on the well-known Hadamard solution (see Batchelor 1967). By balancing viscous drag with the buoyant force on the fluid sphere, the steady settling speed can be determined:

$$V = \frac{1}{3}\frac{a^2 \rho g}{\mu}\left(\frac{\rho_{can}}{\rho} - 1\right)\frac{\mu + \mu_{can}}{\mu + 3\mu_{can}/2}. \quad (4\text{-}5)$$

The settling velocity of a rigid sphere is recovered for $\mu_{can}/\mu >> 1$. The drag on a rigid sphere moving at constant velocity *V*, is given by the well-known Stokes drag formula, $D = 6\pi a\mu V$. The steady settling velocity is computed by equating the drag on the sphere with the buoyant force exerted on the sphere by virtue of its density difference with the salt.

By calculating the drag on the waste package, a similar procedure to compute its settling velocity can be developed. The waste package is a right circular cylinder of radius *a* and length *L*. A drag coefficient is defined for the waste package moving at a speed of *U* (small Reynolds number) as

$$C_D = \frac{D_{can}}{\mu \bar{a} U} \tag{4-6}$$

where we take the effective radius as $\bar{a} = V_{can}^{1/3}$, and $V_{can} = \pi a^2 L$. The dimensionless settling velocity of the waste package can then be written as

$$\frac{\mu U}{\rho g \bar{a}^2} = C_D^{-1}\left(\frac{\rho_{can}}{\rho} - 1\right). \tag{4-7}$$

By computing the drag coefficient the settling velocity can be computed as a function of density ratio and fluid viscosity, for isothermal conditions. Numerical calculations of the drag coefficient were carried out for the waste package ($\bar{a} = 2.504$). The effective viscosity of the waste package was set to 1e22 Pa-s in the numerical calculations to essentially treat the waste package as rigid. Table 4-3 gives the drag coefficients computed for vertical movement of the waste package in horizontal (i.e. centerline axis is horizontal) and vertical orientations. The table also gives the drag on a rigid sphere of radius 1 m for comparison.

Table 4-3. Waste package drag coefficient

Waste Package Orientation	C_D
Horizontal	13.4
Vertical	12.4
Sphere	11.7

It is worthwhile to note that there is less drag on the waste package in the vertical orientation compared to the horizontal orientation. This suggests that given conditions favorable to buoyant motion the waste package would right itself into a vertical orientation, even when it starts out in the horizontal orientation.

Using the waste package dimensions, waste package and salt densities, and computed drag coefficient, the vertical settling velocity (positive downward) of a horizontal waste package as a function of viscosity can be calculated and is shown in (Figure 4-5). Using the temperature dependence of effective viscosity shown in Equation 4-4, the vertical velocity as a function of temperature can be computed as shown in Figure 4-6.

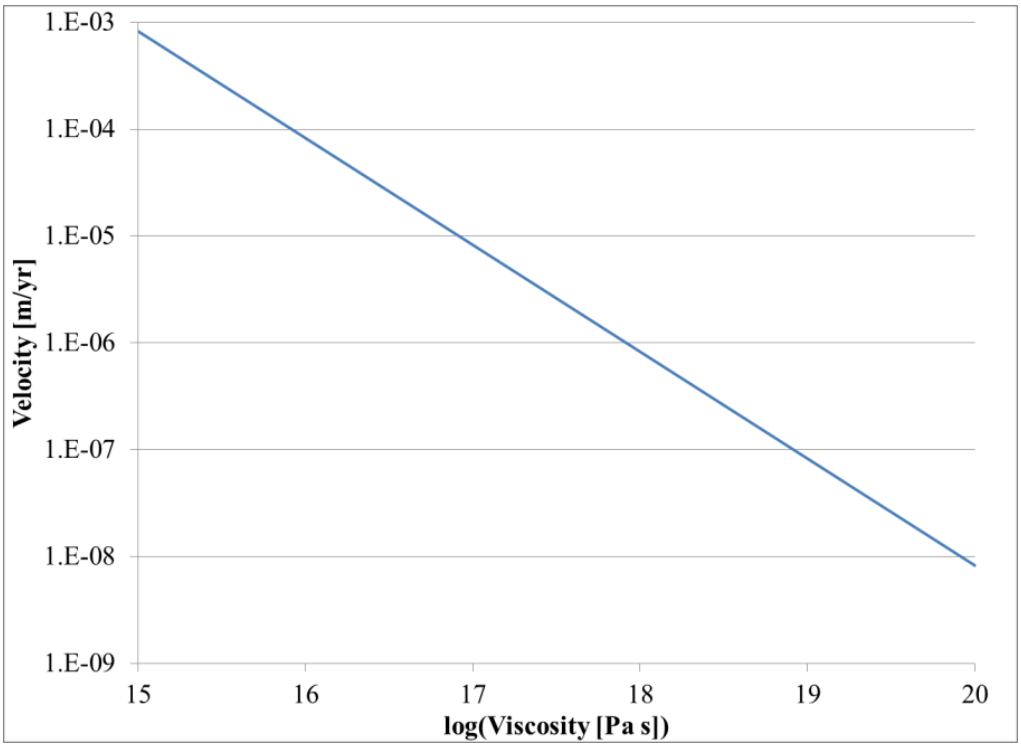

Figure 4-5. Horizontal waste package vertical settling velocity versus salt effective viscosity.

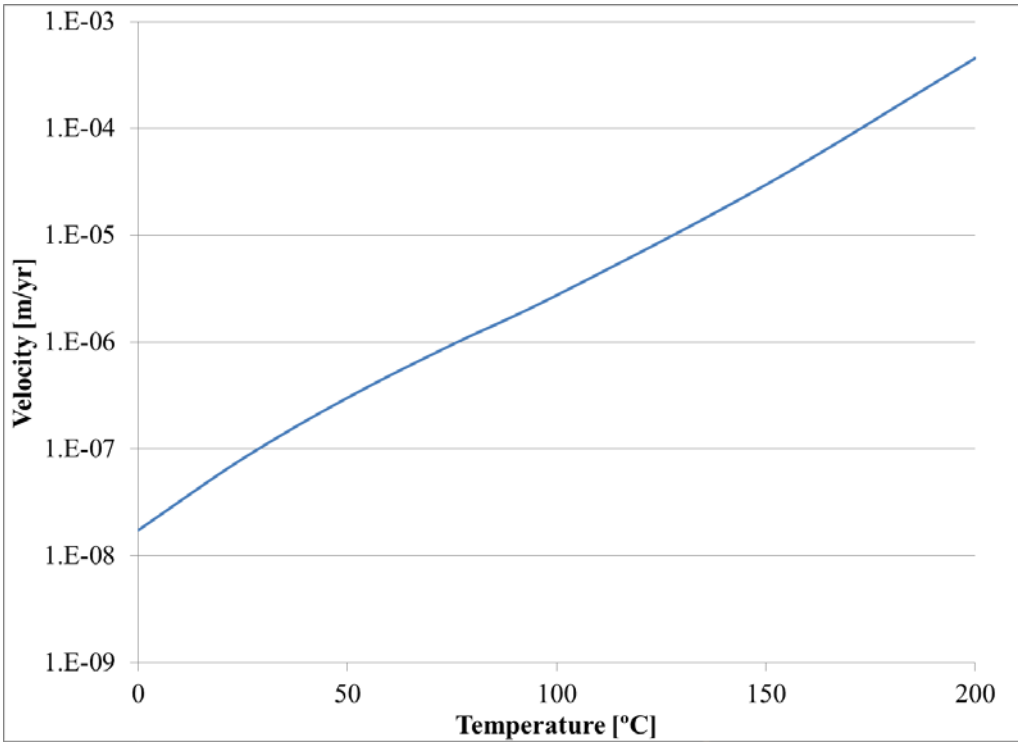

Figure 4-6. Horizontal waste package vertical settling velocity versus salt temperature

4.2 Results

Calculations with the heat generating waste package were conducted using both the thermal-mechanical modeling and thermal-viscous flow modeling on the grid shown in Figure 4-2. To aid in the interpretation of the results, two additional cases were modeled; the first included heat generation and the density of the waste package was set equal to the salt, and the second did not include heat generation and maintained the original waste package density. The results for each case are discussed below.

4.2.1 Baseline Case

The resulting temperature history of the salt at the waste package surface is shown in Figure 4-7. The waste package temperature history was the same for both the thermal-mechanical modeling and thermal-viscous flow modeling. The highest temperatures are within the waste package, with the salt temperature peaking at the waste/salt interface and decreasing with distance from the waste package. The peak waste package temperature of 180°C is reached at ~16 years with the temperature decreasing toward the initial temperature with time as the waste decays.

The resulting waste package vertical displacement history from thermal-mechanical modeling is shown in Figure 4-8. The vertical displacement appears to follow the temperature history. As the waste package and surrounding salt heat up, they expand causing uplift of the waste package and the surrounding salt. As the waste package and surrounding salt cool down and contract, they approach their original positions. From this calculation it is difficult to discern waste package displacement due to the density difference (“sinking”) when compared with the movement due to the thermal expansion. Movement of the waste package relative to the surrounding salt is better discerned from the reduced density case discussed below.

The resulting waste package vertical displacement history from the thermal-viscous flow modeling is shown in Figure 4-9. The waste package sinks faster initially, corresponding to the increased temperatures, then slows down and continues to sink more slowly, with a total displacement of approximately -0.5 mm at 2,000 years. The thermal-viscous flow modeling includes the change in density due to temperature, and tracks the waste package movement relative to the surrounding salt, hence the plotted displacements are negative (not masked by overall upward displacement due to thermal expansion).

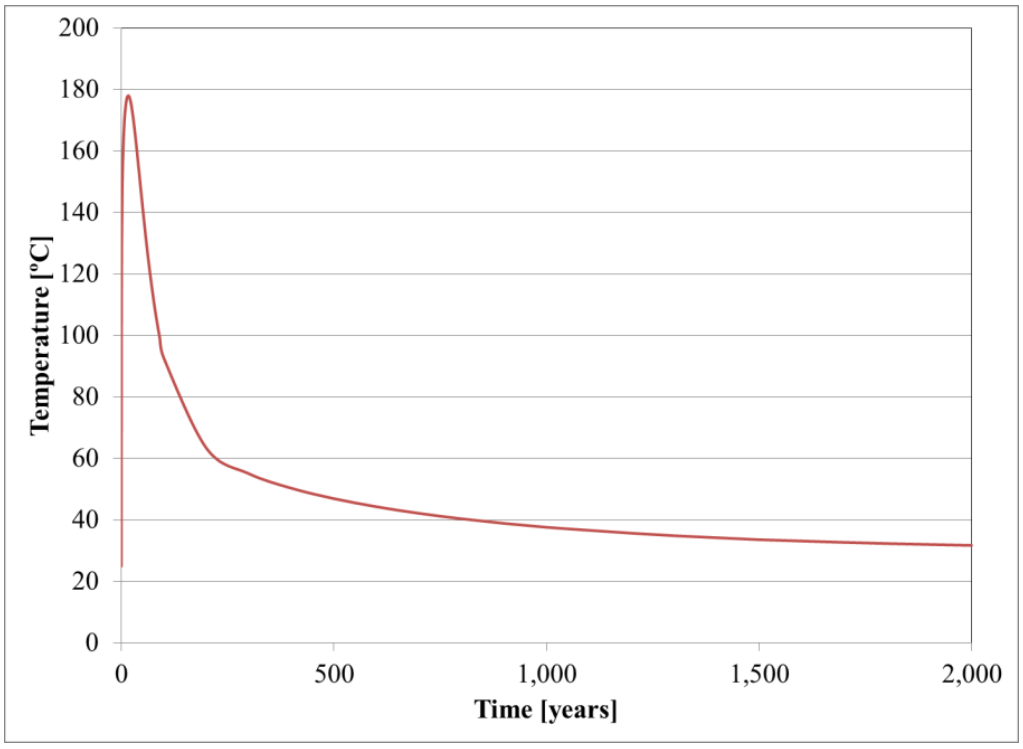

Figure 4-7. Maximum temperature in waste package versus time

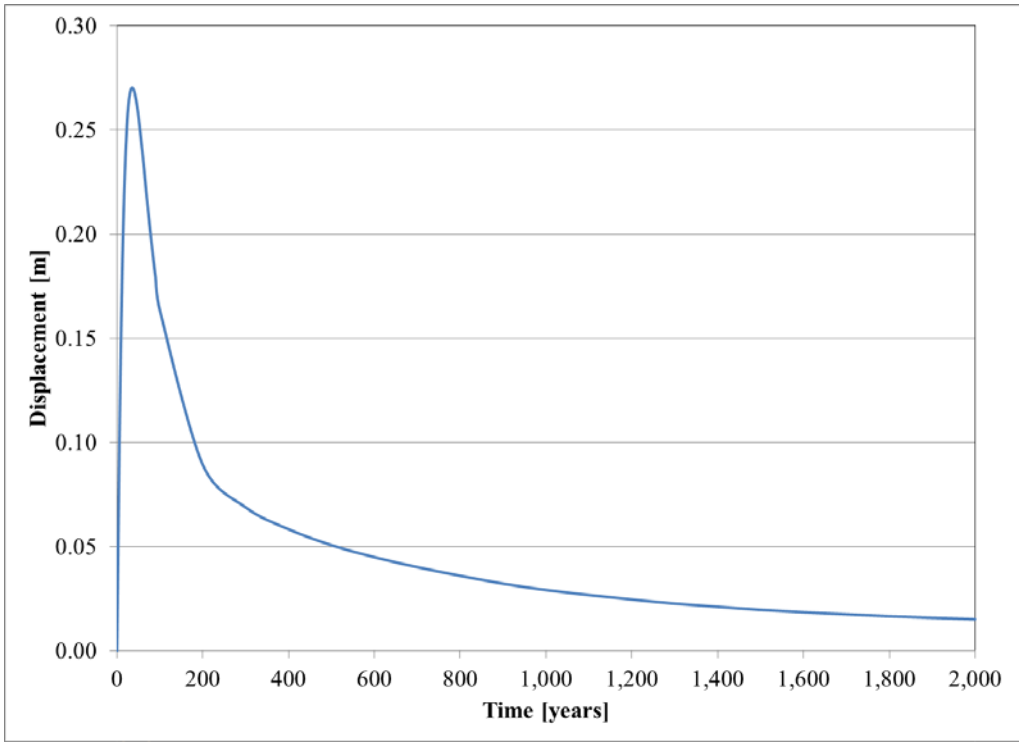

Figure 4-8. Thermal-mechanical modeling, baseline case, waste package vertical displacement versus time

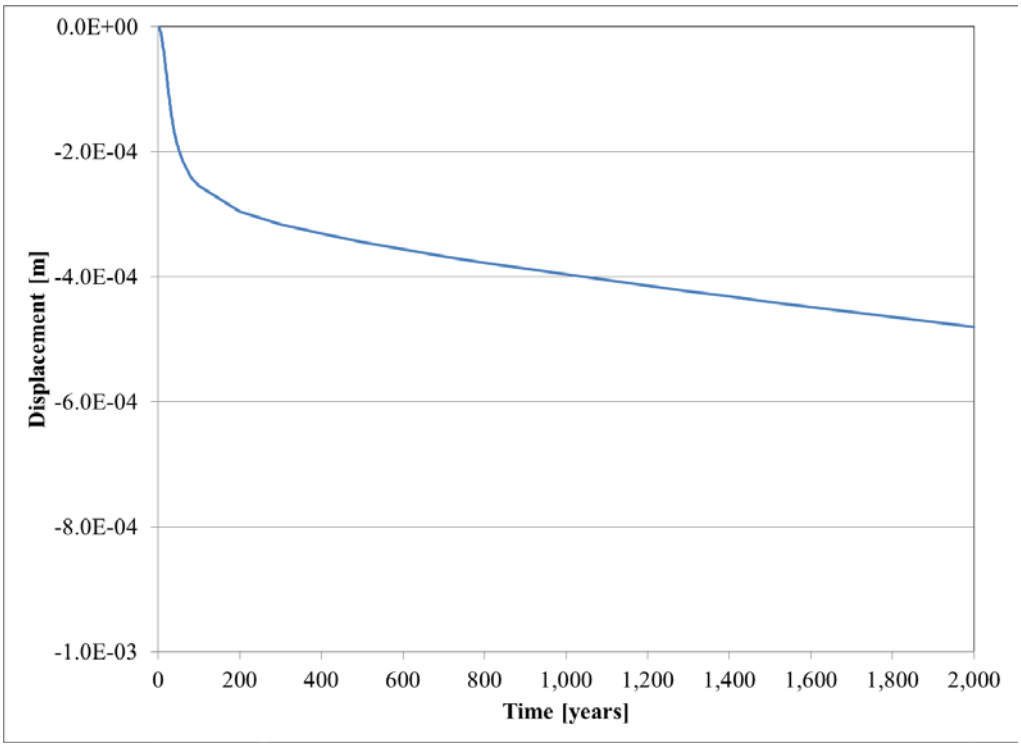

Figure 4-9. Thermal-viscous flow modeling, baseline case, waste package vertical displacement versus time

4.2.2 Reduced Waste Package Density

To investigate the effect of waste package density on vertical displacement, a second case was evaluated in which the waste package density was reduced, and equal to the salt. The resulting waste package vertical displacement history from thermal-mechanical modeling is shown in Figure 4-10. It follows the same general trend as the baseline case. A comparison of the two vertical displacement histories is shown in Figure 4-11. The difference between the two curves at 2,000 years is ~1.2 mm, which compares with the value calculated from the thermal-viscous flow modeling. The thermal-viscous flow modeling of this case shows vertical displacement on the micron scale after 2,000 years, which is essentially no vertical displacement.

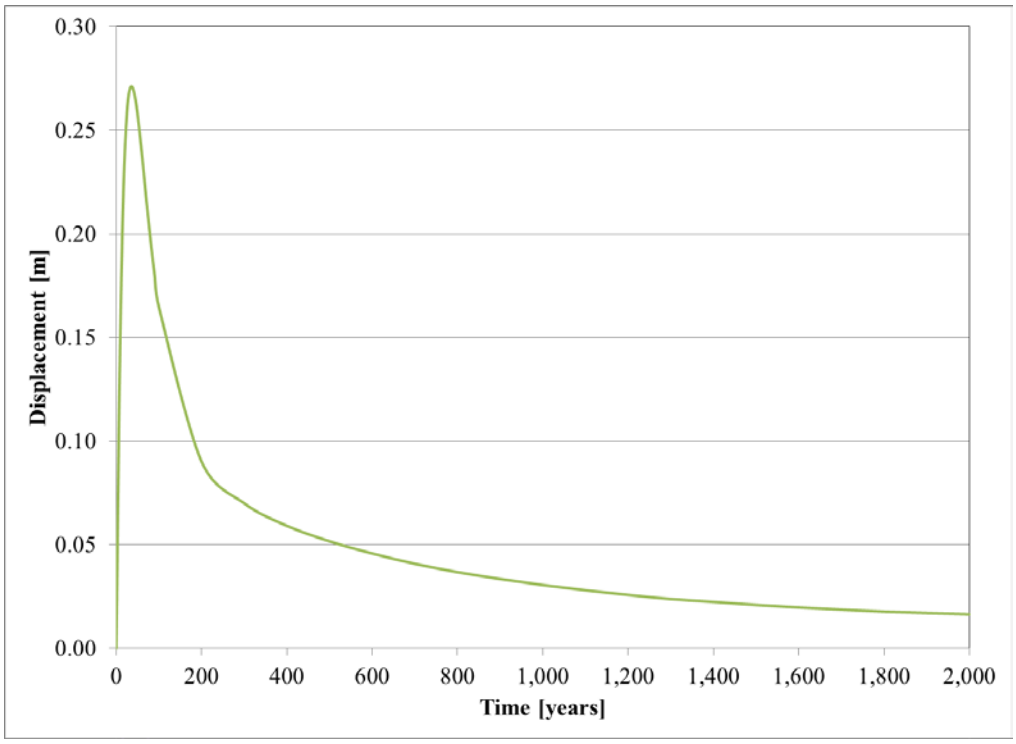

Figure 4-10. Thermal-mechanical modeling, reduced density, waste package vertical displacement versus time

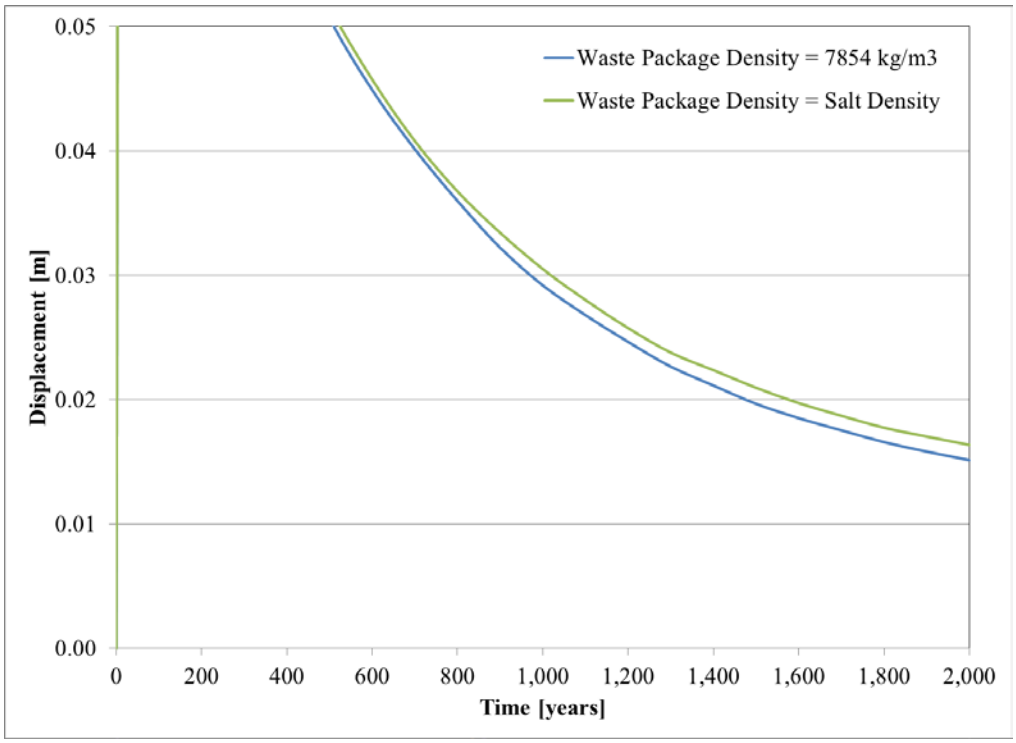

Figure 4-11. Comparison of thermal-mechanical modeling, baseline and reduced density, waste package vertical displacement versus time

4.2.3 No Heat Generation

To determine the effect of heat generation on the vertical displacement, a third case was computed that retained the waste package density contrast, but with no heat generation. The resulting waste package vertical displacement history from thermal-mechanical modeling is shown in Figure 4-12, while the thermal-viscous flow modeling results for the same conditions are shown in Figure 4-13. The thermal-mechanical results show a quick drop of the waste package, which then settles to about -0.06 mm and remains nearly constant after ~1,000 years. The thermal-viscous flow modeling results show a constant downward velocity, with magnitude very similar to the analytical solution given in Figure 4-5, and with a final vertical displacement of approximately -0.14 mm after 2,000 years. Without heat generation, vertical displacement is shown to be at least an order a magnitude smaller.

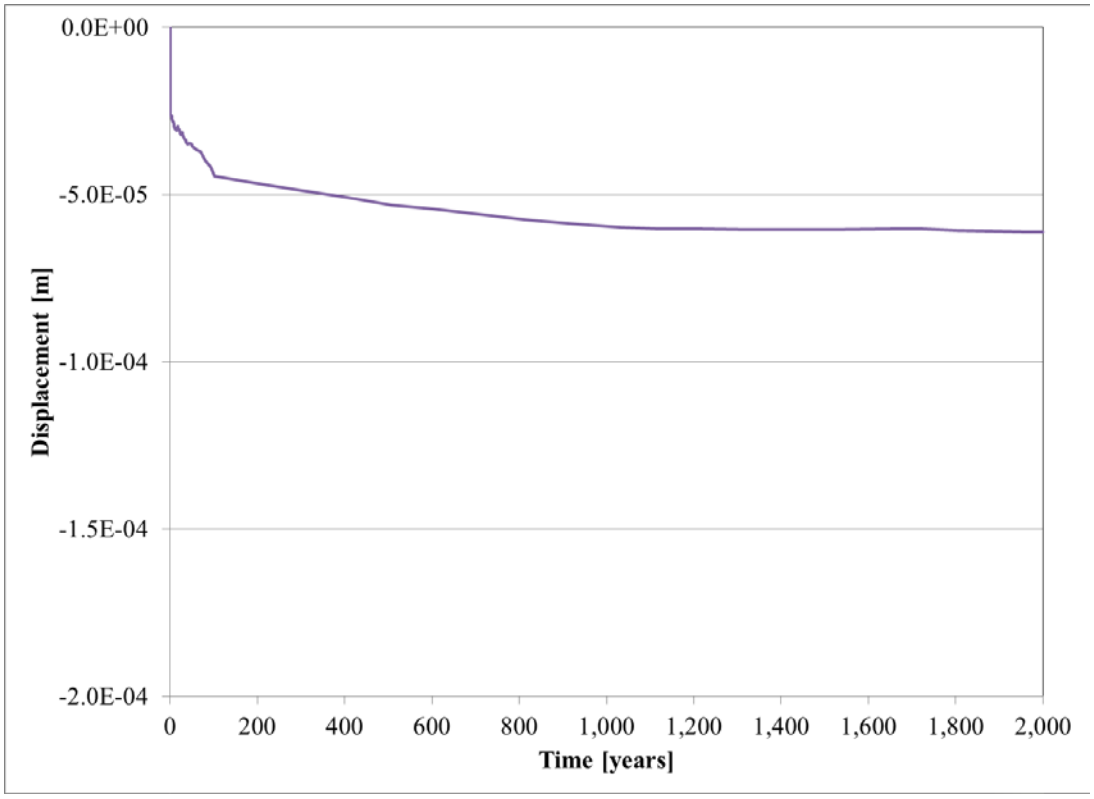

Figure 4-12. Thermal-mechanical modeling, no heat generation, waste package vertical displacement versus time

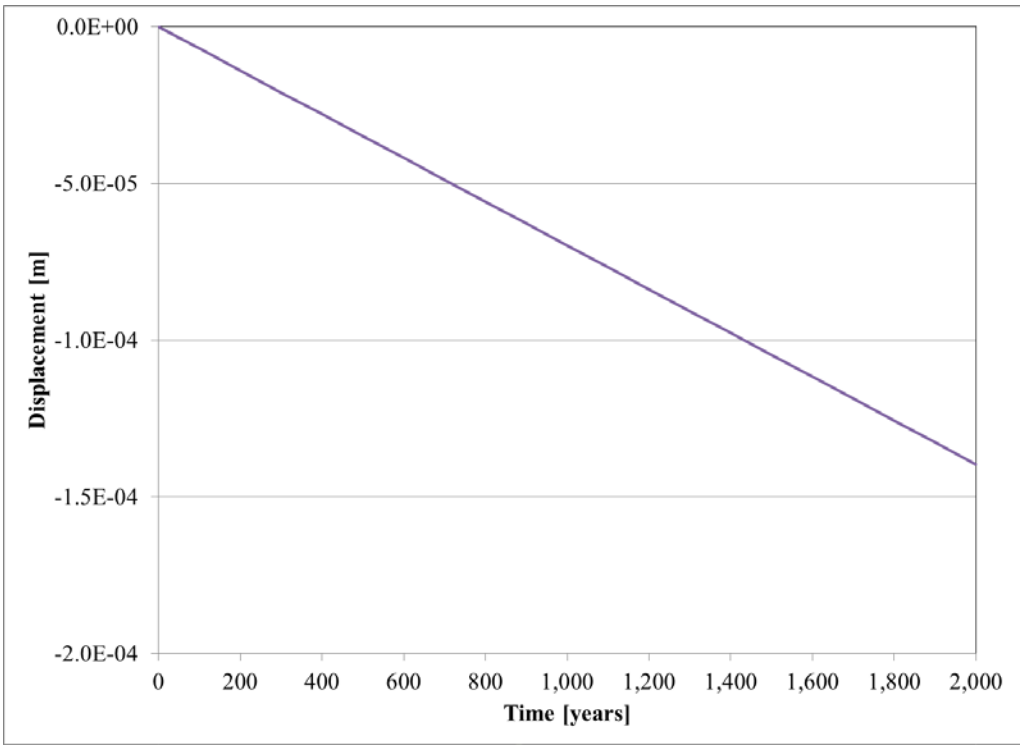

Figure 4-13. Thermal-viscous flow modeling, no heat generation, waste package vertical displacement versus time

4.3 Summary

In order to analyze the potential vertical movement of large, heat generating waste packages, coupled thermal-mechanical and thermal-viscous flow calculations using the Arpeggio, Adagio and Aria codes were conducted. All calculations show potential vertical movement on the order of 1 mm to a few centimeters after 2,000 years. Further displacement beyond 2,000 years is predicted to be much smaller, except for the simpler thermal-viscous model. Even extrapolating the larger velocity from the thermal-viscous model, total displacement after 10^6 years would be a fraction of a meter. With the more realistic M-D constitutive model, total displacement after 10^6 years would be limited to a few millimeters.

References for Section 4

Batchelor, G.K. 1967. *An introduction to fluid dynamic*s. Cambridge University Press.

Clayton, D.J., M.J. Martinez and E.L. Hardin 2013. *Potential Vertical Movement of Large Heat-Generating Waste Packages in Salt*. SAND2013-3596. Albuquerque, NM: Sandia National Laboratories. May, 2013.

Hansen, F.D. and C.D. Leigh 2011. *Salt Disposal of Heat-Generating Nuclear Waste.* SAND2011-0161. Albuquerque, NM: Sandia National Laboratories.

Munson, D.E. 1997. "Constitutive Model of Creep in Rock Salt Applied to Underground Room Closure." *Int. J. Rock Mech. Min. Sci.* Vol.34, No. 2, pp 233-247.

5. Conceptual Design Description for Heavy Shaft Hoists

Sandia National Laboratories (SNL) has contracted DBE TECHNOLOGY GmbH (DBE TEC) to describe the technical basis for a shaft hoisting system suitable for transporting very heavy payloads. A shaft hoisting system is being considered as an option for transporting used nuclear fuel (UNF) in a generic waste repository design concept. SNL is conducting a series of generic waste management studies for the United States Department of Energy, Office of Used Nuclear Fuel Disposition.

This section presents a vertical shaft hoisting system suitable for payloads up to 85 MT, and it goes further to extrapolate the configuration of a system suitable for payloads up to 175 MT. It also describes the safety analyses used to demonstrate how the shaft hoisting concept meets the same risk standards applied in German nuclear power plants (for example, a core-melt scenario with annual probability of occurrence less than 10^{-6}) and relates the analysis framework to the U.S. preclosure safety standards from the Yucca Mountain Review Plan. Finally, rough order-of-magnitude equipment cost estimates are provided for both systems based on anticipated European material costs.

The technical design for the 85 MT hoisting system has been fully developed for implementation at a potential repository at Gorleben, Germany (Filbert et al. 1994b). Demonstration testing was successfully conducted under the project Direkte Endlagerung ausgedienter Brennelemente (DEAB – Direct Disposal of Spent Fuel Elements) from 1985 to 1995. DBE TEC in conjunction with GNS (Gesellschaft für Nuklear-Service mbH) is currently developing the technical design for a hoisting system suitable for shaft transport of payloads up to 175 MT under the recently completed DIREGT II project (Filbert et al. 2012). Specifically, the aspect of the DIREGT II project related to hoisting of heavy loads considers the direct disposal of dual-purpose canisters (DPCs) in a repository constructed in the Gorleben salt dome. Pilot testing of the 175 MT design is currently being planned. The design information presented in this report is based on the experience gained from these projects.

A similar design to the 85 MT hoisting system has been developed as part of the Belgian Agency for Radioactive Waste and Enriched Fissile Materials (ONDRAF/NIRAS) Safety and Feasibility Case (SFC1) R&D program for the disposal of radioactive wastes. SFC1 is intended to demonstrate the constructability and operational functionality of a repository for use in a "go for siting" decision by the Belgian government.

The payloads considered here are consistent with R&D activities that have been conducted in Germany. Specifically, the recently completed Preliminary Safety Assessment Gorleben (Vorläufige Sicherheitsanalyse Gorleben – VSG) considers a repository located at a hoisting depth of approximately 870 m below ground surface. Hoisting payloads of up to 85 MT are considered, while in the separate DIREGT II project hoisting payloads of up to 175 MT are considered.

Generic studies in the U.S. DOE, Used Fuel Disposition (UFD) R&D Campaign focus on the disposal of existing UNF, high-level waste, and potential future waste arisings. Investigations include development of disposal concepts for mined geologic repositories in clay/shale media, salt and crystalline rock. The reference repository design concepts for these host rock types consider repository horizons at depths of approximately 500 m below ground surface (Hardin et al. 2012). The hoisting system concepts described here could be applied to any of these disposal concepts and media. The 85 MT capacity hoist would be suitable for any package up to 12-PWR

size (or BWR equivalent). The 175 MT capacity hoist could accommodate waste packages based on 32-PWR size dual-purpose canisters (or larger, depending on total weight, self-shielding, etc.).

5.1 Shaft Hoisting

Shafts are often used to transport mined material from the subsurface to the surface in deep underground mines. Hoisting systems with payload capacity of up to 50 MT are used in the mining industry. The hoists are generally optimized to address various design constraints imposed by payload requirements; transportation path and velocity; equipment procurement, installation, and maintenance costs; and operational safety and reliability considerations.

Similar constraints are also imposed on hoisting systems for use in repository applications, however with significant differences. Repository hoisting systems are designed to transport heavy payloads to the subsurface, and the payload weight can be significantly greater. Additionally, while safety is always an important factor in any hoisting system, a potential accident in a repository can have significant radiological consequences possibly extending beyond the operational facility. Therefore the systems must be designed to meet not only mining regulatory requirements but radiological safety requirements as well.

The reference salt repository concept developed by the UFD R&D program in 2011 includes a payload weight of 85 MT, which is sufficient for shaft transport of 12-PWR (pressurized water reactor) size waste packages. Thus the feasibility studies for the 85 MT hoist at Gorleben can be directly applied. The dimensions of a 12-PWR waste package are similar to the POLLUX® canister, and smaller than the Belgian Supercontainer for disposal of spent nuclear fuel (SNF) and high-level waste (HLW) (diameter 2,150 mm and length 6,250 mm).

More recently, the UFD R&D program has been investigating the feasibility of direct disposal of DPCs. Waste packages consisting of loaded and sealed DPCs, packaged in disposal overpacks, would weigh 80 to 90 MT. The shielded transporter (e.g., cart) used to carry these packages underground would add up to another 80 tons, hence the U.S. interest in hoisting systems with payload capacity up to 175 MT.

5.1.1 Shaft Safety Requirements

Shafts are the vertical connections between surface and underground facilities, and are important repository components. Damage to shafts or failures in the hoisting systems could directly impact operation of the entire repository. Repository shafts must meet stringent safety requirements which drive the design of hoisting systems. Safety considerations specific to shafts for transporting SNF or HLW into a geologic repository include:

- Fire prevention with emphasis on bearing parts of the static constructions and electrical installations as well as the waste package
- Prevention of a waste package from falling down the shaft or onto shaft equipment
- Prevention of unintended shaft access by loaded or empty transport carts
- Prevention of collisions between the cage and other shaft components
- Prevention overwinding of the cage (i.e., lifting or lowering the cage either above or below design specified bounds)

5.1.2 Design Basis Regulatory Requirements

The hoisting system presented here follows requirements from the relevant German regulations. Specifically, the relevant German regulations used in developing the conceptual design are:

- The German Mining Regulations for Shaft and Inclined Haulage Installations (BVOS – Bergverordnung für Schacht und Schrägförderanlagen from 15.10.2003 (BVOS 2003)
- Technical Requirements for Shaft Hoisting Installations and Inclined Hoisting Installations (TAS – Technische Anforderungen für Schacht und Schrägförderanlagen) from December 2005 (TAS 2005)

The BVOS provides general regulations for the permitting, commissioning, monitoring and operation of hoisting systems in mines, while the TAS provides the detailed requirements for the construction of hoisting systems. TAS further defines calculation methods and identifies applicable construction standards, e.g. DIN EN 12385-1 (Steel wire ropes - Safety - Part 1: General requirements). Additional regulations, e.g., DIN 4118 (Headframes and winding towers for mines; Design loads, calculation principles and design principles) govern the construction of relevant surface installations. TAS is aligned with applicable European Union codes and standards, i.e., Eurocodes.

5.2 Conceptual Design of the Hoisting System for Shaft Gorleben 2

The shaft hoisting system as currently conceived would have an eight-cable Koepe friction winder system for an 85 MT payload. The Koepe winders, as opposed to drum winders, use an “endless” cable configuration looped through large driving wheels. The cables are driven by a wheel at the top of the shaft and looped back up in the shaft sump (i.e. the deepest portion of the shaft, which would extend approximately 40 m below the base of the disposal level shaft station).

The cage and a corresponding counterweight are fixed to the cables so that as one moves up the other moves down the shaft at the same time (see Figure 5-1). This arrangement provides the friction needed between the winder pulley and the cables. The use of a counterbalance configuration produces a much lower starting torque than other hoist types, which in turn allows Koepe winders to use comparatively smaller motors. Employing multiple cables reduces the diameters of the individual pulleys, cable stresses, torque, and power requirements.

Note that the balance cables below the cage and counterweight do not bear the weight of the payload, cage, or hoisting cables. Their function is strictly to balance the variable length of hoisting cables on each side of the winder during operation. As such, the cable separators and cable guide system at the shaft sump would not apply loads to the balance cables except as necessary to turn them and prevent entanglement or contact with shaft internals.

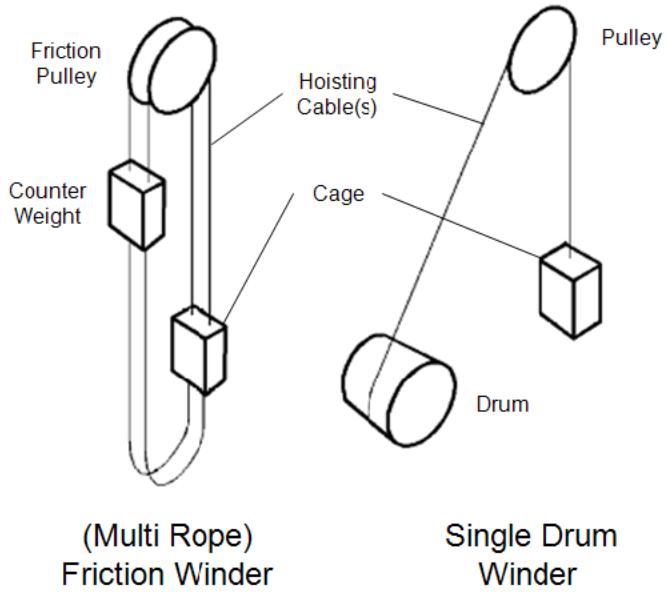

Figure 5-1. Principles of operation for friction and drum winders

During waste transportation the payload (e.g., the 12-PWR package, shielding and transportation cart) is fixed inside the waste transport hoist cage. The maximum hoist velocity is set to 5 m/s. Whereas some mining hoists may operate faster, lower velocity reduces the torque, power and braking requirements and is inherently safer. Because only a small number of transports would be anticipated to occur on a daily basis, hoist velocity would not impact operational efficiency.

The key factors determining the design of the hoisting system are the size, shape and weight of the payload. The 85 MT design is based on the shaft transport of a single POLLUX® type canister with shielding and associated transportation cart. The POLLUX® canister is a cylindrical container with a length of 5.5 m and an outer diameter (including trunnions) of 1.96 m (Bollingerfehr et al. 2012, Section 2.1).

In addition to the maximum payload weight, for purposes of designing the overall hoisting system the hoist cage and the hoist cables must also be taken into account. The hoist cage for an 85 MT payload would have an approximately weight of 36 MT (Filbert et al, 1994f). The total weight of the cables depends on the selection of cables in the design, the length of the cables determined by the hoisting depth, and the loads connected to them. Cable requirements as designed for the Gorleben 2 shaft are discussed below.

5.2.1 Cable Requirements and Safety Factor

Selection of the cable type depends on the diameter and weight of the individual cables. The diameter in turn depends on cable material composition, the selected winder, the winding pulley, the cable guide track, the payload mass distribution, intended hoisting velocity and distance, and anticipated environmental conditions inside the shaft (which impact the selection of cable material type).

The cables are looped over the hoist pulley and translated into a vertical orientation for shaft operations. The cables have the highest safety function of all hoisting system components during

hoisting operations. They must ensure that the cage with its payload cannot fall down the shaft during transport. To this end safety factors established for modern cable hoist systems preclude a fall accident related to a cable rupture failure. German TAS requirements (Part 6.8.1) for hoist cables used for material transportation establish a minimal safety factor (S) for static loads as a function of cable length (L) as follows:

$$S \geq 7.2 - 0.0005 \times L$$

The cable length is measured between surface and subsurface shaft stations. The required factor of safety S for the total cable length of one strand is 6.72, or almost seven times higher than the designed load. The German requirements moderately exceed similar US cable requirements given in 30CFR§77.1431.

The hoisting cables for the Gorleben 2 shaft design have a diameter of 50 mm. They are manufactured in a three-layered configuration of oval strands (Figure 5-2). The Gorleben 2 design length for a single cable is approximately 950 m, based on the hoisting distance (i.e., 870 m) and the additional cable length needed to loop over the winder and attach to the counterweight. The performance of the hoist cables over their designed lifetime was tested and confirmed suitable in a specialized laboratory to simulate the expected lifetime loads as part of the DEAB project (Filbert et al. 1994c).

Three flat balance cables with a thickness of 38 mm and width of 264 mm, and a total weight equal to that of the hoist cables, are connected below the cage and the counterweight to ensure an overall equal distribution of cable loads. The balance cables are non-load carrying and therefore have lower design performance requirements than the hoist cables. In accordance with TAS (Part 6.8.3) balance cables must meet a minimum safety factor exceeding six times their total weight.

The counterweight compensates for 50% of the payload weight as well as the weight of the hoist cage and cable attachments during the hoisting cycle. To avoid entanglement of the counter balance cables, the cables are looped through cable separators in the shaft sump. As needed, additional performance assurance can be achieved through the use of a cable guide system installed in the shaft sump.

The total load on the hoist cage plus cable component is approximately 214.2 MT. The load on the counterbalance plus cable component is approximately 171.7 MT for a maximum overload of 42.5 MT (half the payload capacity).

In accordance with TAS, the overall factor of safety (S) for the cables is determined to be:

$$S = \frac{tensile\ strength \times number\ of\ cables}{highest\ static\ load} = 7.27 \geq 6.72$$

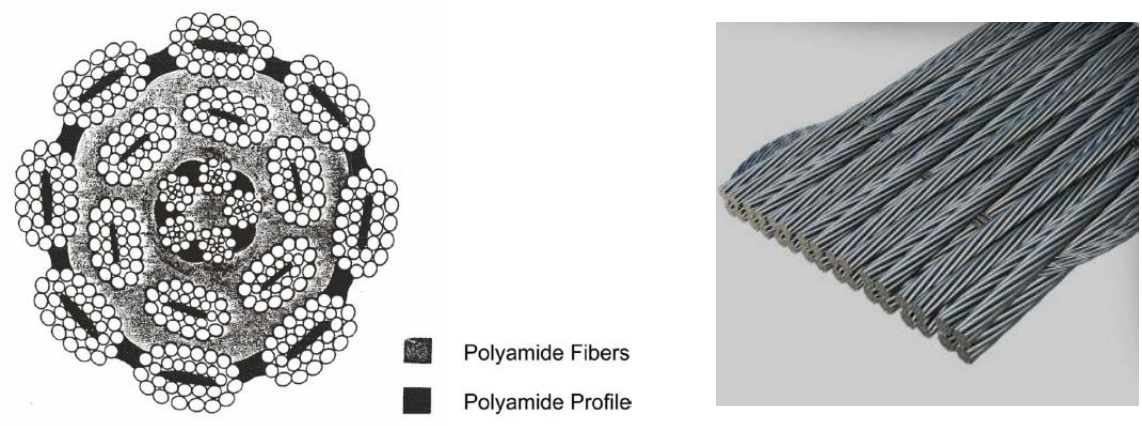

SOURCE: Filbert et al. 1994c, Figure 2-3 SOURCE: Bridon 2013

Figure 5-2. Three-layer oval cable strand (left); and an example of flat balance cables (right)

Some advantages of a Koepe winder over a drum winder were described in the introduction to this section. A significant disadvantage with a Koepe winder is the possibility of cable slip. The hoisting system includes several design features which help to prevent cable-slip events. Technical details, and control and monitoring systems that prevent cable slip are distributed in different components of the hoist system. Important design measures with cable-slip control functions include:

- Selection of a suitable cable load ratio (e.g., counterweighting scheme discussed above)
- Monitoring of the cable load ratio
- Acceleration limits for the winder and monitoring of the acceleration
- Defined braking rates, forces and pressures
- Monitoring of the braking rates, forces and pressures
- Assurance of adequate friction values
- Hoist cage design features specifically intended to avoid high-rate load transfers

As a part of the DEAB project a separate study (Filbert et al. 1994d, Section 7) evaluated the risk of cable slippage and developed associated technical recommendations. The study calculated the relevant load ratios and critical accelerations during hoisting and showed that the system as designed, would successfully prevent cable-slip events.

In addition to the technical requirements of TAS, the BVOS (BVOS 2003) requires several monitoring functions to be incorporated in the hoist design. The general safety strategy of the German regulations includes both technical design and stringent monitoring of the hoisting equipment and cables to detect and mitigate potential failure conditions.

5.2.2 Hoist Cage and Cable Attachments

The transport cage consists of two main components, the frame and the transport platform. The transport platform is a false bottom construction that is free to move vertically within the cage

frame. The transport platform is the load carrying floor of the cage during hoisting. During loading and unloading operations the transport platform is latched to fixed supports at the shaft stations, thus isolating transient loads from the hoist cables.

The frame of the transportation cage is constructed from bolted and welded steel beams. The outer and inner cage dimensions are defined by waste package requirements, the shaft, and the required safety buffer distance between the cage and the shaft wall. Sockets for the cage-latch system are installed on both short sides of the transport platform (Figure 5-3). The cable attachments for the hoist and balance cables are affixed at the top and bottom, respectively, of the cage frame. The attachments used in the design are state-of-the-art and extensively used in modern mine hoisting systems. The whole cage system, consisting of the cage and the cable attachments is approximately 12 m high.

Four guide blocks are installed on one long side of the hoist cage to maintain distance from the shaft wall. They connect the cage with the guide rails and hold the cage in correct position. With heavy hoists of this type the shaft must be very close to plumb, minimizing side loads during hoisting.

The cable attachments for the hoist and balance cables are affixed at the top and base of the cage frame. The cable attachment assemblies are connected to the hoist cage using universal joints. Each assembly is approximately 4.2 m in height and weighs approximately 1.1 MT (included in the total weight of the cage). The individual attachment assemblies use a clamping thimble to secure and lock the cable in place. Each clamping thimble is attached to a vernier adjustment mechanism that allows fine tuning adjustments for slight differences in cable lengths ensuring that stresses can be evenly distributed. Adjustment mechanisms are needed only at the hoist cage and not at the counterweight assembly. The cable attachments used in the design are state-of-the-art and extensively used in modern mine hoisting systems.

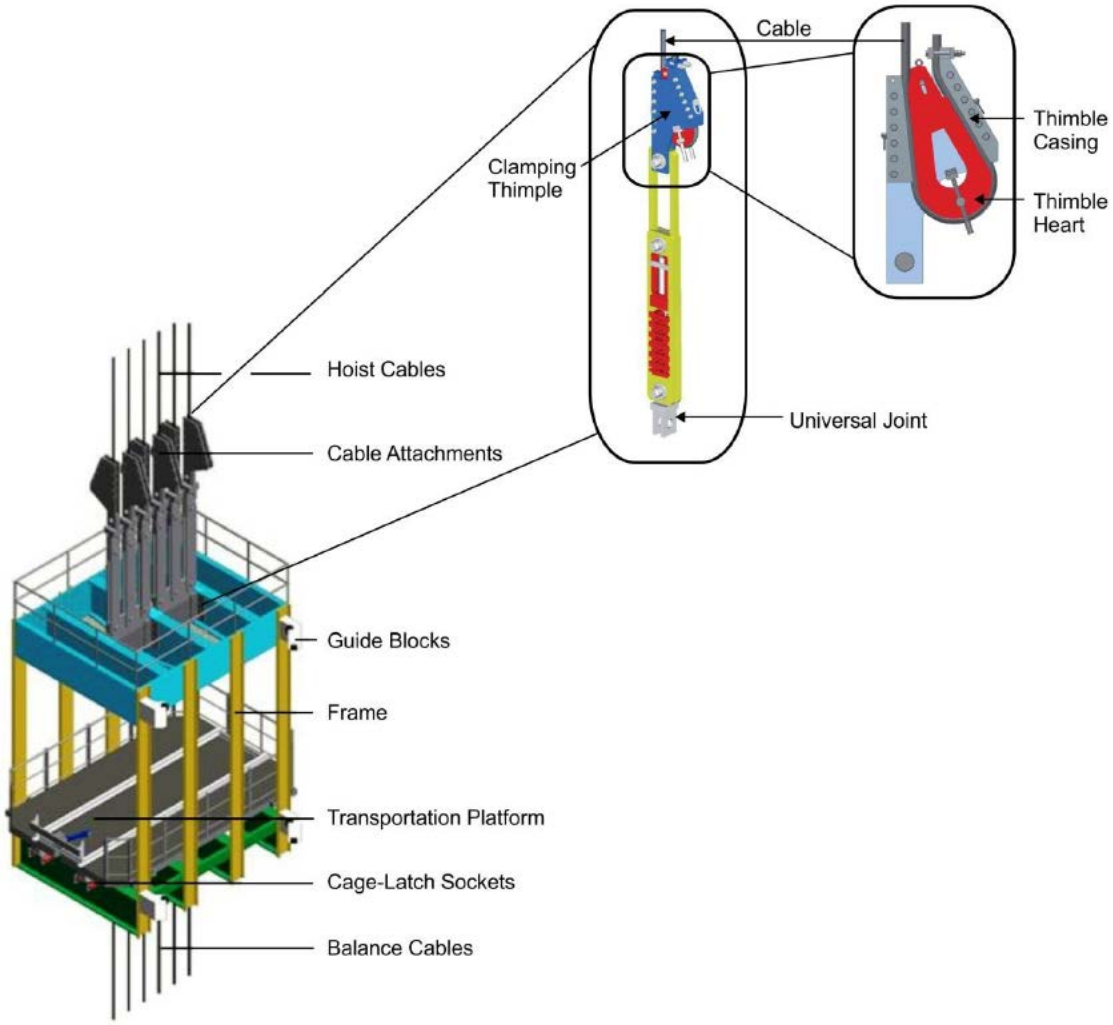

SOURCE: (Filbert et al. 2012, Figure 2-6)

Figure 5-3. Hoisting cage with mounting attachments as planned for a 175 MT system

The transport platform weighs approximately 6 MT. The platform supports the waste shipment during the hoisting process and is equipped with grooved rail tracks to hold the waste transport cart. During on-setting of the waste shipment, the transport platform is held in place by the cage-latch system. With the transport platform firmly held by fixed supports, the cage frame is lowered slightly to release tension in the cables and to retract the arresting pins. Once the waste shipment has been moved onto the transport platform the cage frame is slowly raised into its former (operating) position. Rubber gaskets between cage bottom and transport platform abate potential impact loads. The arresting pins are matched with locking sockets in the transport cart and the cables are pulled taut to assume the combined weight of the cage and waste shipment. Once the cables have been pulled taut in this fashion the cage-latch system is disengaged and the cage is ready for hoisting. This process ensures that dynamic loading of the system associated with on-setting the waste shipment (i.e., loading and unloading) do not result in large, rapid load transfers to the cables that would have a negative impact on cable life.

The counterweight (Figure 5-4) is designed to balance the loads imposed by the cage and provide adequate friction between the cables and the winding pulley. It consists of a supporting steel frame filled with steel block weights to achieve the mass needed for balance. Using this system the total weight of the assembly can be adjusted by adding or removing the steel blocks as needed based on the type of waste package to be transported.

The proposed dimensions for the counterweight frame are: (Filbert et al. 1994b, Section 4):

- Length: 3,300 mm
- Width: 900 mm
- Height: 11,500 mm

The required mass for the counterweight assembly is determined by adding the weights of the hoist cage and one half that of the payload. For example, for transporting a POLLUX® canister the cage weight (36 MT) plus half the weight of the transport cart (0.5 × 20 MT) plus half the weight of the loaded canister (0.5 × 65 MT) sums to 78.5 MT.

5.2.3 Hoist Mechanism

The hoist mechanism is installed in the shaft headframe and powers the hoisting system for the waste transport. The hoist consists of:

- Hoisting pulley
- Brake system
- Engine
- Control and safety systems

The hoist is designed consistent with TAS requirements (TAS 2005) and is characterized by parameters identified in Table 5-1.

Table 5-1. Hoisting System Design Parameters

Parameter	Value
Hoisting distance	870 m
Number of cables	8
Cable diameter	50 mm
Maximum overload	42,500 kg
Friction pulley diameter	5,000 mm
Engine power	2 x 2800 kW
Hoisting velocity	5 m/s

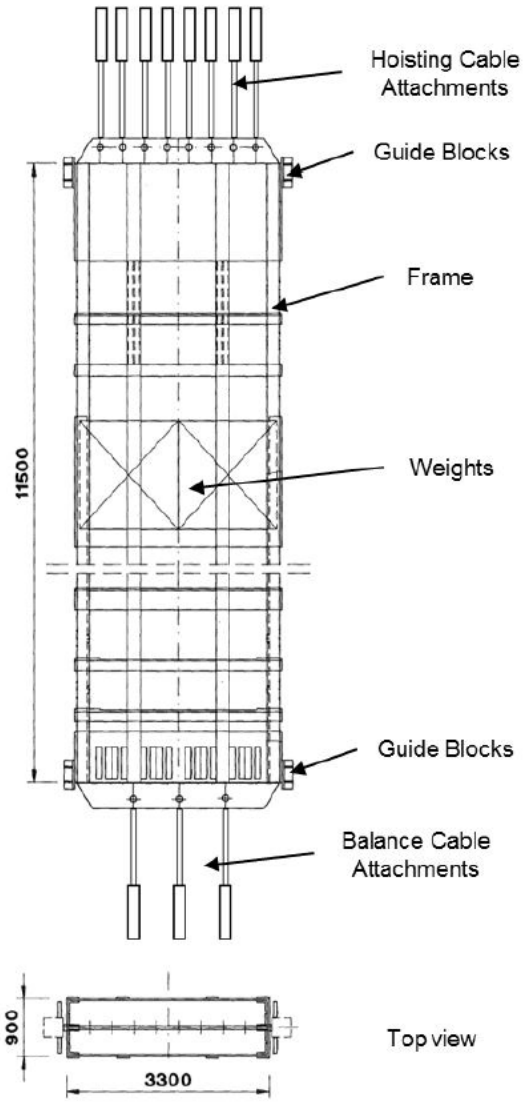

SOURCE: Filbert et al. 1994b, Figure 4-6

Figure 5-4. Counterweight assembly

5.2.3.1 Friction Winder

The friction-winder component of the hoisting system (also referred to as the drive sheave or pulley) is installed in the headframe directly above the shaft. The placement of the drive pulley is based on the shaft diameter and the standoff between the cage and the counterweight assembly. The pulley diameter at the cable liner surface is 5,000 mm. An additional deflection pulley defines the distance between cage and counterweight (which is less than 5 m).

An important performance factor for the drive pulley is the friction coefficient between the cables and the pulley. TAS Part 3.10.2 requires a minimum friction coefficient of 0.25 between the pulley and an individual cable. Because the friction factor for steel on steel is approximately 0.15, a material other than steel is required as a cable liner for the pulley to achieve the minimum

friction factor. Selection of the pulley lining material depends on the cable design and the technical and environmental conditions at the shaft. Several parameters such as the cable guide profile, the lining material, and the attachment of the liner to the pulley must be considered in the design.

5.2.3.2 Hoist Motor

The hoist motor is designed as a dual-motor system consisting of two identical DC motors installed on each side of the main drive pulley as shown in Figure 5-5, that directly power the hoist. The work associated with hoisting the payload is split between the two motors, which allows the use of existing off-the-shelf technology, which is preferred from both reliability and economic considerations. Additionally, the dual motor configuration minimizes static and dynamic loads placed on the drive shaft, bearings, and other components. The dual motor configuration allows completion of a hoisting operation in the case of a single motor failure, at a reduced speed. However, the use of two motors to drive the hoisting system requires a higher level of engineering control for synchronizing the motors.

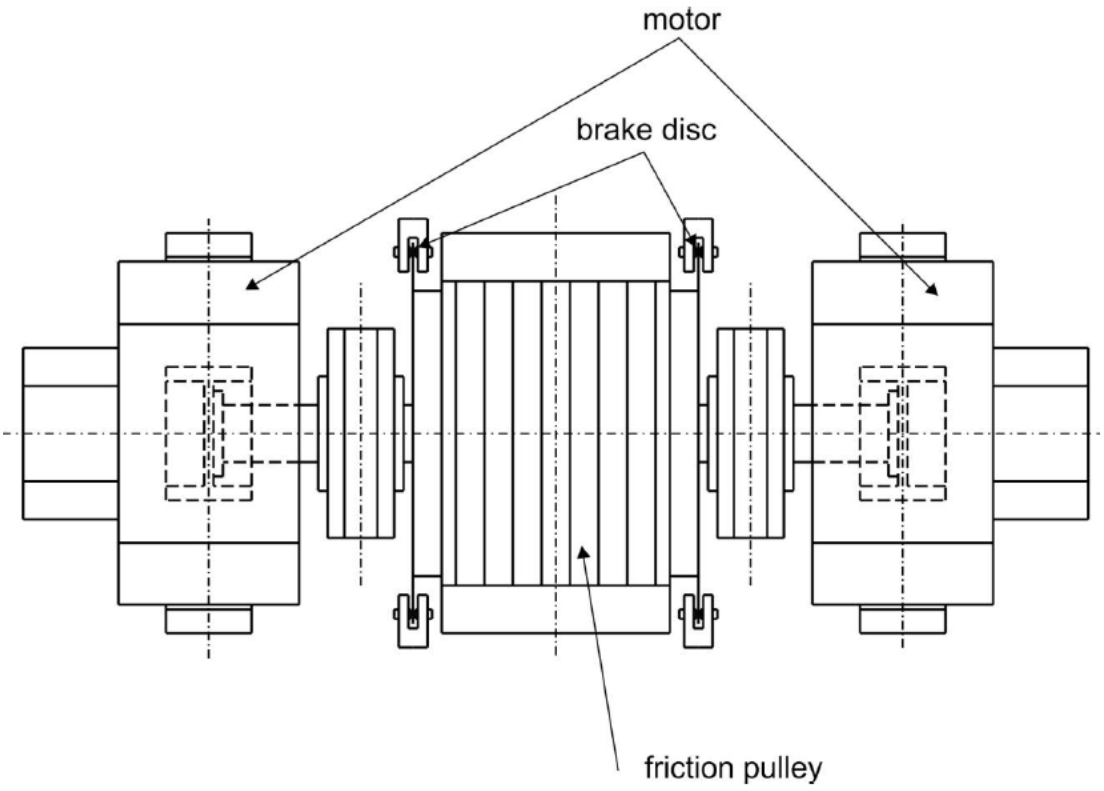

SOURCE: Filbert et al. 1994b, Figure 4-8

Figure 5-5. Friction pulley and dual motors

5.2.3.3 Braking System

The braking system is designed to normally operate with a controlled braking force to ensure that constant retardation levels are maintained during all operating situations, regardless of the

direction of travel, speed, load or other factors. This greatly improves the safety performance of the hoist while limiting mechanical stresses on the equipment. There are two operational braking modes for the system: normal braking and emergency braking. The brakes are designed as an electrohydraulic disc brake system consistent with the requirements of TAS (Section 3.9).

During normal operations the hoist speed is slowly increased or decreased by the motor drive system. When the hoist has been decelerated to a creeping speed and the cage is located approximately 1 m from the station level, the hydraulic brakes are actuated by reducing the pressure in the brake units to obtain a smooth contact with the brake discs. The pressure is further reduced to zero to reach a full stop.

For emergency stops, braking is accomplished exclusively by means of the hydraulic disc brake system. All functions of the hoist that are required for safe operation are monitored by sensors connected to the electrohydraulic system. Should an unsafe condition be indicated by any one sensor the emergency braking system of the hoist is activated. Possible circumstances under which an emergency stop could be initiated are monitored by the sensors identified in the Table 5-2 (Filbert et al. 1994b, Table 4-4).

Table 5-2. Hoist safety system sensors

Original German System Designation	English Translation of System Designation
Kontinuierliche Geschwindigkeitsüberwachung	Continuous monitoring of hoisting speed
Punktweise Geschwindigkeitsüberwachung	Selective point monitoring of hoisting speed
Gegenseitige Überwachung des Drehzahlgebers und Winkelschrittgebers	Mutual monitoring of the speed sensor and the incremental angle encoder
Gegenseitige Überwachung Ständerwicklung	Mutual monitoring of the stator winding
Motortemperaturüberwachung, Auslösung	Motor temperature monitoring, triggering
Stromflußüberwachung der Thyristoranlage des Ständerkreises mit Auswertung	Power supply control system monitoring of the thyristor stator circuit and evaluation
Auslösung des Sicherheitskreises "Ungeregelte Sicherheitsbremsung" (Signal aus Bremssteuerung	Activation of the safety circuit "Unregulated safety braking" (signal from brake control)
Einsatzüberwachung Hüllkurve	Monitoring of the envelope curve
Gegenseitige Überwachung der Drehzahlgeber für Regelung und Überwachung	Mutual monitoring of the rotational speed sensors used for regulating and monitoring systems
Schachtschalterüberwachung	Shaft-switch monitoring
Ständer-Erdschlußüberwachung, Auslösung	Stand-ground fault monitoring, triggering
Elektronische Rücklaufsperre	Electronic backstop
Schachtzähler/Sprungüberwachung	Shaft position and target depth monitor
Soll/Istwertüberwachung der Drehzahl und des Ständer und Erregerstromes	Target-value monitoring of the stator speed and exciter current

SOURCE: (Filbert et al. 1994b, Table 4-4)

Conditions that could initiate an emergency braking sequence include, among others:

- Excessive hoist speed
- Higher than permissible motor temperatures
- Higher than permissible motor torque or speed
- Electrical failures inside the motors
- Electrical power supply failures

In addition to these automatic responses the braking system can also be activated manually.

Additional initiating events are associated with release of the cage from the shaft stations. The safety brake system cannot be released at either the surface or subsurface shaft stations if for example the motor temperature is too high, electrical problems are indicated, or on-setting of the payload has not been fully realized.

The brake system consists of hydraulically controlled brake calipers affixed around the brake disc at both sides of the friction winder (Figure 5-5). In principle the brake system works similarly to a common hydraulic disc brake system such as those used in cars (except that braking force is exerted when pressure is released). In accordance with TAS requirements the braking system must have a safety margin so that braking capacity is at least 3 times greater than the highest expected load. In the Gorleben 2 design the braking system uses 24 brake calipers (Figure 5-6) with 12 calipers on each brake disc divided between two brake stands, yielding a safety factor greater than that required by TAS. The orientation of the brake calipers is shown in Figure 5-7.

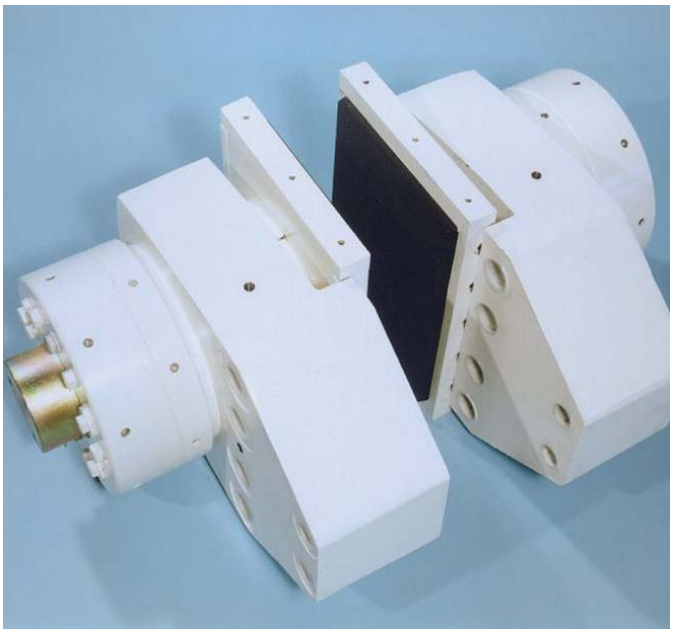

SOURCE: SIEMAG 2013a

Figure 5-6. Brake caliper (Type SIEMAG BE 100)

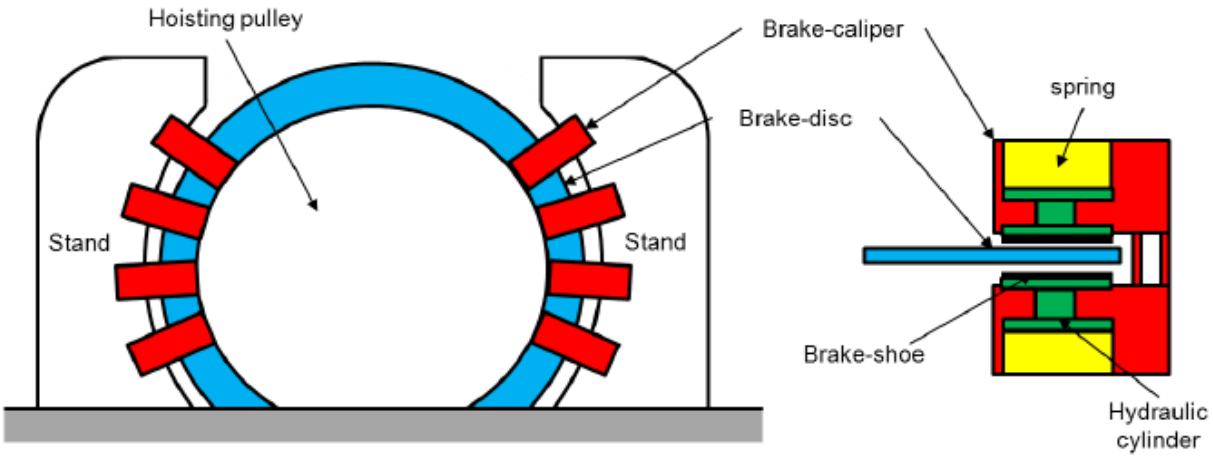

Note: the Gorleben 2 design uses 12 brake calipers, with six each on two stands, for each of two brake discs.

Figure 5-7. Conceptual design of the braking system (left) and structure of the brake caliper (right)

The brake calipers are hydraulically actuated. The hydraulic cylinders inside the brake calipers compress pre-set disc springs. The cylinder is attached to the brake shoes (pads) and releases

them during hoist operations. Without the hydraulic pressure the springs relax, the calipers close, and the cable pulley is locked. In the event of emergency braking, the pressure is reduced automatically to a predefined value which allows the gradual activation of the system without initiating a cable slip event. Without the predefined pressure the disc springs inside the brake caliper would close immediately and the sudden stop could cause cable slippage. The braking system is controlled electronically, integrated with the previously described electrohydraulic system. Braking is automatically initiated in case of a power failure or overwind or other serious incidents. All safety-relevant elements of the braking system are installed in redundant configurations.

5.2.4 Headframe and Shaft House

The main mechanical and electrical components of the hoisting system are located in the shaft headframe. Operational supporting functions are located in the shaft house. The shaft house is located immediately adjacent to and forms an integrated structure with the headframe.

The headframe provides the structural support function under both static and dynamic load conditions for the hoisting system, including the Koepe pulley, deflection pulley, hoist cage and counter weight, hoist cables, and the payload. Additionally, the headframe is designed to provide fire protection for load bearing components and equipment. The headframe as represented in this report would be a steel framework with load-bearing capacity sufficient for functionality under both normal and low-probability seismic conditions.

The main components of the headframe and shaft house, relevant to hoisting operations, are shown in Figure 5-8. The following components of the hoisting system are contained within the headframe:

- Machinery level and overhead crane
- Safety winder
- Clamping and lifting device for maintenance
- Lift and stairway
- Guiding stand with Strain Energy Linear Ductile Arrestor (SELDA) system
- Impact beam
- Catching bolts
- Interior support structure with air lock

Additional details of the headframe and shaft house are discussed in the following subsections.

The Koepe hoist and the safety winder are located in the highest floor of the headframe, referred to as the winder floor. The winder floor is at an elevation of approximately 44 m above ground surface and is equipped with an overhead crane to facilitate maintenance and repair activities on the winder.

A clamping and lifting device is installed below the winder floor, at a height of approximately 24 m above ground surface. This device is used to grasp and secure the hoist cables during maintenance and repair operations (e.g., servicing the winder). The device can lift and lower the cables to facilitate repairs.

The surface shaft station, including access to the safety winder, is located on the ground floor level. A stairway and lift provide access via the shaft station to the various floors of the headframe.

The guiderail support structure at the shaft station is a steel framework designed to allow the cage and counterweight guide rails to extend above ground for loading and operation of the hoist cage.

Multiple safety features and systems minimize hazards associated with overwind accidents, including impact beams, SELDA systems, and catch gears. (Note similar systems are also used at the disposal level shaft station.) Impact beams are installed at the top of the guiderail support structure as a safety barrier to protect the Koepe winder. Under normal operating conditions the highest position of the hoist cage is 12 m below the impact beams (reversed at the lower shaft station). The SELDA system is installed in this gap and the catch gears are integrated into the upper portion of the guide rails. These catch gears are intended to hold the hoist cage in position in the event of an overwind accident requiring the SELDA system (Section 5.2.4.2).

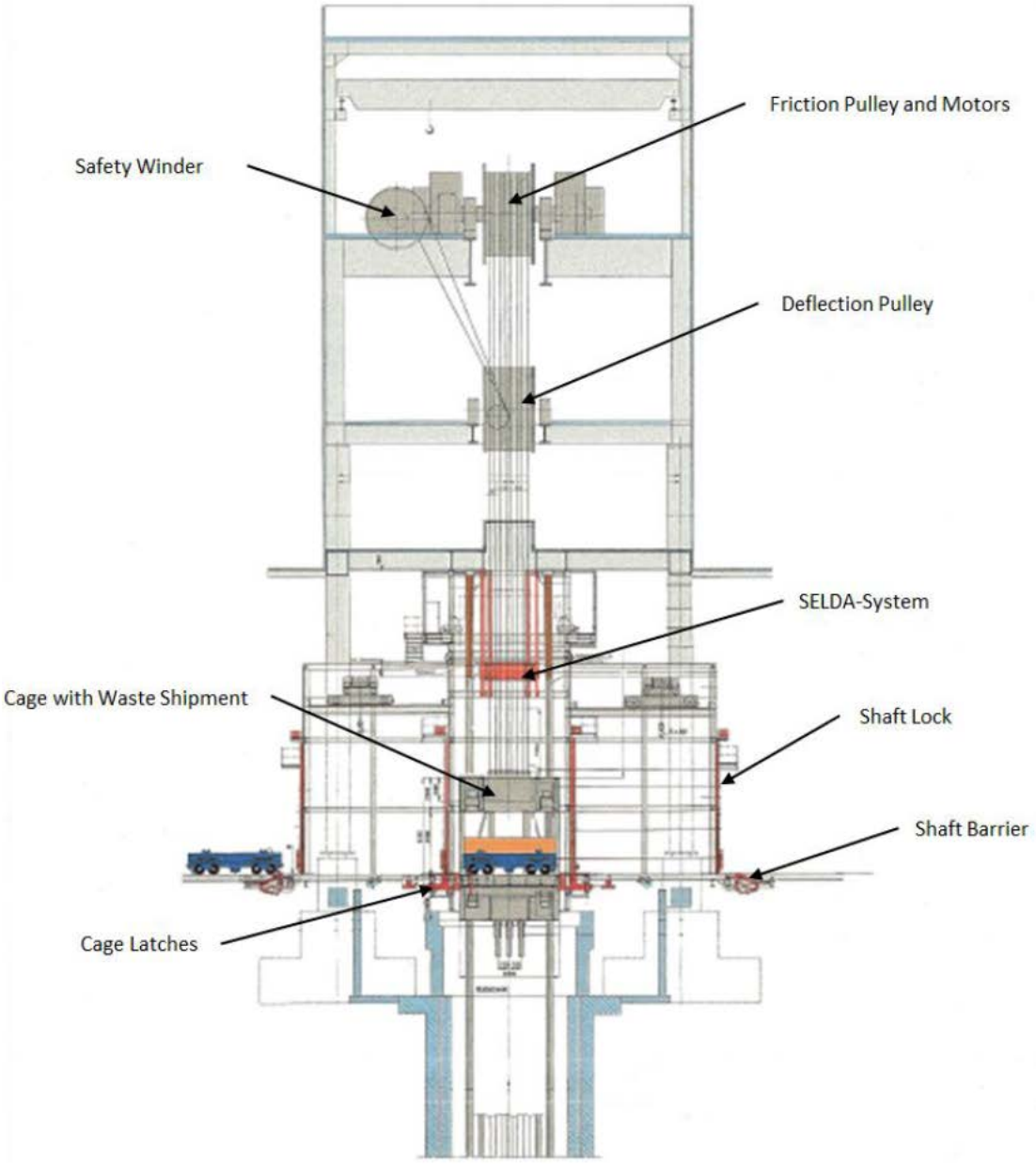

SOURCE: Filbert et al. 1994b, Figuire 4-1

Figure 5-8. Design of the shaft hoisting system for the Gorleben 2 design, surface shaft station

5.2.4.1 Shaft House Surface Station Safety Features

The shaft house surface station is located at the base of the headframe. Potential options for configuration of the station are shown in planar view in Figure 5-9 and cross-sectional view in Figure 5-10. It functions to transition the waste shipment from horizontal surface transportation to vertical shaft transportation. To preclude the fall of a waste shipment or locomotive down the shaft there are no direct rail tracks to the shaft. Rather, a traverse table as shown in Figure 5-9 or a turntable should be installed to interrupt the direct rail linkage to the shaft. This precaution

eliminates the possibility of a combined fall of a locomotive and waste shipment down the shaft. Additionally a shaft barrier is installed directly in front of the shaft to preclude the fall of a waste shipment. On-setting machines are used to move the waste shipment at these transition points.

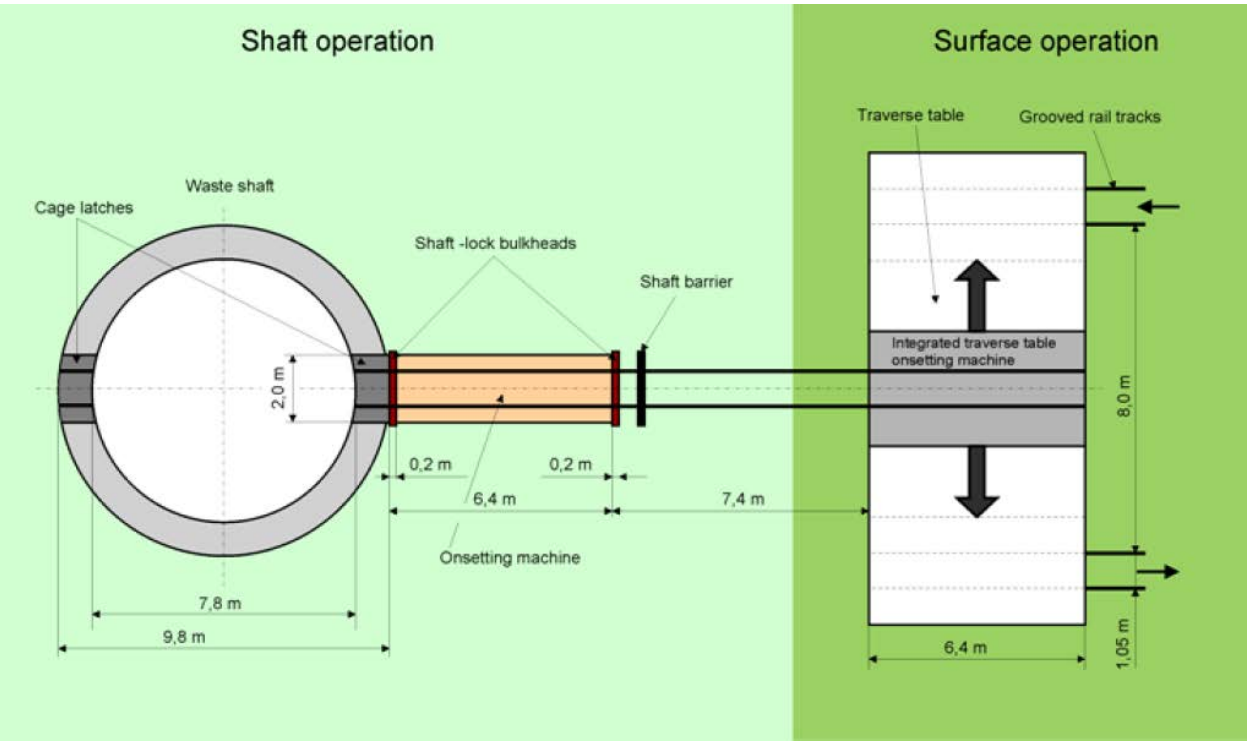

SOURCE: Herold et al. 2013, Figure 21

Figure 5-9. Configuration of surface station systems for loading waste shipments

Before the transition maneuver can be initiated the hoist cage must be in place at the shaft surface station and the cage-latch system must be grasping the transport platform in the hoist cage. Mechanical and procedural controls are used to ensure that the transition maneuver is not initiated until these requirements have been met.

Once the hoist cage has been properly positioned either a locomotive or an on-setting machine moves the waste transportation cart from the delivery rail tracks onto either a traverse table or turntable. The traverse/turntable brings the waste shipment into position in front of the outer shaft-lock bulkhead and the shaft barrier. An integrated on-setting machine pushes the waste shipment from the traverse/turntable. The shaft barrier is in the raised position to protect the outer shaft-lock bulkhead. The outer bulkhead is opened, the shaft barrier is lowered and the on-setting machine moves the waste cart into position directly in front of the inner shaft-lock bulkhead. Once the waste cart has been positioned in the shaft-lock the outer bulkhead is closed, the shaft safety barrier is again raised, and the inner bulkhead is opened. A second on-setting machine located in the shaft-lock floor pushes the waste transport cart onto the waste transport platform in the hoist cage. The inner shaft-lock bulkhead is closed and the hoist cage with payload is readied for shaft transport.

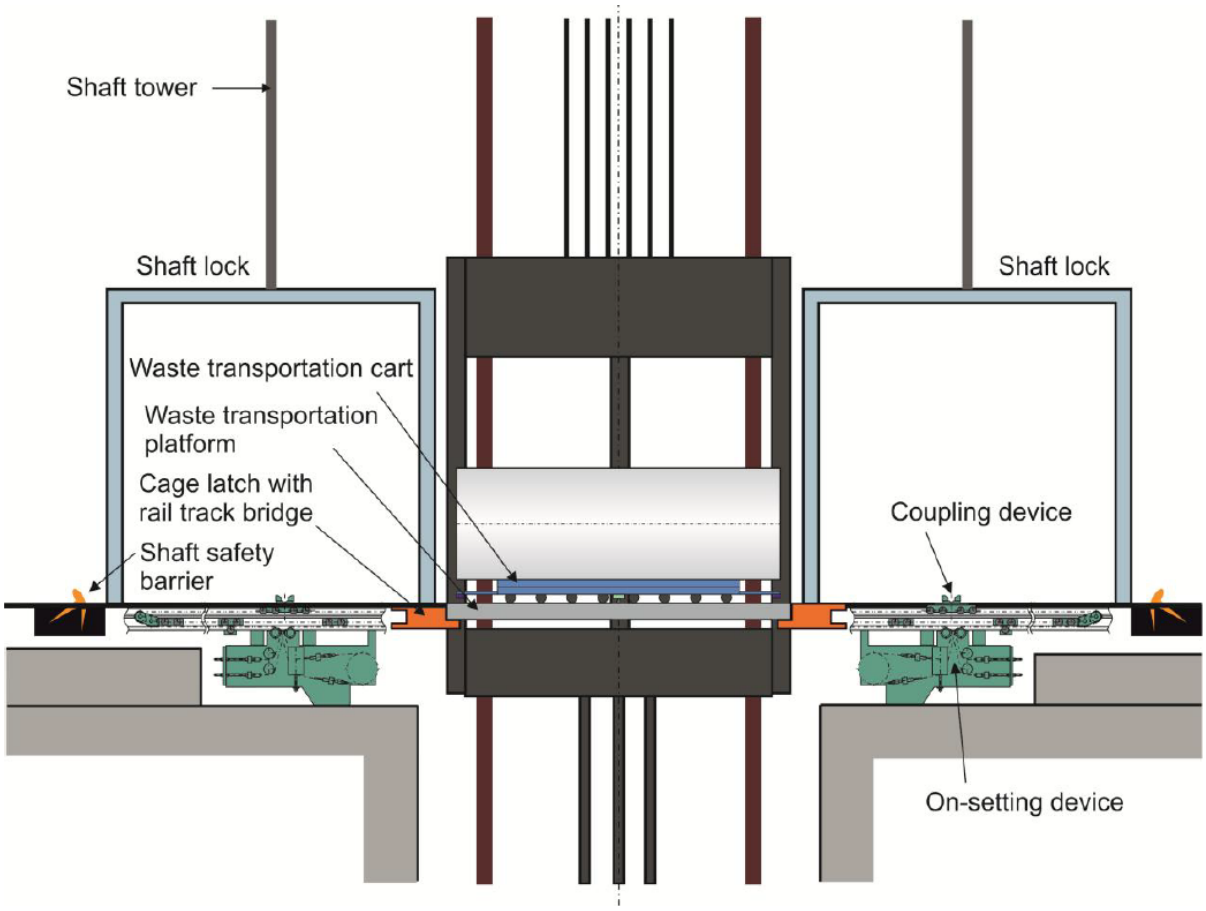

SOURCE: Herold et al. 2013, Figure 22

Figure 5-10. Potential Configuration of a Shaft House Surface Station with Safety Systems

The feasibility of a similar shaft safety barrier concept was confirmed for a simulated waste transport of 85 MT as part of the DEAB demonstration project (Filbert et al. 1994a). The demonstration test is described in Section 5.3.

A safety circuit is used to monitor all of the functions related to the execution of each step in the loading and unloading process. The safety circuit ensures that each step in the loading and unloading process can only be executed if all of the prerequisite actions have been performed.

5.2.4.2 SELDA System

This safety system protects against accidental overwinds, that is, unintentional hoisting of the cage beyond the prescribed loading and unloading positions at the shaft stations (i.e., surface and disposal levels). Shaft stations at the top and bottom of the shaft are equipped with SELDA-systems and impact beams. Additionally, catch gears are used at the shaft house location. SELDA braking devices function to slow down the cage and the counterweight at a defined rate in an emergency situation without causing damage to equipment or station installations. The system was developed by Fairport Engineering Ltd. and is licensed for distribution outside of the United Kingdom by SIEMAG TECBERG GmbH. The SELDA system was successfully tested for heavy loads by DBE as part of the DEAB demonstration tests for the Gorleben 2 heavy load

hoisting system (Schrimpf 1989) for both the hoist cage and counterweight. The use of a SELDA system with the counterweight (in addition to the hoist cage) avoids the possibility of a cable failure associated with arresting.

A SELDA system consists of several steel bars fixed to a guide frame (Figure 5-11). Each steel strip is connected to a SELDA roller box, which is attached to a brake frame. In the event of an overwind accident the deformation of the steel bars functions to absorb the kinetic energy and brake the cage. The maximum braking distance can be precisely set based on the material properties of the steel bars and the total mass of the hoist cage including the heaviest expected payload.

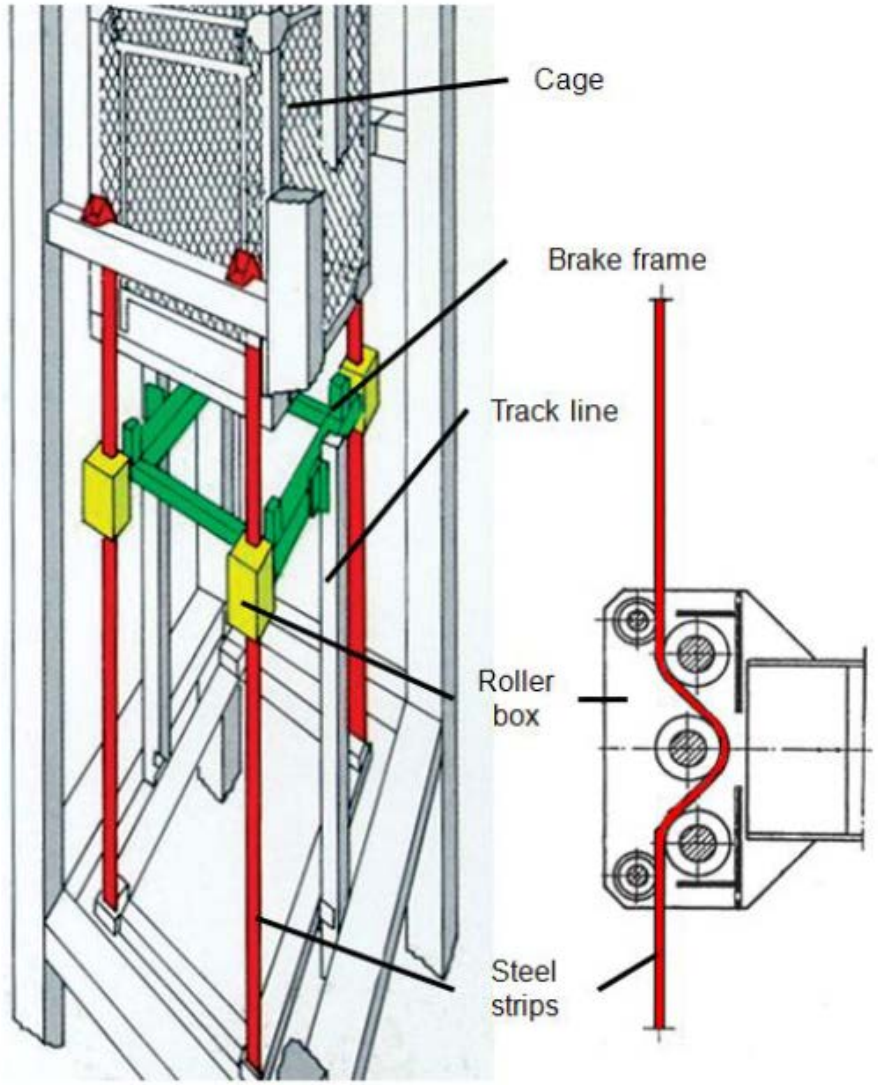

SOURCE: SIEMAG 2013c

Figure 5-11. Concept of the SELDA braking system as designed for the shaft sump

The SELDA system is installed at both ends of the shaft; in the inner support structure of the headframe and in the corresponding structure in the shaft sump. Both SELDA systems function identically.

In addition to the SELDA system impact beams are also installed at both ends of the shaft as an additional safety measure against a possible overwind accident. These impact beams function as a final barrier in case of a failure in the SELDA system. If during an overwind accident the hoist cables also fail, the catch gears are activated (Figure 5-12). The catch gears are installed inside the guiderail to catch the hoist cage after it rises past them. Multiple catch gears are installed in sequence to prevent the cage from falling. Similar catch gears are installed along the guide rails used for the counterweight.

SOURCE: Barker-Davies 2013

Figure 5-12. Example catch gears

5.2.5 Safety Winder/Hoist System

In addition to the main hoist system for waste transportation operations a safety winder/hoist system is also installed in the shaft. The safety winder has a dual role: the hoist provides access to the shaft for maintenance and inspection, as well as an emergency evacuation route for subsurface personnel.

The safety winder consists of a single personnel cage with a maximum payload capacity of 1.1 MT. A single-cable drum winder is sufficient for expected loads. The drum winder is

operated by an external DC motor. The safety winder is operated by an independent energy supply. The system is installed on the machine floor of the headframe. The safety winder is equipped with disc brakes and calipers.

TAS requires that auxiliary and safety winder/hoist systems demonstrate a minimal safety factor of 7.5. The safety factor for the cable is determined from the coefficient of the breaking force of the cable and the maximal expected load.

The safety winder/hoist cage is mounted in the shaft opposite the counterweight construction. The cage is held in place by two steel guide rails. Two pairs of guide blocks equipped with guide rollers (Figure 5-13) mounted on each side of the safety hoist cage maintain correct position of the cage. The maximum hoisting velocity is 4 m/s.

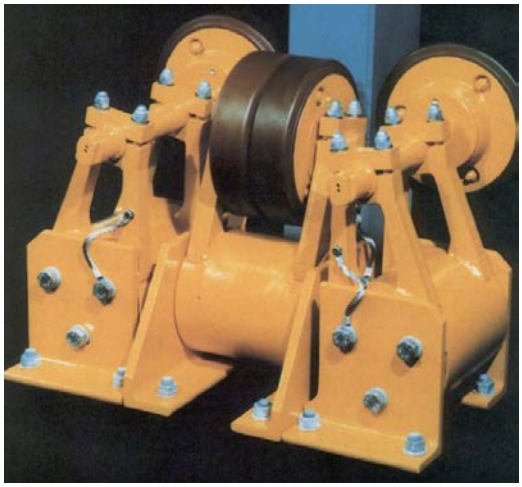

SOURCE: SIEMAG 2013b

Figure 5-13. Safety Winder Roller Guides

The guide rails for the payload hoist cage and the counterweight are similar, but mounted in different parts of the shaft cross-section (Figure 5-14).

5.2.6 Shaft Cross-Section

A shaft cross-section configuration that meets the requirements discussed in this report (based on the Gorleben 2 design) is presented in Figure 5-14. This cross-section provides adequate space for the both the waste hoist cage and counterweight system as well as an emergency personnel hoist cage. Additionally space is available for ventilation ducts if needed, and for various utilities (energy, communication, water, compressed air, piping, etc.).

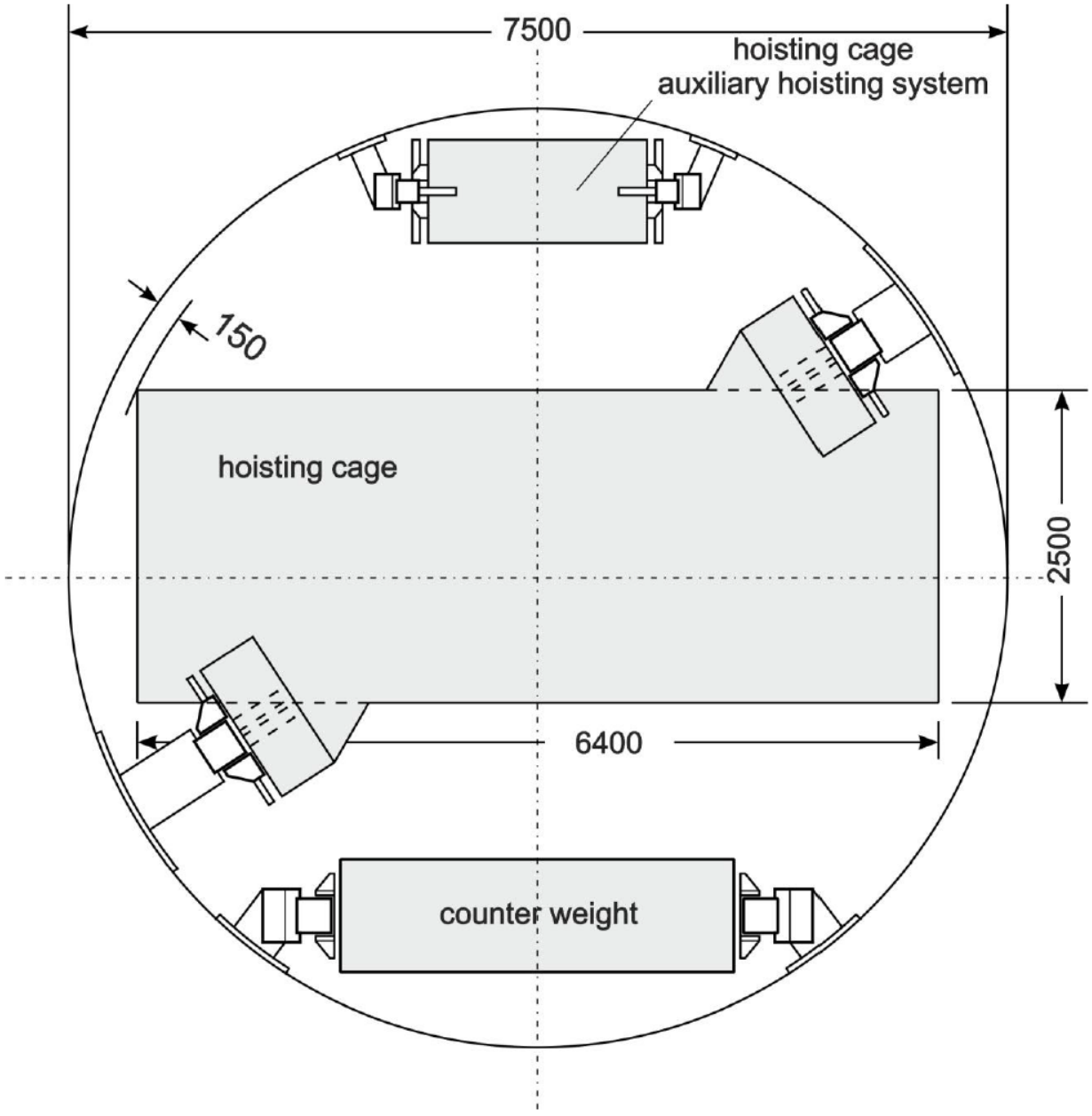

SOURCE: Filbert et al. 1994b, Figure 3-1

Figure 5-14. Schematic of the shaft cross-section

5.3 Operational Safety Analyses and Demonstration Analysis (Gorleben)

A shaft hoisting system for the transportation of waste packages to repository disposal depths fulfills a major function in repository operations and as a result has an important safety function. Currently, no operational shaft hoisting systems have been fully constructed for payloads greater than 50 MT. Such capabilities have not previously been needed in the mining industry. Only since the advent of deep geologic repository R&D, has the potential for hoists with significantly greater payload capacity been of economic interest.

The key concern related to shaft hoisting of nuclear waste payloads is a failure that could result in the uncontrolled fall of a waste shipment down the shaft and the associated potential for release of radioactive materials. The reliability of a hoist for transporting 85 MT payloads was demonstrated in the DEAB project conducted by DBE (discussed below). The main goal of the DEAB project was to demonstrate the technical feasibility and constructability of such a heavy hoist system, and assess the safety of the system in repository applications, under the relevant German mining and nuclear licensing requirements. The DEAB project consisted of two major components:

- Probabilistic safety assessment (PSA) (Filbert et al. 1994e)
- Demonstration testing (Filbert et al. 1994a; Schrimpf et al. 1989)

A preliminary operational safety evaluation, developed at a conceptual level (nonquantitative), assumes the transport of a shielded waste package (Appendix A). The evaluation was originally developed in support of the ONDRAF/NIRAS conceptual repository design (Herold et al. 2013, Appendix C). The hoisting system design proposed for ONDRAF/NIRAS was based on the Gorleben 2 concept.

5.3.1 Probabilistic Safety Assessment

Probabilistic safety analysis was used to evaluate the proper safety criteria for implementation in the design of the hoisting system. The probability of occurrence of significant events associated with the hoisting system, including loading and unloading of waste shipments was evaluated. Two safety related scenarios were evaluated using the probabilistic safety analysis method:

- The potential for exposure of operational personnel to increased radiation doses as a function of worker proximity to waste packages
- Potential for release of radioactive materials to the environment

The analysis includes the payload on-setting process at the shaft surface station, the shaft hoisting process, and payload off-setting process at the shaft subsurface station. As an initial step in the analysis process all steps associated with the planned operation were thoroughly evaluated, reviewed, and described, including both operational processes and equipment requirements. The performance of the majority of the hoisting system components and processes had been considered and evaluated in earlier PSAs, thus providing insight and confidence in the results from the DEAB PSA. The operational process steps were evaluated to assess the relationship of the two potential scenarios (i.e., exposure and release) with the hoisting system, and to describe mechanisms leading to potential system and component failures.

For the first event (exposure of operational personnel) the assessment results showed that higher worker radiological dose rates would exceed operational background rates on average 14 times per operational year (with 5,000 operational hours) or 3×10^{-3} events per operational hour. The main source of disturbance would be the hydraulic system. Disregarding the hydraulic system the number of events decreases to 0.03 per operational year or 6×10^{-6} per operational hour. The study did not evaluate the level and the period of radiation exposure, which were evaluated separately as part of a followup study to DEAB. The average duration for a waste shaft transport, including the on- and off-setting processes, would be approximately 30 minutes per shipment (Filbert et al. 1994e, Section 6).

For the second event, the potential release of radiation to the environment, the assessment considered four fault trees (Filbert et al. 1994e, Section 6):

A) The uncontrolled fall of the hoist cage with the waste package

B) The impact of a heavy load falling on the waste package

C) The accidental fall of a waste shipment down the shaft

D) Pulley overwind events

Event A could result from breakage of six or more hoist cables or breakage of the driving shaft inside the cable hoist pulley. The breakage of the cables includes also the failure of the cable attachments at the cage and counterweight and of the vernier adjustments inside the cable attachments.

Event B could result from the impact of a heavy load. A falling component impacts the waste package inside the cage. Such a heavy component could be the deflection pulley, weights or parts from the counterweight, or parts of the guide rails. The initiation of the fall/impact accident requires an additional initiating event.

Event C could result from the unexpected faulty operation of several shaft barriers. Those barriers are the shaft barrier itself, the bulkheads of the shaft lock, the shaft gate and the on-setting device.

Event D could occur at the head frame and at the shaft sump. The SELDA system at both shaft stations is designed to handle overwinding events with the normal hoisting velocity. If the cage exceeds this velocity the overwinding could result in damage to a waste package and a release of radiation. Overwinding associated with higher velocities could occur related to failures in both the braking system and the drive control system.

The probability of occurrence estimated for the different events A through D varies. The lowest probability 1.3×10^{-11} per year was determined for Event C, the fall of the waste shipment down the shaft. The redundant design of the different barriers and the lock systems essentially exclude the uncontrolled fall of a loaded cart from further consideration. The highest probability was determined for Event A under the assumption that six cables break associated with a single initiating event. The probability lies at 5×10^{-7} per year. Event B would occur with a maximum probability of 5.3×10^{-7} per year and Event D with 3×10^{-7} per year. The combined probability of occurrence was determined to be 1.3×10^{-6} per operational year. (Filbert et al. 1994e, Section 6).

Reduction in probability results from the redundant connection of the control and safety elements of the hoisting system. A release of radiation is only possible if several failures occur in combination. The German regulations do not define exact values for the acceptable probability of exposure or release. According to the state of the art and science this probability depends on the technical system and the risk potential. Technical systems are never 100% without risks. A residual risk remains even if all technically viable and economically sound safety measures are considered. In general the maximum accepted probability for radiological release from a German nuclear facility is approximately 10^{-6} per year. The probability of occurrence for release, although small, could be further reduced (e.g., to less than 10^{-6} per year) by including additional mitigating systems such as damping in the shaft sump.

Residual risk as implemented in DEAB can be compared to the preclosure safety standards used in the Yucca Mountain Review Plan for beyond-Category-2 event sequences, which were

defined as those events having less than 1 chance in 10,000 of occurring over the lifetime of the operating facility, before permanent closure (NRC 2003). It is noted that the analytical methods used in the DEAB and the Yucca Mountain license review, although similar, should not be directly compared. The Yucca Mountain analysis was finalized in 2008, and represented a further development in the state-of-the-art compared to the DEAB project which was conducted from 1989 to 1994.

For comparison the use of redundant and diverse safety design features was also considered in the Yucca Mountain Safety Analysis Report to meet the design basis reliability demands for operational safety (DOE 2008, Section 1.9.1.12).

5.3.2 DEAB Demonstration Test

The demonstration test of the hoisting system was designed with respect to relevant German mining regulations and nuclear safety considerations. Previous studies, as summarized in Filbert et al. 1994b, were conducted to determine the appropriate safety requirements associated with both conventional transport and radiological transport. The theoretical safety assessment was complimented by the full-scale demonstration tests intended to verify the reliability of the safety features considered in the analysis and to provide evidence of compliance for system reliability considerations (Schrimpf et al. 1989). The goal of the test was to evaluated functioning and reliability each of the systems components. Surface and subsurface shaft station are designed in the same manner. Therefore the demonstration test was suitable for evaluating operations for both loading and unloading of the cage. The configuration of the DEAB demonstration testbed is illustrated in Figure 5-15. During the demonstration test, the performance of the following components of the Gorleben 2 hoisting system design was confirmed:

- Shaft barrier
- On-setting machine
- Bulkheads of the shaft lock
- Movable transportation platform
- SELDA system
- Safety circuit

The testing rig contained a completely equipped shaft station with a SELDA system and a hoist cage. The winder was simulated by a crane inside the hall. The test bed was equipped with a fully functional hoist monitoring and control system and safety circuit. In addition to the demonstration itself, other programs within the DEAB project analyzed the reliability of the individual system components.

Cable reliability during the expected operational conditions was confirmed separately in a specialized facility for the testing of hoisting ropes (Filbert et al. 1994d). The cable testing facility confirmed the suitability of the selected cables. The cables resisted the expected loads. During the testing no failures either on the exterior or interior of the cables were detected. Based on the testing results cable life was determined to be primarily a function of corrosion.

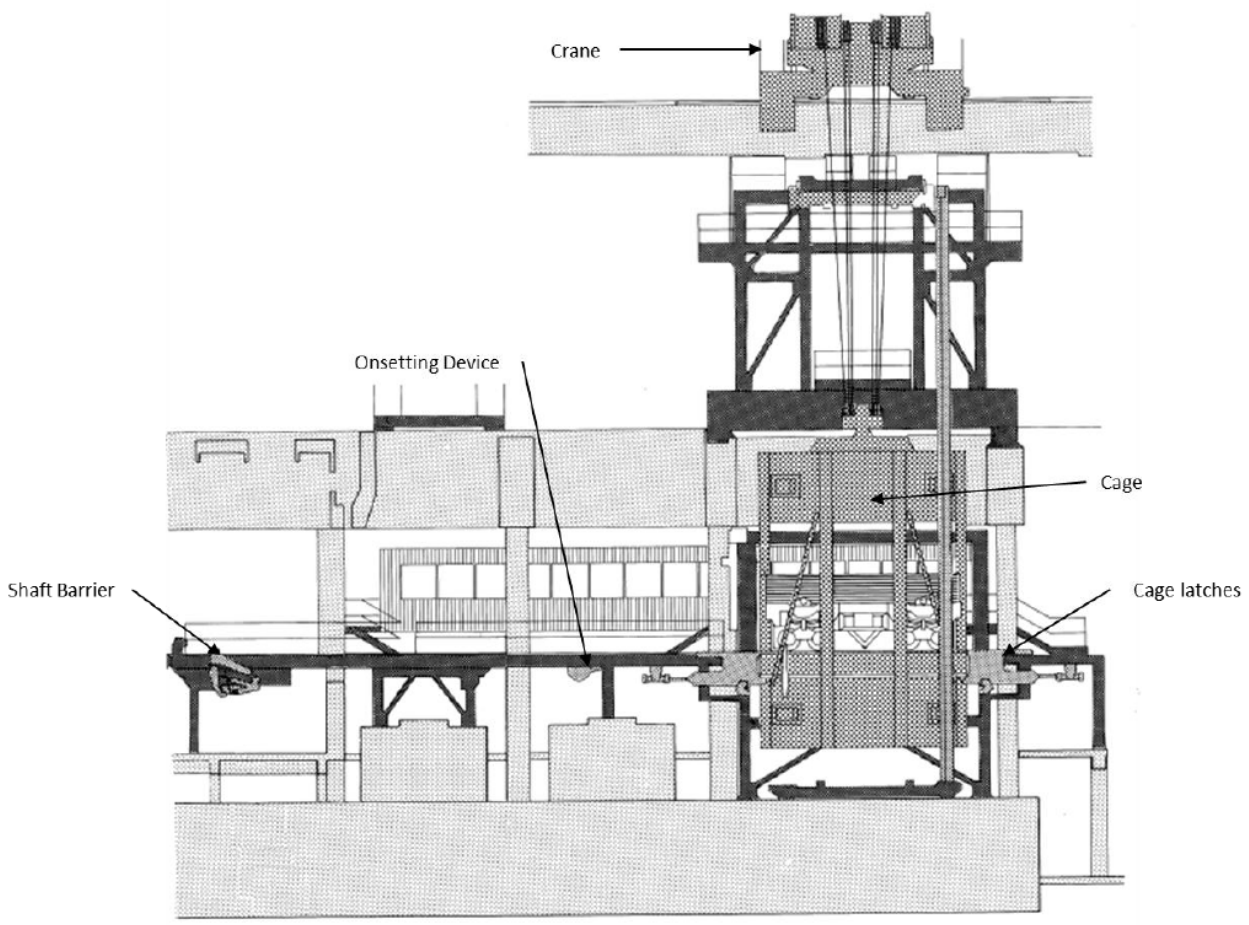

SOURCE: Filbert et al. 1994a, Figure 2-6

Figure 5-15. Configuration of the DEAB demonstration testbed

5.4 Upscaling to a 175 MT Hoist

DBE on behalf of GNS has recently completed conceptual designs for upscaling hoisting capacity to allow direct disposal of waste transportation and storage canisters (Project DIREGT II). Specifically, the design focused on shaft transport of shielded CASTOR® type waste canisters to repository level for disposal, assuming a repository disposal level at approximately 830 m below ground surface. The transport of these types of canisters increases the design payload from 85 MT to 175 MT, or twice that considered previously (Filbert et al. 2012).

Upscaling of the existing hoisting concept to 175 MT was one of the main goals of the DIREGT II project. The project produced a detailed plan for the hoist and an initial rough order-of-magnitude cost estimate.

Based on the experience gained form the DEAB project it was already understood that 175 MT capacity heavy hoist system could be realized from off-the-shelf equipment commonly used in the mining industry. The systems and components are essentially identical to those used in numerous mines around the world. The main questions are with respect to adapting the systems and components to greater payloads.

The general system concept for a 175 MT capacity heavy hoist remains unchanged from the 85 MT hoist. A detailed design was completed in DIREGT II that included three dimensional modeling and engineering calculations on all relevant parts, consistent with the relevant requirements defined in TAS and BVOS. The detailed design completed under DIREGT II includes:

- Hoisting tower
- Clamping and lifting devices for maintenance
- Electrical installations
- Six-cable Koepe winder and gear box
- Braking systems
- Cage with movable platform
- Hoisting and balance cables with cable attachments
- Friction pulley
- Surface and subsurface shaft station with on-setting device and shaft barriers
- Safety equipment (e.g. SELDA system, fire dampers, impact beams)
- Safety winder

The hoisting system is designed for the following parameters:

- Shaft diameter 7.5 m
- Hoisting depth 870 m
- Payload (i.e., loaded waste package, cart, and shielding if needed) weight 175 MT
- Transport cage weight 48 MT
- Counterweight 133 MT
- Hoist cable weight 83.29 MT

The greatest weight differential between the two strands (i.e., hoist cage and counterweight is approximately 89 MT at maximum displacement). Based on these loads, the required power of the winder was determined to 800 kW. The friction pulley has a diameter of 2.8 m and the cables lie on 500-mm intervals. The selected pulley diameter eliminates the need for additional deflection pulleys thus increasing the lifetime of the cables. Six hoisting cables and six balance cables are used in the design. The six balance cables are identical to the hoisting cables. All cables have a nominal diameter of 66 mm (6x36 – Warrington-Seal-Cable). The calculated safety factor of safety for the cables is 6.77 compared with a required safety factor of 6.75.

Hoisting velocity is reduced to 1 m/s. This also reduces the required engine and braking power. In the DIREGT II design only a single DC electric motor is needed. The hoisting tower includes all important system internals. The overall height is 40 m. All floors are connected by a lift and stairways.

The loading and unloading facilities at the shaft stations were designed consistent with the proven DEAB design. Guide rails and deployable cage latches for the transportation platform were designed for both hoisting stations. The cage latches allow an exact positioning of the movable platform during on-setting. The cage latches assume the full weight of the cage during loading and unloading and thus avoid any sudden changes in load on the cables. To manage potential overwinding events SELDA braking systems are installed at both shaft stations.

The DIREGT project has developed the shaft hoisting system design, stepwise to the state-of-the-art. The DIREGT II study demonstrates the technical feasibility of the increased payload requirements for disposal of CASTOR® type canisters. A detailed safety analysis of the DIREGT II design is included in the current DIREGT III project. A schedule for the realization of safety analysis and possible demonstration tests has not yet been finalized.

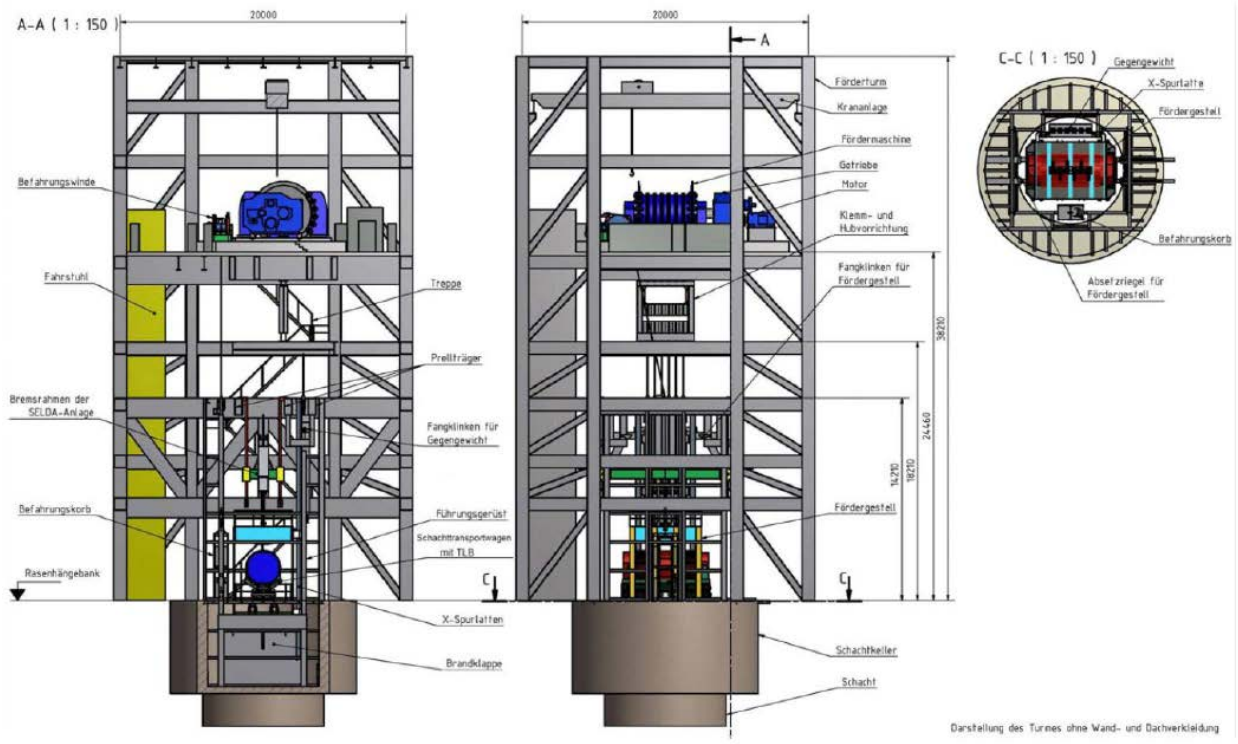

SOURCE: Filbert et al. 2013, Figure 3-1

Figure 5-16. Hoisting tower without lining (DIREGT)

5.5 Preliminary Cost Estimate for 85 MT and 175 MT Hoist Systems

The preliminary cost estimate presented in this section is based on the designs described in the DEAB and DIREGT projects (Filbert et al 2012, Section 4). The DEAB estimate has been updated to reflect current costs in Euros. It includes only estimates for required equipment and materials for completing the hoist system. Neither shaft excavation nor subsidiary systems such as ventilation and utilities are included. Installation costs are not considered. Costs for cables and cable attachments are not included. Cost estimates for the 85 MT hoist are based on a conceptual design developed by DBE TEC for ONDRAF/NIRAS (note that the estimate for this hoist has

been adjusted to the Gorleben 2 depths). Cost estimates for the 175 MT hoist are based on a similar system developed for the DIREGT II project. Costs are estimated for the major system components only as presented in Table 5-3.

Table 5-3. Preliminary cost estimation for major system components

Component	Rough Estimate [1] (85 MT)	Rough Estimate [2] (175 MT)
Headframe	8.0 Million €	10.0 Million €
Surface and subsurface shaft station installations	1.3 Million €	1.3 Million €
Shaft internals	2.3 Million €	2.3 Million €
Koepe winder	3.3 Million €	3.6 Million €
Monitoring and control systems	0.5 Million €	0.5 Million €
Safety winder	0.6 Million €	0.6 Million €
Total	16.0 Million €	18.3 Million €???

SOURCES: [1] After Herold et al. (2013); [2] Filbert et al. (2012), Section 4.

Equipment costs for the 85 MT and 175 MT hoisting systems are expected to be approximately 16 Million € and 18.3 Million €, respectively. The additional cost for the transport cart would be approximately 0.35 Million €.

Based on experience gained from the design, construction and fitting of the personnel shaft (Shaft 1) at the Gorleben exploratory facility it can be assumed that the total cost for hoist engineering, procurement and installation could be on the order of twice the equipment cost. This estimate does not include planning, site characterization, shaft design, licensing, surveying, shaft construction, shipping, development costs such as road building and power supply, and related costs such as project management and quality management. Installation of such a hoisting system would require a company with specialized expertise.

5.6 Summary

The eight-cable Koepe winder hoist system proposed for the shaft Gorleben 2 would handle a total payload of 85 MT, sufficient for the combined weight of the waste canister and waste transportation cart. The system would transport POLLUX® waste canisters to the disposal level in a specially designed hoist cage. The hoist cage features a false bottom, i.e., a waste transport platform that is free to move vertically within the cage framework. At the shaft stations cage latches would be used to grasp and immobilize this platform. With the platform immobilized the stresses on the cables can be equalized and controlled prior to conducting loading and unloading operations.

The Gorleben 2 hoisting concept for an 85 MT capable system has undergone full-scale demonstration testing (except for shaft construction, and using a crane instead of the hoist winder). The Gorleben concept uses known technologies and engineering solutions in its design and is ready for implementation. Additionally, a detailed safety analysis was prepared as part of the demonstration to evaluate the probability of occurrence for certain safety relevant failures.

The demonstration tests included full testing of the hoisting process consisting of on-setting, hoisting and removal of the waste shipment from the shaft. The shaft station was built at full scale (in a shallow excavation). The testing confirmed the reliability of the system with many repeated operations. The hoist cables were tested separately at a specialized laboratory. German mining authorities attested to the possibility of license.

Upscaling of payload capacity from 85 MT to 175 MT was verified by an additional study. The components of the hoisting system described here are derived from available conventional mining technologies. Where appropriate these technologies have been modified and confirmed by demonstration testing to accommodate the greater payloads associated with waste disposal (up to 85 MT). The design as proposed is feasible and represents the current state-of-the-art in hoisting system design. By inference (subject to further testing) upscaling to 175 MT is also feasible.

This section provides a conceptual description of shaft hoists that could be built to transport waste packages underground for disposal, but a hoisting concept has not been selected for implementation in the U.S., nor is it known where such a repository would be sited. The description refers (in simple present tense) to features of a generic hoist system design, but not to an existing hoist or to one that is currently planned for construction in the U.S.

References for Section 5

Barker-Davies 2013. Reliance Barker Davies – Homepage: Overwind Catchgear/Barker-Davies Catchgears. (http://www.reliancebarkerdavies.com)

Bollingfehr, W., W. Filbert, Ch. Lerch and M. Tholen 2012. “Vorläufi-ge Sicherheitsanalyse für den Standort Gorleben, Endlagerauslegung.” *Bericht zum Arbeitspaket*. 5. (GRS – 272). Köln. Dezember, 2012 .

Bridon International Ltd 2013. Homepage: Underground Mining Products/Flat Balance Ropes. (http://www.bridonltd.com/site/products/undergroundmining/flatr ope.php)

BVOS 2003 (Bergverordnung für Schacht- und Schrägförderanlagen – BVOS). vom 15.Oktober 2003 (Nds. MBI. S. 769).

DOE (U.S. Department of Energy) 2008. *Yucca Mountain Repository License Application for Construction Authorization*. DOE/RW-0573. Washington, D.C.: U.S. Department of Energy.

Filbert, W., J. Rissel and W. Weber 1994a. Direkte Endlagerung ausgedienter Brennelemente DEAB, Simulation des Schachttransportes - Versuchsstand zur Simulation des Schachttransportes (T 13). Peine. März, 1994.

Filbert, W., P. Kipka, K. Simmich and H. Weber 1994b. Direkte Endlagerung ausgedienter Brennelemente DEAB, Simulation des Schachttransportes - Konzeption einer Schachtförderanlage für Schwerlasten bis 85 t (T 42). Peine. März, 1994.

Filbert, W., D. Fuchs and F. Langebrake 1994c. Direkte Endlagerung ausgedienter Brennelemente DEAB, Untersuchungen der Seil-beanspruchung bei der Übernahme der Nutzlast von 85t (T48). Peine. März, 1994.

Filbert, W., K. Simmich, H. Weber, A. Gerlach and W. Sindern 1994d. Direkte Endlagerung ausgedienter Brennelemente DEAB, Untersuchungen zum Seilrutsch (T49). Peine. März, 1994.

Filbert, W., C. Schrimpf, R. van Hecke, R. Leicht and R. Schaub 1994e. Direkte Endlagerung ausgedienter Brennelemente DEAB, Probabilistische Sicherheitsanalyse zur Schachtförderanlage (T 50). Peine. Mai, 1994.

Filbert, W., M. Heda, M. Khamis and C. Schrimpf 1994f . Direkte Endla-gerung ausgedienter Brennelemente DEAB, Funktionsprüfung der SELDA-Anlage (DEAB T47). Peine. Mai, 1994.

Filbert, W., P. Herold, F. Kristek, D. Schelkmann and M. Sonn-tag 2012. Realisierbarkeit der Schachtförderanlage für Transport-und Lagerbehälter (TLB) bis 160 Mg - DIREGT II. Peine. 2012.

Hardin, E., T. Hadgu, D. Clayton, R. Howard, H. Greenberg, J. Blink, M. Sharma, M. Sutton, J. Carter, M. Dupont and P. Rodwell 2012. *Repository Reference Disposal Concepts and Thermal Load Management Analysis*. FCRD-UFD-2012-00219 Rev. 2. U.S. Department of Energy, Used Fuel Disposition R&D Campaign. November, 2012.

Herold, P., W. Filbert and B. Haverkamp 2013. Technical Support for the R&D Feasibility Program for the Geological Disposal of Category B&C Radioactive Waste, R&D Study Conceptual Design for the Hoisting System of the Waste Shaft, Final Report. Peine. 2013.

NRC (U.S. Nuclear Regulatory Commission) 2003. *Yucca Mountain Review Plan, Final Report*. NUREG-1804, Rev. 2. Washington, D.C.: U.S. Nuclear Regulatory Commission. July, 2003.

Schrimpf, C. 1989. Direkte Endlagerung ausgedienter Brennelemente DEAB, Auslegung und Erprobung des SELDA-Systems Versuchsprogramm (T10). Peine. Februar, 1989.

Schrimpf, C., W. Filbert, M. Heda and R. Leicht 1989. Direkte End-lagerung ausgedienter Brennelemente DEAB, Demonstrationsversuche (T 14). Peine. April, 1989.

SIEMAG 2013a. SIEMAG – Homepage: Technical Information Disc Brake Units Be 100, Be 125, and Be 200. (http://www.siemag-tecberg.com/cms/upload/downloads/en//TI_06_Disc-Brake- Units_be-100_125_200_e.pdf)

SIEMAG 2013b. SIEMAG – Homepage: Technial Information Roller Guide for Skips and Cages. (http://www.siemag-tecberg.com/infocentre/technical-information/ti_22-roller-guides.html)

SIEMAG 2013c. SIEMAG – Homepage: Technical information Safety Arrestor (SELDA Principle). (http://www.siemag-tecberg.com/cms/upload/downloads/en//TI_11_Safety-Arrestor_e.pdf)

TAS 2005 Technische Anforderungen an Schacht-und Schrägförderanlagen (TAS) Stand. Dezember, 2005.

6. Summary

Reference geologic disposal concepts for the Used Fuel Disposition R&D campaign, are expanded to include backfill and unbackfilled open-mode alternatives for sedimentary rock (e.g., clay/shale) and hard rock (e.g., crystalline). Also, the cavern-retrievable concept is recognized as a possible alternative that combines elements of storage and disposal packaging.

Thermal analysis of alternative disposal concepts is extended to open emplacement modes (those allowing long-term repository ventilation to remove heat), with calcuations of minimum ventilation time for various waste types and geologic settings. Also, waste package thermal power limits at the time of emplacement in the repository, are calculated for a range of package spacings and storage/ventilation timing cases, to be used as input to logistical simulations that model disposition and ultimate disposal of used nuclear fuel. These calculations are sensitive to the maximum temperature target adopted for host rock and engineered materials such as clay-based backfill. Disposal in salt and hard rock, which have relatively high thermal conductivity and tolerance for elevated temperatures on the order of 200°C, allows the highest thermal power limits (10 to 15 kW at emplacement). Disposal in sedimentary rock, which has relatively low thermal conductivity, could be facilitated by longer decay storage, larger repository drift and package spacings, or by heating a thin region of the near-field host rock to peak temperatures greater than 100°C. Use of temperature-sensitive backfill is associated with the lowest emplacement power limits (on the order of 1 kW to meet a 100°C temperature target) which would require protracted surface decay storage.

Questions about the potential for large, hot waste packages to sink due to creep in a salt repository are addressed using coupled thermal-mechanical finite-element simulations. These calculations were performed using the Adagio and Aria codes, and using constitutive models developed from tests performed in the laboratory at the Waste Isolation Pilot Plant and elsewhere. They show that based on these inputs, sinking is limited to 0.1 m or possibly much less over 10^6 years, even for a large, heavy waste packages (containing 32 PWR assemblies, and having average density equivalent to solid steel).

Finally, the technical details and safety analysis for a heavy shaft hoist with payload capacity of 85 MT are discussed, based on previous work done in Germany at the Gorleben site. Such a capacity would facilitate transport of packages weighing about 60 MT (e.g., 12 PWR assemblies, canister, disposal overpack, and shielding). For larger packages (e.g., containing 32 PWR assemblies) the hoist design concept could be extended to 175 MT. Costs for hoist hardware would be approximately $20 to $30 million, plus shaft construction, hoist installation, and other costs associated with management, engineering, procurement, and construction.

Appendix A – Operational Safety Evaluation

Primary System Component	Description of Failure/Hazard	Result	Corrective or Preventive Actions
Shaft barrier	Shaft barrier closes during the on-setting process. • The waste shipment is directly above the shaft barrier • The shaft barrier strikes the bottom of the cart	The cart may become temporarily inoperable; components of the cart may be damaged (e.g., Hydraulics, wheels and axels, bearings, braking system). Personnel may be subject to higher radiological dose during recovery/repair operations.	• Maintain spare components for repairs • Station emergency equipment capable of transferring the waste container from the cart to an auxiliary transportation system near the shaft • Evaluate the repair requirements if needed transfer the waste package to the auxiliary system and move to a temporary storage facility • Conduct repairs and test system before resuming operations
		The cart may be lifted off of the rails resulting in a derailment accident. Personnel may be subject to higher radiological dose during rerailing operations.	• Maintain rerailing equipment at the facility • Provide additional personnel protective equipment for conducting repairs
	Malfunction of the traverse table	Waste shipment is stranded between rail-track connections. Personnel may be subject to higher radiological dose during recovery/repair operations.	• Provide manual backup systems to operate the traverse table in case of a failure of the primary systems
	Malfunction of the traverse table's integrated on-setting machine	Waste shipment strikes the shaft barrier at the maximum velocity of the on-setting machine. No radiological exposures to personnel are expected	• Shaft barrier is designed to resist the impact at the highest velocity that can be generated by the on-setting • Bumpers integrated into the cart absorb the impact and avoid derailing
Shaft lock	Malfunction of shaft on-setting machine	Waste shipment strikes a shaft-lock bulkhead gate at the maximum velocity of the on-setting machine. No radiological exposures to personnel are expected	• Bulk heads are to be designed to resist the highest potential impact from the on-setting machine • Bumpers integrated into the cart absorb the impact and avoid derailing
	A bulk head gate prematurely closes during the on-setting process • The waste shipment is located below the bulk head	The bulk head strikes the waste shipment • The waste shipment is trapped by the bulkhead and cannot be moved	• The bulkheads are designed to allow manual operation in the case of this accident scenario • The lift height is limited to minimize the potential fall of a bulkhead thus reducing the impact energy avoiding significant damage to a waste package • Consequences depend on the waste package construction and materials • Operational procedures should be designed to avoid occurrence • Electronic and mechanical systems can be integrated into the operating systems to eliminate any possibility of occurrence. • In the event of this accident scenario affected waste packages are returned to the buffer storage facility for inspection and repair if needed

Primary System Component	Description of Failure/Hazard	Result	Corrective or Preventive Actions
On-setting machine	Malfunction of the on-setting machine during the loading process	Mechanical failure or control failure is possible at any position between shaft barrier and fixed transportation platform. As a result the waste shipment cannot be moved in normal operating manner. Repairs can result in higher potential radiation exposures to personnel.	• Manual operation of the coupling device to release the waste shipment • Subsequent return of the waste shipment to a standby position on the on-setting machine (e.g., an auxiliary cable wench system can be used to move the waste shipment into the standby position)
	Coupling device does not open	Mechanical failure is relevant at the beginning and end of an on-setting maneuver and completion of the on-setting process is hindered. As a result the waste shipment cannot be moved in normal operating manner. Repairs can result in higher potential radiation exposures to personnel of working beside the waste package.	• Manual operation of the coupling device to release the waste shipment if required • Subsequent return of the waste shipment to a standby position on the on-setting machine (e.g., an auxiliary cable wench system can be used to move the waste shipment into the standby position)
Cage latches	Malfunction of one or more cage latches; fail to extend properly • Fixing the transport platform into its loading position is not possible • Both shaft stations	The securing of the transport platform into the loading position is disturbed. The on-setting process cannot be completed. The cage cannot be lowered into the loading position until the failure is rectified.	• Sensors are used to confirm that the cage latches are fully engaged • The control system will only allow the hoist cage to be lowered into its loading position when the latches are properly engaged. • Cage latches can be manually operated
	Malfunction of one or more cage latches; fail to retract properly • Shaft transport is not possible • At surface shaft station	The one or more cage latches cannot be retracted however because the hoist cage has been raised to its shaft transportation position and the cables have been pulled taut a fall accident is not possible. Repairs can result in higher potential radiation exposures to personnel.	• Sensors are used to confirm that the cage latches are fully engaged • The control systems only allow shaft transport to commence if all cage latches have been retracted. • Cage latches can be manually operated
	Metal fatigue and material flaw results in one or more cage latches breaking during loading of the transport platform • Relevant to both shaft stations	The failure leads to uneven loading on the remaining latches. Failure of one latch is accounted for in the design of the complete cage latch system. Failure of more than one latch would result in a drop down of the transport platform onto the hoist cage (app 20 cm drop). The hoist cage in turn can experience cable slipping.	• Cage latches are specifically designed to preclude breaking accidents. • Regular inspection includes assessing load-bearing components for metal fatigue and material flaws. • Design requirements for the cage latches ensure that three latches are adequate to secure the loaded waste transportation platform in place pending removal of the waste shipment to allow repairs • Emergency brakes ensure that cable slippage cannot exceed a defined length before being activated
Shaft	Failure of one cable	A single cable can fail (i.e., rupture) as a result of material fatigue however the safety factors included in the design of the remaining cables preclude a fall accident from occurring.	• TAS provides strict safety requirements for hoist cables • Design and construction criteria placed on the cables minimizes potential risks • Cables are continuously monitored to detect material weaknesses • Regular inspection and maintenance of the

Primary System Component	Description of Failure/Hazard	Result	Corrective or Preventive Actions
			cables ensures that flaws are identified and repaired • Sensors at the cable attachments provide early warning if load distribution becomes uneven • The factor of safety for the remaining cable is such that sufficient safety is given • Upon arrival at the subsurface shaft station the waste shipment is immediately offloaded following emergency protocols and the hoist cage is returned to the surface station (if possible) for repairs (including the potential replacement of all cables)
Shaft, continued	Failure of all cables	Failure of more than one cable as a result of material weakness results in a cascade failure of all of the cables and the waste shipment falls in an uncontrolled manner down the shaft.	This failure most be avoided by design considerations: • TAS provides strict safety requirements for hoist cables • Design and construction requirements placed on the cables minimizes potential risks • Cables are continuously monitored to detect material weaknesses • Regular inspection (including inspection during construction) and maintenance of the cables ensures that flaws are identified and repaired (It is noted that a residual risk will always remain, however the probability of failure is seen as extremely low. A detailed safety analysis of the final design will be required to quantify the residual risk.)
	Cable slippage	Cables slip as a result of uneven loading: • Can result due to an excessive change in velocity (braking or accelerating) • The friction between the cables and the winder is not sufficient • Difference in torques on the cables determines the slippage distance • In the worst case the hoist cage slips down the entire length of the shaft	• Adequate frictional surface area is included in the design of the winder pulley • Braking systems are designed so that the maximum braking velocity/distance is not exceeded • Initiation of the hoisting maneuver is controlled so that the maximum acceleration is not exceeded • Sensors are used to monitor cable load ratios during hoisting • Regular maintenance and inspection of the winder pulley liner, the cables, and lubricants • Controlled/steered braking system (i.e., similar to an antilock braking system) can be installed to further reduce the likelihood of this failure scenario
	Failure of a single cable attachment assembly	A single cable attachment assembly can fail as a result of a mechanical or material failure material however the safety factors included in the design of the remaining assemblies	• TAS provides strict safety requirements for hoist cables attachments • Design and construction criteria placed on the attachments minimizes potential risks • Regular inspection and maintenance of the

Primary System Component	Description of Failure/Hazard	Result	Corrective or Preventive Actions
		precludes a fall accident from occurring.	attachments ensures that flaws are identified and repaired • Sensors at the cable attachments provide early warning if load distribution becomes uneven • The factor of safety for the remaining attachments is such that sufficient safety is given • Upon arrival at the subsurface shaft station the waste shipment is immediately offloaded following emergency protocols and the hoist cage is returned to the surface station (if possible) for repairs (It is noted that a residual risk will always remain however the probability of failure is seen as extremely low. A detailed safety analysis of the final design will be required to quantify the residual risk.)
Shaft, continued	Failure of all cable attachment assemblies	Failure of more than one cable attachment assembly results in a cascade failure of all of the cable attachments and the waste shipment falls in an uncontrolled manner down the shaft.	This failure most be avoided by design considerations: • TAS provides strict safety requirements for hoist cables attachments • Design and construction requirements placed on the attachments minimizes potential risks • Regular inspection (including inspection during construction) and maintenance of the cable attachments ensures that flaws are identified and repaired
	Failure of a single cable attachment assembly	A single cable attachment assembly can fail as a result of a mechanical or material failure material however the safety factors included in the design of the remaining assemblies precludes a fall accident from occurring.	• TAS provides strict safety requirements for hoist cables attachments • Design and construction criteria placed on the attachments minimizes potential risks • Regular inspection and maintenance of the attachments ensures that flaws are identified and repaired • Sensors at the cable attachments provide early warning if load distribution becomes uneven • The factor of safety for the remaining attachments is such that sufficient safety is given • Upon arrival at the subsurface shaft station the waste shipment is immediately offloaded following emergency protocols and the hoist cage is returned to the surface station (if possible) for repairs
	Failure of all cable attachment assemblies	Failure of more than one cable attachment assembly results in a cascade failure of all of the cable attachments and the waste shipment falls in an uncontrolled manner down the shaft.	This failure most be avoided by design considerations: • TAS provides strict safety requirements for hoist cable attachments • Design and construction requirements placed on the attachments minimizes potential risks

Primary System Component	Description of Failure/Hazard	Result	Corrective or Preventive Actions
			• Regular inspection (including inspection during construction) and maintenance of the cable attachments ensures that flaws are identified and repaired
	Failure in the guide rail system • Rupture above the hoist cage • Rupture below the hoist cage	• Hoisting path is interrupted • Components of the damaged guide rail system fall off • Falling parts can damage other components of the hoisting system • If the failure is not detected the cage could collide with the broken guide rail during down hoisting • Derailing can result • Damage to ventilation, power cables, emergency system, countebalance	• TAS and related requirement documents provide detailed requirements and instructions for maintenance of hoisting systems including guiderails • Strict requirements must be placed on the design of the guiderail system • Regular inspection and maintenance to the guiderails is required • The waste package is adequately secured to avoid any damage due to a collision between the cage and a damaged guiderail.
Shaft, continued	Loss of power to brake system	The system is designed so that in the event of a power outage the brakes are automatically engaged. No radiological impacts are expected.	• Power losses to the hoisting system are anticipated under normal operating conditions.
	Loss of power to the winder	The system is designed so that in the event of a power outage the brakes are automatically engaged. No radiological impacts are expected.	• Power losses to the hoisting system are anticipated under normal operating conditions.
Surface or subsurface shaft station	Waste shipment is dropped down an open shaft	Waste package falls down the shaft, resulting in the complete failure of the waste package containment and a significant radiological release	Several systems are included in the design to preclude this unlikely scenario: • Traverse table ensures that there is no direct path to the shaft from the surface rail transport • Shaft safety barrier and shaft lock secure the shaft • Mechanical control systems ensure that the shaft barrier can only be opened when the bulkhead door is open and the cart is grasped by the on-setting device, Next the cart can then only be moved onto the cage when the outer bulkhead is closed and the inner bulkhead is open. The inner bulkhead can only be open when the transport platform is in its loading position. • Bulkhead gates can only be opened one at a time interrupting the movement of each waste shipment • The waste shipment is loaded onto the transport platform via on-setting machine; no locomotives are used in the immediate shaft area.
	Overwind accident	Hoist cage fails to stop at the shaft station • SELDA system used to brake the cage • Cage ratchets at surface shaft	• The SELDA system is a safety feature integrated into the hoisting system • Regular inspection and maintenance of all relevant components and parts

Primary System Component	Description of Failure/Hazard	Result	Corrective or Preventive Actions
		station catch the cage after braking by the SELDA system • No serious consequences, however the SELDA system will require replacement if used • No radiological exposures to operational personnel.	• In the event of an overwind accident all components of the SELDA system are inspected and replaced as needed.
Surface shaft station	Overwind accident exceeding SELDA design criteria at the surface shaft station	Cage collides with the SELDA system under normal hoisting velocity exceeding the braking capacity of the SELDA system. The momentum of the cage is arrested by the impact beams. Concurrently, the counterweight strikes the SELDA system installed at the shaft sump • Cage ratchets catch the cage avoiding a fall accident • Impact may damage components of the hoisting system and shaft • Waste package could be damaged resulting in higher radiation exposures	• The SELDA system, including impact beams, is a safety feature integrated into the hoisting system at both the shaft and sump locations • Regular inspection and maintenance of all relevant components and parts • In the event of an overwind accident all com ponents of the SELDA system are inspected and replaced as needed.
Subsurface shaft station	Overwind accident exceeding SELDA design criteria at the subsurface shaft station	Cage collides with the SELDA system under normal hoisting velocity exceeding the braking capacity of the SELDA system. The momentum of the cage is arrested by the impact beams. Concurrently, the counterweight strikes the SELDA system installed at the headframe: • Cage ratchets catch the counterweight at the surface station avoiding a fall accident • Impact may damage components of the hoisting system and shaft • Waste package could be damaged resulting in higher radiation exposures	The SELDA system, including impact beams, is a safety feature integrated into the hoisting system at both the shaft and sump locations Regular inspection and maintenance of all relevant components and parts In the event of an overwind accident all components of the SELDA system are inspected and replaced as needed.
Surface shaft station	Non-related piece of equipment or other materials is accidentally dropped down the shaft.	• The falling piece of equipment damages one or more components of the shaft hoisting system. • Damages a waste package during shaft transportation resulting in a potential radiological exposure	• The roof of the cage is closed to protect the waste shipments from falling objects • No serious damage to the waste package is expected as shaft safety features preclude the dropping of any significant component (e.g. the locomotive) down the shaft • Should an object be inadvertently dropped down the shaft all potentially exposed components of the hoisting system and related safety features must be thoroughly inspected and repairs initiated as appropriate